Assessing the role of Sorting Nexins in the nervous system: Insights from "stressed" synapses

Gisela Cristina Vieira Armada

UMinho | 2020

Universidade do Minho
Escola de Medicina

Gisela Cristina Vieira Armada

Assessing the role of Sorting Nexins in the nervous system: insights from "stressed" synapses

Novembro de 2020

Universidade do Minho
Escola de Medicina

Gisela Cristina Vieira Armada

Assessing the role of Sorting Nexins in the nervous system: insights from “stressed” synapses

Dissertação de Mestrado
Mestrado em Ciências da Saúde

Trabalho efetuado sob a orientação da
Doutora Neide Marina Vieira Pereira
e do
Doutor André Miguel Lopes Miranda

Novembro de 2020

DIREITOS DE AUTOR E CONDIÇÕES DE UTILIZAÇÃO DO TRABALHO POR TERCEIROS

Este é um trabalho académico que pode ser utilizado por terceiros desde que respeitadas as regras e boas práticas internacionalmente aceites, no que concerne aos direitos de autor e direitos conexos.

Assim, o presente trabalho pode ser utilizado nos termos previstos na licença abaixo indicada.

Caso o utilizador necessite de permissão para poder fazer um uso do trabalho em condições não previstas no licenciamento indicado, deverá contactar o autor, através do RepositóriUM da Universidade do Minho.

Licença concedida aos utilizadores deste trabalho

Atribuição-NãoComercial-SemDerivações
CC BY-NC-ND

https://creativecommons.org/licenses/by-nc-nd/4.0/

ACKNOWLEDGMENTS

Agradeço aos meus orientadores, Neide Vieira e André Miranda, pela mentoria e dedicação durante a realização deste projeto. Obrigada por todo o conhecimento que me transmitiram e por acima de tudo terem acreditado no meu trabalho. Obrigada pela vossa ajuda constante e incondicional!

Agradeço aos meus colegas de equipa e a todo o grupo MCN por toda a ajuda proporcionada e pelo bom ambiente de trabalho.

Aos meus amigos de laboratório, obrigada pelos momentos de descontração e pelas horas de reflexão. Obrigada por tornarem isto possível e por contribuírem para o sucesso deste trabalho!

Aos meus amigos de sempre, obrigada por compreenderem todos os momentos ausentes e tornarem a distância um pouco mais tolerável. Obrigada por mesmo longe estarem tão perto!

À minha família, principalmente aos meus pais, obrigada pela preocupação, por serem um suporte incansável e por sempre acreditarem em mim ao longo destes anos. Obrigada por tudo!

Ao Vitor, por ter sido o apoio incondicional que eu não sabia que precisava. Obrigada por veres sempre o lado positivo e por tornares tudo mais fácil!

Agradeço a todos aqueles que das mais variadas formas contribuíram para a realização deste trabalho.

Agradeço ao Doutor Nuno Sousa, Presidente da Escola de Medicina da Universidade do Minho, ao Professor Jorge Correia-Pinto, Presidente do Instituto de Investigação em Ciências da Vida e Saúde (ICVS), ao Doutor João Bessa, Coordenador do Domínio de Neurociências, e à Professora Doutora Patrícia Maciel, Diretora do Mestrado em Ciências da Saúde pelo apoio institucional.

The work presented in this thesis was performed in the Life and Health Sciences Research Institute (ICVS), Minho University. Financial support was provided by grants from the NARSAD Young Investigator Grant from Brain and Behavior Research Foundation, NY, USA, for Neide Vieira, ICVS Scientific Microscopy Platform, member of the national infrastructure PPBI - Portuguese Platform of Bioimaging (PPBI-POCI-01-0145-FEDER-022122; by National funds, through the Foundation for Science and Technology (FCT) - project UIDB/50026/2020 and UIDP/50026/2020; and by the projects NORTE-01-0145-FEDER-000013 and NORTE-01-0145-FEDER-000023, supported by Norte Portugal Regional Operational Programme (NORTE 2020), under the PORTUGAL 2020 Partnership Agreement, through the European Regional Development Fund (ERDF).

STATEMENT OF INTEGRITY

I hereby declare having conducted this academic work with integrity. I confirm that I have not used plagiarism or any form of undue use of information or falsification of results along the process leading to its elaboration.

I further declare that I have fully acknowledged the Code of Ethical Conduct of the University of Minho.

RESUMO

As *Sorting Nexins* (SNXs) surgiram como uma família de proteínas que facilitam o tráfego proteico e sinalização intracelular sendo reguladoras chave de processos endocíticos subjacentes à plasticidade sináptica e cognição. Curiosamente, a sua desregulação tem sido associada a doenças neurológicas, nomeadamente doença de Alzheimer (AD) e doença de Parkinson (PD). Particularmente, a SNX27 contribui para os défices cognitivos observados no Síndrome de *Down* (DS). Um estudo desenvolvido num modelo animal de DS demonstrou que a sua expressão reduzida contribui para disfunções sinápticas e défices cognitivos através da redução da reciclagem de recetores de glutamato para a superfície celular. Outras SNXs, como a SNX3 e SNX12, mostraram ser relevantes para a regulação da homeostasia do sistema nervoso sendo associadas a processos de neurodesenvolvimento e neurodegeneração. Apesar disto, pouco se sabe relativamente à expressão e função das SNXs no sistema nervoso, em particular, como são moduladas pelo *stress*, condição associada à desregulação endocítica, e um conhecido potenciador de défices cognitivos e disfunção sináptica. Recorrendo ao estudo de roedores e de uma linha celular, propomos desvendar o papel das SNXs no sistema nervoso central e estudar os efeitos modulatórios do *stress* na performance comportamental, morfologia neuronal e na localização subcelular de reguladores da plasticidade sináptica. Para tal, geramos um modelo de murganho heterozigótico para a SNX27 com *background* em C57BL/6J e caracterizamos o impacto da redução da SNX27 durante o desenvolvimento pós-natal e na performance comportamental durante exposição a *stress* crónico. Adicionalmente, exploramos os efeitos da modulação dos níveis de PI3P e glucocorticoides (GC) na função das SNXs numa linha celular de neuroblastoma. Neste trabalho demonstramos que a redução dos níveis de SNX27 não interfere com o desenvolvimento somático e neurológico animal. A avaliação comportamental demonstrou que o bem-estar de animas heterozigóticos é afetado e que estes animais apresentam aumento de comportamentos do tipo ansioso no teste NSF. Curiosamente, não foram encontrados défices cognitivos nestes animais. Resultados *in vitro* indicam que, sob condições de redução de PI3P e aumento de GC, os níveis de SNX27 estão aumentados, facto não observado para a SNX3. Este facto pode ser indicativo de papéis opostos para a SNX27 e SNX3 após modulação do tráfego endolisossomal. Em suma, este trabalho fornece novas perspetivas sobre o papel da SNX27 durante o desenvolvimento e performance comportamental e como é modulada por processos associados ao *stress* assim como a localização subcelular e modulação de várias SNXs.

Palavras-chave: Sorting Nexins, Tráfego intracelular, Comportamento, Stress, Desenvolvimento

ABSTRACT

Sorting Nexins (SNXs) have emerged as a family of highly conserved proteins that facilitate protein trafficking and intracellular signaling being key regulators of endocytic processes underlying synaptic plasticity and cognition. Interestingly, SNXs mis-regulation has been associated with neurological disorders such as Alzheimer's disease (AD) and Down's syndrome (DS). Particularly, SNX27 was shown to be a major contributor to intellectual impairments in DS. A study developed in a DS mouse model demonstrated that downregulation of SNX27 contributes to synaptic dysfunction and cognitive deficits by decreasing the recycling of glutamate receptors to the cell surface. Other SNXs, such as SNX3 and SNX12, have also been shown to be relevant for nervous system homeostasis regulation being associated with neurodevelopment and neurodegeneration. Despite this, much is unknown concerning SNXs' expression and function within the nervous system, and particularly how they are modulated by stress, a condition linked to endocytic dysregulation, and a known inducer of cognitive decline and synaptic malfunction. Using both rodents and an established cell line, we set out to unveil SNXs role on the central nervous system and to study the modulatory effects of stress on behavioral performance, neuronal morphology and subcellular localization of regulators of synaptic plasticity. For such, we generated a SNX27$^{+/-}$ mouse model backcrossed to C57BL/6J background and characterized the impact of SNX27 reduction on postnatal development and behavioral performance, particularly under chronic stress-exposure. Furthermore, we explored the pharmacological modulation of phosphatidylinositol-3-phosphate (PI3P) and glucocorticoids (GC) on SNXs expression in an established neuronal-like cell line. Our results indicate that reduced levels of SNX27 do not interfere with the acquisition of somatic and neurological development milestones. Concomitantly, behavioral analysis showed that the well-being of SNX27$^{+/-}$ C57BL/6J animals is affected and that these animals display increased anxious-like behaviors in the NSF test. Interestingly, we did not find any cognitive deficits in SNX27$^{+/-}$ C57BL/6J mice. *In vitro* findings indicate that SNX27 levels are increased under conditions of PI3P reduction or elevation of GC levels, which is not observed for SNX3. This might be indicative of opposing roles of SNX3 and SNX27 upon endolysosomal trafficking modulation. Overall, this work provides new insights on SNX27 role during development and behavioral performance in a pure genetic background, and how SNX27 is affected by stress-related processes as well as on the subcellular localization and modulation of additional SNXs by the above-mentioned.

Keywords: Sorting Nexins, Intracellular trafficking, Behavior, Stress, Development

TABLE OF CONTENTS

ABREVIATIONS

A	
A	Ampere
ACTH	Adrenocorticotropic Hormone
AD	Alzheimer's disease
AMPA	α-amino-3-hydrozy-5-methylisoxa-zole-4-propionic acid
ANOVA	Analysis of Variance
ANS	Autonomic Nervous System
APP	Amyloid Precursor Protein
Aβ	Amyloid β
B	
BAR	Bin, amphiphysin, Rvs
BBB	Blood Brain Barrier
BNST	Bed Nucleus of the Stria Terminalis
Bp	Base Pair
C	
CFC	Contextual Fear Conditioning
CNS	Central Nervous System
CON	Control
CORT	Corticosterone
CRH	Corticotropin-releasing hormone
CUS	Chronic Unpredictable Stress
D	
DEX	Dexamethasone
DG	Dentate Gyrus
DNA	Deoxyribonucleic acid
DS	Down's syndrome
E	
EGFR	Epidermal growth factor receptor
EPM	Elevated Plus Maze
F	
FBS	Fetal Bovine Serum
FERM	4.1 protein, ezrin, radixin, moesin
FST	Forced Swim Test

G	
GAS	General Adaptation Syndrome
GC	Glucocorticoid
GLUT	Glucose Transporter
GR	Glucocorticoid receptors
H	
Het	Heterozygous
Hip.D	Dorsal hippocampus
Hip.V	Ventral hippocampus
HPA	Hypothalamic-Pituitary-Adrenal
HSP	Hereditary Spastic Paraplegia
I	
IF	Immunofluorescence
ILVs	Intraluminal vesicles
L	
LDP	Long-term depression
LTP	Long-term potentiation
L/D Box	Light/Dark Box
M	
MWM	Morris Water Maze
MR	Mineralocorticoid receptors
N	
NMDA	N-methyl-D-aspartate
NORT	Novel Object Recognition Test
NSF	Novelty Suppressed Feeding
O	
OF	Open Field
P	
PBS	Phosphate buffered saline
PCR	Polymerase Chain Reaction
PD	Parkinson's disease
PDZ	Postsynaptic density protein-95
PFA	Paraformaldehyde
PFC	Prefrontal cortex

PI	Phosphatidylinositol
PNS	Peripheral Nervous System
PtdIns3P	Phosphatidylinositol-3-monophosphate
PX	Phox-homology
Q	
qRT-PCR	Quantitative Real-Time PCR
R	
RT	Room temperature
S	
SAM	Sympathomedullary
SEM	Standard Error of the Mean
SNP	Single Nucleotide Polymorphism
SNX	Sorting Nexin
U	
uCMS	unpredictable Chronic Mild Stress
V	
V	Volt
Vps	Vacuolar protein sorting
W	
WB	Western Blot
WHO	World Health Organization
WT	Wild-type
Y	
Y-Maze	Two-Trial Place Recognition Test in the Y-Maze

LIST OF FIGURES

LIST OF TABLES

INTRODUCTION

In developed societies, NEURODEGENERATIVE and NEUROPSYCHIATRIC disorders are socio-economical burdens of great concern with major implications and devastating consequences in individual's well-being and society overall. Most of these pathologies arise from extended human life expectancy and worldwide population aging, but also from environmental challenges that are increasingly present in our daily lives (Peña-bautista, Casas-fernández, Vento, Baquero, & Cháfer-pericás, 2020). Mental and psychiatric disorders manifest in different forms through the individuals, nonetheless are generally characterized by a combination of abnormal thoughts, perceptions, emotions and behaviors (WHO 2019). According to the World Health Organization (WHO), depression is one of the main causes of disability worldwide and it is estimated that approximately 264 million people are affected by depression globally (WHO 2019). Individuals suffering from this disorder usually describe sadness, loss of interest, disturbed sleep, poor concentration and physical complaints as main clinical symptoms that impair their personal and social lives.

Recently, it has become evident that stress, a ubiquitous aspect of everyday life, is a major risk factor for the development of these brain disorders (Mcewen, 2004). In fact, stress exposure potentiates neurodegeneration and is linked to the onset of several neuropsychiatric disorders, such as depression and anxiety, as well as neurodegenerative disorders, including Alzheimer's disease, Parkinson's disease, among others (Peña-bautista et al., 2020). Curiously, many studies describe an association between stress, aging and cognitive decline (Miller & Callaghan, 2005), suggesting that aging and stress may share common cellular mechanisms (Tatar, Tatar, Bartke, & Antebi, 2003). In addition to emotional and cognitive impairments and synaptic malfunction, endocytic dysregulation is also a hallmark of neurodegeneration that strongly correlates with the development of stress-associated pathologies. As follows it is crucial to understand the molecular mechanisms underlying the behavioral and functional impairments in stress-related pathologies.

1. Stress and the brain network

The constant evolution of the modern world has challenged the population with more demanding and performance-oriented societies. Particularly, stress exposure appears to be increasing in our daily lives influencing every aspect of our body and brain. Stress can be perceived at different dimensions and has major influence upon mood, behavior and overall health. Life time exposure to intense stressors increases the risk for structural changes in the central nervous system (CNS) precipitating anxiety and mood disorders, impulsive aggression, immune dysfunction, medical morbidity and early death (Schneiderman, Ironson, & Siegel, 2005).

The term stressor can be defined as any endogenous or exogenous challenge that is perceived as unpleasant, aversive or threatening and that activates a coordinated response with the goal of re-establishing homeostasis (Lucassen et al., 2014). In fact, the nature of different types of stressors (physical or physiological) requires engagement of distinct neuronal networks, which may overlap at some instances. Stimuli that causes disturbances on the physiological status that overwhelm the organism, e.g. hemorrhage, infection or inflammation, are considered physical stressors. On the other hand, physiological stressors are generally defined as uncontrollable stimuli that threaten the homeostatic state and include the perception of physical threat, e.g. aversive environmental stimuli, predator-related cues and failure to satisfy internal drives. These type of stressors usually elicit both physical and cognitive stress responses (Godoy, Rossignoli, Delfino-pereira, Garcia-Cairasco, & Umeoka, 2018). The processes that underlie the stress response are termed 'allostasis' and whenever this response is inadequate or excessive, consequently leading to incapability to reinstate homeostasis, we face a condition termed allostatic load (Kloet, Joëls, & Holsboer, 2005). Given that, stress is regarded as a major environmental element of susceptibility for mood disorders (Calabrese, Molteni, Racagni, & Riva, 2009), contributing to several disabilities and imposing severe socio-economical burdens (Lucassen et al., 2014). Stressful life experiences can impact on a variety of physiological systems, including the central nervous system, the peripheral nervous system (PNS), the cardiac system and the immune system (Kemeny, 2003).

1.1. Mediators of the stress response

The complexity of the stress response is not restricted to neuroanatomy or mediator molecules, but also diverge according to timing and duration of stressor exposure (Godoy et al., 2018). The body responds in different ways to short-term stress and long-term stress following a pattern syndrome known as the general adaptation syndrome (GAS). On the first phase of GAS, also considered "the alarm reaction", the stress response is mediated by epinephrine and norepinephrine via the sympathomedullary (SAM) pathway and their function is to prepare the body for extreme physical activity. Once this stress is relieved, the body quickly returns to normal. However, if the stress continues for a long period of time, the body adapts to the stress in a second phase called "the phase of resilience". This phase is mediated by glucocorticoid (GC) hormones released as a result of signals from the hypothalamic-pituitary-adrenal (HPA) axis (Lucassen et al., 2014) (figure 1). The mediators of the stress response will be described in more detail in the following sections.

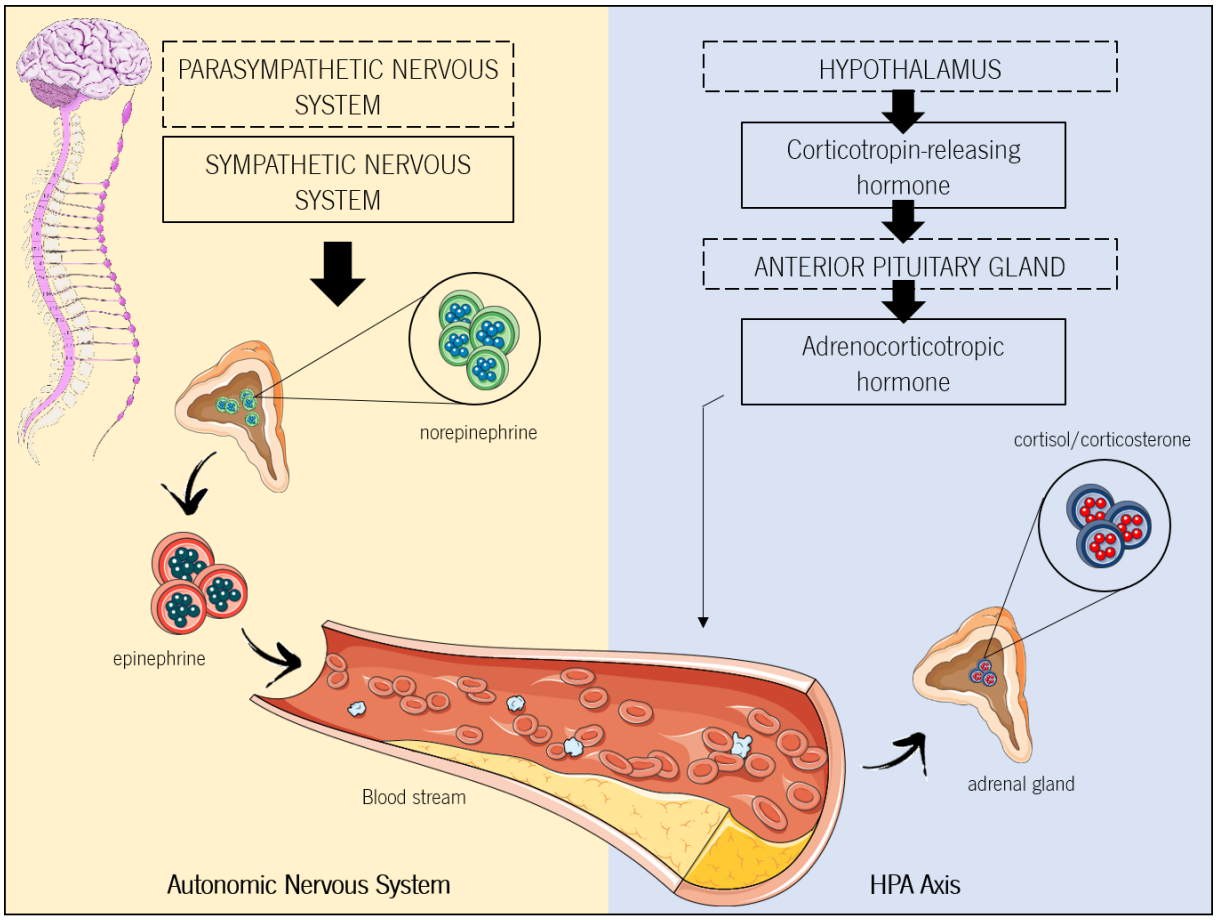

Figure 1 – Mediators of the stress response. Schematic representation of the association between the autonomic nervous system (ANS) and the hypothalamic-pituitary-adrenal (HPA) axis when exposed to stress. **Autonomic Nervous System.** Fibers of the sympathetic nervous system release the neurotransmitter norepinephrine that causes the release of epinephrine into the blood stream. **Hypothalamic-Pituitary-Adrenal Axis.** The activation of the HPA axis leads to an integrated response between the hypothalamus, causing the release of corticotropin-releasing hormone, and the pituitary gland, leading to the release of adrenocorticotropic hormone into the blood stream. This hormone travels to the adrenal gland and causes the adrenal cortex to release glucocorticoids, cortisol (humans) or corticosterone (rodents).

1.1.1. The Autonomic Nervous System and the SAM pathway

Earlier work developed by Walter Cannon in the XX century on the fight-or-flight response, a near-instantaneous sequence of hormonal changes and physiological responses that helps in the decision of fighting the threat off or flee to safety, revealed the release of the hormone epinephrine from the adrenal medulla in exposure to emergency situations (Cannon, 1929). This effect was shown to be accomplished by the activity of the autonomic nervous system (ANS) (Mccorry, 2007). Two different systems of the ANS are required to respond to physical threats: the parasympathetic nervous system, responsible for controlling involuntary resting functions, and the sympathetic nervous system, crucial in

the response of threatening situations and responsible for increases in involuntary processes (e.g. heart rate and respiration). In case of encounter with a potential armful situation, the adrenal medulla is stimulated and secretes the amine hormones norepinephrine and epinephrine into the blood stream (Kemeny, 2003). The stimulation of the medulla and consequent release of epinephrine is controlled by the SAM pathway through impulses from the hypothalamus via neurons from the thoracic spinal cord. Several researchers have demonstrated that exposure to different stressors (e.g. being confronted with a predator) can activate this system leading to an increase in the output of norepinephrine and epinephrine, as well as an increase in autonomic indicators of sympathetic arousal (e.g. increased heart rate, blood pressure and respiration; constricted muscle vasculature; increased peripheral vascular resistance) (Lucassen et al., 2014; Ziegler, 2012). The activation of this system occurs within seconds and results in the "adrenaline rush" that occurs after encounter with an unexpected threat (Mccorry, 2007).

1.1.2. The Hypothalamic-Pituitary-Adrenal axis

Following the first phase of the stress response, a second phase occurs with the activation of the HPA axis. In this classic neuroendocrine circuit, the magnitude and specificity of an individual's behavioral, neural and hormonal responses to stress is determined by limbic and hypothalamic brain structures that together coordinate emotional, cognitive neuroendocrine and autonomic inputs. At this phase there is a subacute increase in the levels of cortisol in the body fluids, including blood, saliva and urine (D. Y. Lee, Kim, & Choi, 2015). A stressful stimulus triggers an integrated response in the paraventricular nucleus of the hypothalamus resulting in the release of corticotropin-releasing hormone (CRH). This hormone stimulates the anterior part of the pituitary gland to release adrenocorticotropic hormone (ACTH), which then travels to the blood stream to the adrenal glands and stimulates the release of glucocorticoids in the adrenal cortex (cortisol in humans and corticosterone in rodents) (Kemeny, 2003). The GC hormones generally act in a slow manner as transcriptional regulators of glucocorticoid responsive genes, and as such activation of this system occurs over minutes rather than seconds (Lucassen et al., 2014) (Herman, Mcklveen, Ghosal, Kopp, & Wulsin, 2016). Regulation of this process occurs through negative feedback loop after GC binding to high-affinity mineralocorticoid receptors (MR) and lower affinity glucocorticoid receptors (GR). At low levels of glucocorticoids in the blood, the high affinity to the MRs instigates them to bind, which is thought to be critical in the glucocorticoid signaling processes (e.g., monitoring basal secretion by the circadian cycle). Just when

the circulating concentration of glucocorticoid is elevated (e.g. in a stressful event), it binds to the GRs that induce the decrease of ACTH release from the anterior pituitary and consequently reduce glucocorticoids production. This feedback loop is an important mechanism to timely regulate responses to stress. However, if stress is perceived in a chronic manner (chronic stress), it may cause pronounced long-lasting alterations in both baseline and on-demand HPA function, such as hypersecretion of corticosterone, ACTH and prolactin. Moreover, HPA responsive organs also undergo evident somatic changes. For example, hyperstimulation of the adrenal gland from repeated exposure to ACTH induces hyperplasia and increased sympathetic drive. In addition, glucocorticoid-sensitive immune organs, such as the thymus, undergo accelerated cell death and involution, favoring increased glucocorticoid release (Herman et al., 2016). On the other hand, repeated exposure to the same stressor ("homotypic" stressor) can result in habituation of the HPA axis response, characterized by a long-term decrease in glucocorticoid response. Ultimately, a more prolonged exposure to a stressful event can lead to negative consequences that adversely affect the immune, cardiovascular, neuroendocrine and central nervous system.

1.2. Impact of stress on physiology

An adequate stress response requires an interplay between a variety of complex systems, such as the CNS, the endocrine system and the immune system, that act together to reinsure the homeostasis of the organism. Nevertheless, as in the CNS, stressful life events dysregulate other organic systems, including the cardiovascular and the immune systems, among others (Pruett, 2003).

The relationship between stress and the immune system has been considered for decades. The prevailing opinion between the association of stress and the immune system has been that people under stress are more likely to have an impaired immune system and, as a result, suffer from more frequent illness. Studies have shown that stress mediators can pass through the blood-brain barrier (BBB) and exert their effects on the immune system (Yaribeygi, Panahi, Sahraei, & Johnston, 2017). For instance, cortisol, a hormone released by the mediators of the stress response, can inhibit the production of anti-inflammatory cytokines and suppress some immune functions (Seiler, Fagundes, & Christian, 2019). Moreover, recent findings have demonstrated a direct pathway between inflammation and depression, in which depression facilitates inflammatory responses and inflammation promotes depression. Elevated inflammatory signaling, a consequence of chronic stress exposure, dysregulates neurotransmitter metabolism, impairs neuronal health and alters neuronal activity in mood-relevant brain regions (Kiecolt-Glaser, Derry, & Fagundes, 2015; Slavich & Irwin, 2014). In fact, inflammation also impairs neuronal growth and survival through oxidative damage of glial cells in key regions, such as the prefrontal cortex and amygdala (Leonard & Maes, 2012).

Additionally, stress, whether acute or chronic, also has deleterious effects on the function of the cardiovascular system. Upon the activation of the sympathetic nervous system, the initial effect of stress on heart function is usually increased heart rate followed by increased strength of contraction, vasodilation in the arteries of skeletal muscles, contraction of the arteries in the spleen and kidneys and decreased sodium excretion by the kidneys. Vasoconstriction mediates an increase in blood pressure and may precipitate arrhythmias and subsequent myocardial infarction (Yaribeygi et al., 2017).

1.3. Stress as a trigger for brain pathology

The effects of stress in the brain involve a complex network and occur in a multimodal fashion. Particularly, the effects of stress on brain function depend on the timing and duration of the adverse experience (Calabrese et al., 2009). While stress responses are important for maintenance of homeostasis and preservation of mental and physical health, more prolonged stress exposure may become deleterious for the brain. In fact, stress was shown to be associated with the etiology of mood disorders and depressive episodes, which result from maladaptive changes occurring in the brain, namely through alterations in neuronal plasticity (Kloet et al., 2005). Indeed the expression of neurotrophic molecules, such as the neurotrophin BDNF, is reduced in patients with these pathologies as well as in experimental animals exposed to adverse experiences at early stages of life or adulthood (Calabrese et al., 2009). Depressed patients also present elevation of cortisol levels that strongly correlates with brain as well as other systemic pathologies. Evidence for the effect of cortisol in such organs is supported by Cushing disease, a primary gland disease, in which autonomous production of glucocorticoids causes hippocampal atrophy, white mater intensities and cognitive impairment (Brown, Varghese, & Mcewen, 2004) (Chen, Zhang, Tan, Li, & Yu, 2020). Furthermore, chronic stress and high glucocorticoids levels were also demonstrated to have an impact in the neuronal population of the hippocampus and prefrontal cortex with significant decreases in the total length and number of spines in the apical dendrites (Cerqueira, Taipa, & Uylings, 2007; Sotiropoulos et al., 2008) .

Moreover, recent evidence suggests a causal role for stress in the onset and progression of Alzheimer's disease pathology. From a critical analysis of the available data, the picture that emerges is that stress promotes AD-related pathogenesis. Particularly, exposure to stress increases the expression of Amyloid Precursor Protein (APP) and the generation and accumulation of amyloid-beta (Aβ) peptides in plaques, a pathological hallmark of AD (Justice, 2018). Stress also accelerates loss in cognitive performance in AD animal models (Big Han et al., 2017; Bing Han et al., 2016).

Overall, stress exposure activates a network of tightly-interconnect brain areas that together with alterations in the levels of GC and are subject to several structural and synaptic deficits.

1.3.1. Acute stress exposure

Acute stress is defined as a single exposure to a stressor (e.g. an argument with a loved one, someone breaking into your house), limited in time, without cycles of recovery or re-exposure, which are often novel and unpredictable (Kirby et al., 2013). In fact, exposure to acute stressors can, in some circumstances, improve memory formation and cognitive flexibility. This phenomenon is explained by the inverted U function model. This model states that brief or moderate stressors can actually enhance neural function, while severe and prolonged stressors are detrimental for the brain (Lupien & McEwen, 1997) and is able to explain the variable consequences of stress for the healthy brain. Although the individual susceptibility threshold to environmental challenges may be genetically determined, the consequences of the stress response rely on the perception of an individual to a stressor. For example, Posttraumatic Stress Disorders (PTSD), a prevalent anxiety disorder, typically follows an acute psychological traumatic event and has deleterious effects to the organism. Interestingly, behavioral studies in rodents focusing on the memory functions of the hippocampus have demonstrated that moderate stress enhances memory performance, yet more severe stress impairs it (Conrad, Lupien, & Mcewen, 1999).

1.3.2. Chronic stress exposure

On the other hand, chronic stress exposure can become maladaptive and lead to deleterious consequences, including neurodegeneration (Mcewen, 2004). The effects of chronic stress in the nervous system are elevation of the glucocorticoid levels and dysregulation of the HPA axis, reduced proliferation and survival of newborn cells and cognitive and emotional impairment (Kirby & Kaufer, 2010; Mirescu & Gould, 2006). A model widely used by researchers to understand the pathologic effects of chronic stress exposure is the unpredictable chronic mild stress (uCMS) paradigm. This model is reported to induce a depressive-like state characterized by anhedonia and apathy, along with anxious-like behavior and cognitive dysfunction (Nollet, Guisquet, & Belzung, 2013).

1.3.3. The chronic mild stress protocol

The chronic mild stress protocol (CMS) was first described by Katz and colleagues in the early 1980s to assess the effects of stress and antidepressant drugs in behavioral changes (Katz & Hersh, 1981; Katz, Roth, & Carrol, 1981) and since validated as a model of stress-induced anhedonia and extensively used to study depression in several preclinical models (Willner, 2017b). The CMS stress paradigm is known to induce depressive-like behavior, an anxiety- and anhedonic-like phenotype and cognitive deficits (Willner, 2017b) and consists in a chronically, random and variable exposure to unpredictable mild stressors, including confinement to a restricted place, shaking in a container, placement in a tilted cage or overcrowded environment, housing on a damp bedding, exposure to stroboscopic lights or dark room and reversed light/dark cycle, over a period of weeks (Willner, 2017a). Nevertheless, the CMS model is susceptible to individual differences caused by strain variability, genomic manipulations and natural variations, which collectively reflect in distinct extent of anxiety- and depression-like phenotypes in different backgrounds (Willner, 2017b). For example, the C57BL/6 strain is considered to be the most resilient strain, in opposition to BALB/c strain, considered to be more susceptible (Farley, Dumas, Mestikawy, & Giros, 2012). Interestingly, inter-individual variability in susceptibility to stress was also observed within inbred strains. For instance, C57BL/6J mice subjected to chronic social defeat can be separated into susceptible and unsusceptible individuals based on their social interaction scores (Ebner & Singewald, 2017; Razzoli, Carboni, Andreoli, Ballottari, & Arban, 2011).

2. Protein homeostasis

Protein homeostasis is an essential for cellular survival and a large number of human diseases arise from proteostasis network disruptions. In fact, many observations support proteostasis dysregulation as a pivotal feature of neurodegenerative diseases in particular. Under normal conditions, the proteostasis network sense and rectify disturbances in the proteome to restore basal homeostasis. Nevertheless, despite the robustness and adaptability of the proteostasis network, proteostatic balance is challenged in the presence of chronic stressors, culminating in the development of proteotoxicity (Kaushik & Cuervo, 2015). Protein homeostasis is thus a balanced and dynamic network of interconnected processes tightly regulated by a series of quality control mechanisms (synthesis, folding, trafficking and clearance of proteins) that act together to ensure proteome stability (Sin & Nollen, 2015), crucial to cellular survival, particularly in neurons.

The neuronal proteome requires robust intracellular trafficking machinery and quality control mechanisms to support the long-term viability and functionality of neurons (Y. Wang, Lauwers, & Verstreken, 2017). Neurons are extremely large and active cells that have to sustain their activity for the entire lifespan of an individual. Their large size imposes significant challenges for regulating transport of membrane components, both from the biosynthetic pathway to deliver membrane proteins to their correct locations, as well as for removing membrane proteins from the surface and transporting them to new sites or to degrade them via the endolysosomal system (Winckler et al., 2018). Several players are involved in the maintenance of proteostasis, namely chaperones and two proteolytic systems: the ubiquitin-proteasome system and lysosome-autophagy system (Kaushik & Cuervo, 2015).

Besides, transcription factors, chromatin remodelers, structural components, signaling pathways, metabolic factors, regulators of post-translational modifications and stress response pathways are also critical to the protein homeostasis network function (Walter & Ron, 2011). An enormous amount of human diseases are caused by impairments of the proteostasis network, such as cancer, immunological and metabolic diseases and neurodegenerative diseases (Morimoto, Driessen, Hegde, & Langer, 2011). In fact, loss of proteostasis is common to late-onset neurodegenerative diseases such as Alzheimer's disease or Parkinson's disease, which are potentiated by stress exposure. These pathologies are histologically characterized by misfolding and accumulation of specific disease-related proteins in insoluble inclusions or aggregates (Douglas & Dillin, 2010), namely Aβ and tau, and alpha-synuclein, respectively, which ultimately lead to synaptic and cellular dysfunction (Sin & Nollen, 2015).

Given the challenges in regulating intracellular trafficking and proteostasis, it is not surprising that defects in these processes have been implicated in the pathogenesis of major neurodegenerative diseases. Particularly, members of the vacuolar protein sorting (VPS) 10 family of receptors and components of the retromer complex (VPS35 and VPS26) have been linked to multiple neurodegenerative diseases (Lane, George-hyslop, Hempstead, Small, & Strittmatter, 2012). The retromer complex is a protein complex that plays a central role in sorting endosomal cargo back to the cell surface for reuse, to the trans-Golgi network (TGN), or to specialized endomembrane compartments and its dysfunction has been linked to many neurological disorders, such as Alzheimer's and Parkinson's diseases, among others (C. Li, Zahid, Shah, Zhao, & Yang, 2016). This complex contains two sub-complexes: the cargo selective complex (VPS26, VPS29, VPS35) responsible for the interaction with the protein cargoes, and the Sorting Nexins (SNXs) BAR membrane-associated complex of proteins which directs the cargoes to the membranes of the endosomal system (C. Li et al., 2016).

3. Sorting Nexins family: regulators of the membrane trafficking

The Sorting Nexins (SNXs) family was firstly discovered in 1996 when Gordon Gill isolated the mammalian sorting nexin-1, using a yeast two-hybrid screen designed to identify proteins binding to the epidermal growth factor receptor (EGFR) (Kurten, Cadena, & Gill, 1996). Sorting Nexins have been identified across phyla, from yeast to mammals, and at present have been described 10 yeast and 33 mammalian sorting nexins (figure 2)(Cullen, 2008; Gallon & Cullen, 2015).

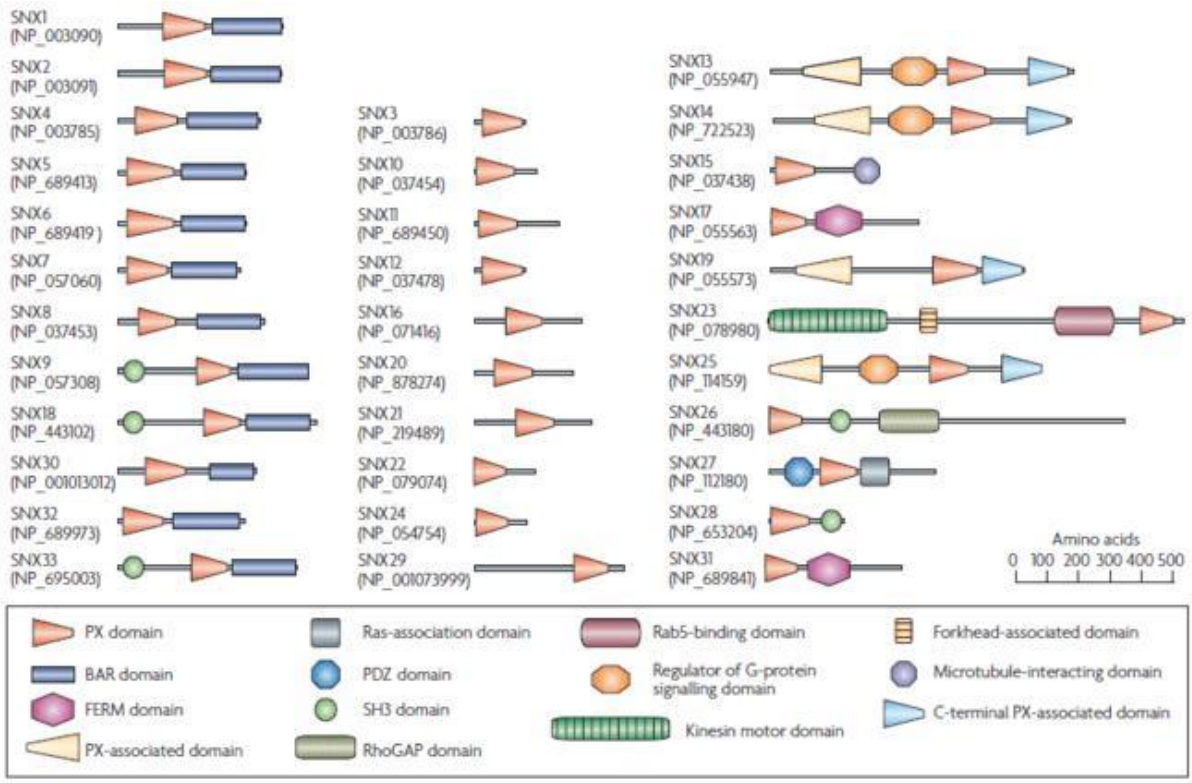

Figure 2 – Architecture of the mammalian sorting nexins predicted domains. The predicted domains of the 33 mammalian sorting nexins are represented. The sorting nexins family is divided in three different subfamilies: those containing a C-terminal BAR (Bin, amphiphysin, Rvs) domain in addition to the SNX-PX domain (on the left); those containing only a SNX-PX domain (middle group); and those containing other recognized domain in addition to the SNX-PX domain, many of which are involved in cell signaling: FERM (protein 4.1, ezrin, radixin, moesin); PDZ (PSD-95/disks large/zonula occludens); Discs-large, Zona-occludens-1; RhoGAP (Rho GTPase-activating protein); SH3 (Src-homology-3) (on the right). Adapted from Cullen 2008.

Sorting Nexins have emerged over the years as a distinct family of cytoplasmic and membrane-associated proteins with function in diverse cellular processes, including endocytosis, endosomal sorting and signaling (figure 3) (Teasdale & Collins, 2012) and can be divided into five subfamilies according to their members' domain organization: the SNX-PX only, SNX-BAR (Bin/Amphiphysin/Rvs) ,

SNX-FERM (protein 4.1/ezrin/radixin/moesin), SNX-PXA-RGS-PXC (Gallon & Cullen, 2015). SNXs are characterized by the presence of a particular type of phox-homology domain – the SNX-PX domain. The PX domain binds to phosphatidylinositols (PIs), mostly to phosphatidylinositol-3-monophosphate (PtdIns3P), therefore most SNXs are associated with PtdIns3P-enriched elements of the early endocytic network (Cullen, 2008; Teasdale & Collins, 2012). Nevertheless, SNXs have other binding motifs that makes them essential for targeting protein cargoes to different cellular compartments, and thus for proper cell functioning. The BAR domain, for example, is responsible for targeting to high-curvature membranes and phosphoinositide-containing subdomains of the early endocytic network, due to membrane-binding properties common of all SNXs. Over the years, several authors have demonstrated a role for SNXs in nervous system homeostasis regulation being associated with neurodevelopment and neurodegeneration processes. In fact, several SNXs were described to be brain-enriched and thus being associated with pathologies that affect the brain, namely with AD and DS.

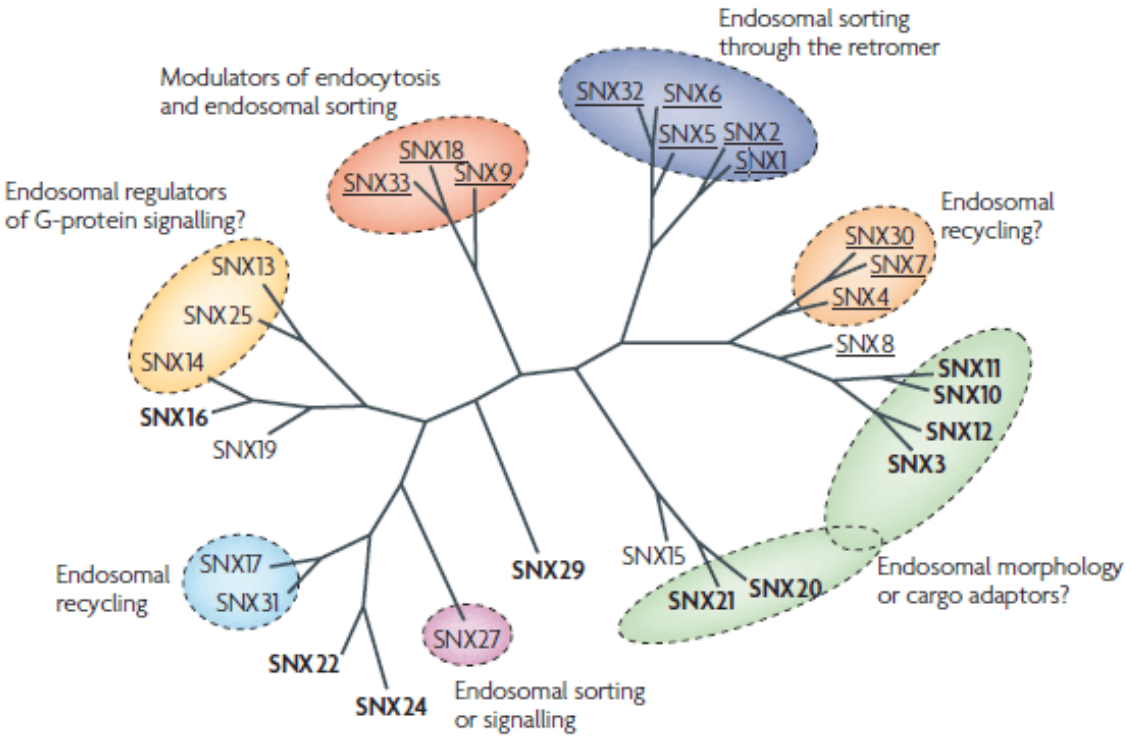

Figure 3 – Phylogenetic analysis of the mammalian sorting nexins based on their amino-acid sequences. The sorting nexins family was divided in different groups according to their biological functions. SNX-BAR (Bin, amphiphysin, Rvs) proteins are indicated in underlined text and SNX-PX (phox-homology) proteins are indicated in bold text. SNX1, SNX2, SNX5, SNX6 and SNX32 have a role in retromer function. SNX4 exists in a complex with SNX41 and SNX42 and regulates cargo recycling. SNX3, SNX10, SNX11, SNX12, SNX20 and SNX21 are grouped together because their manipulation leads to an alteration in endosomal morphology. SNX27 has a role in endosomal sorting and signaling. SNX17 and SNX31 have a similar role in regulating endosomal sorting of various cargo. SNX13 has been suggested to regulate endosomal heterotrimeric G-protein signaling. Recent data on SNX9 have highlighted that SNX18 and SNX33 might also function in endocytosis and endosomal sorting. Adapted from Cullen 2008.

3.1. Sorting nexins in (neuro)development

The formation of the mammalian CNS occurs during the early stages of development and requires the proper formation of precise circuits to function correctly (Mcallister, 2007). Particularly, in the mouse nervous system, the early postnatal period includes important steps of brain growth such as myelination, gliogenesis, apoptosis, and the appearance of most sensory and motor abilities (Hill, Lim, & Stone, 2008). Genetic defects such as those occurring in Down's syndrome, Rett syndrome or mental retardation culminate in different neurodevelopmental pathologies (Berger-sweeney, Ricceri, & Branchi, 2003), characterized by motor impairments and cognitive deficits. Therefore, comprehension of developmental processes during prenatal and postnatal periods of mice development is essential.

Several SNXs have been implicated in development. For example, SNX1 and SNX2 genetic ablation has been shown to arrest midgestation indicating that these sorting nexins are fundamental during the early developmental stages (Schwarz, Griffin, Schneider, Yee, & Magnuson, 2002). Similar to $SNX1^{-/-}$ $SNX2^{-/-}$ embryos, a knockout for SNX13 displayed comparable defects and phenotype. Targeted disruption of the SNX13 gene resulted in embryonic lethality, growth retardation and, in particular, abnormities in the yolk-sac endoderm (Zheng et al., 2006). Moreover, studies from our laboratory using a *Caenorhabditis elegans* model indicated that the SNX3/12 homolog gene plays a crucial role in the nervous system, as SNX3 KO worms showed impairments in neurodevelopment, neuronal wiring, and behavioral performance, as well as reduced stress tolerance (Vieira et al., 2017). Studies conducted in Drosophila mutants have reported SNX3 as an essential molecule for Wg secretion. Particularly, mutants of this SNX show marked defects in Wg secretion and its signaling activity suggesting that SNX3 acts as a cargo-specific component of retromer and is required for endocytic recycling of Wg/Wnt secretion (P. Zhang, Wu, Belenkaya, & Lin, 2011). Others SNXs were also reported to have a role in development, such as SNX14, SNX8 and SNX6, however their exact association remains to be fully verified.

SNX27, another retromer-associated protein, was previously demonstrated to have a role during embryonic development. Moreover, $SNX27^{-/-}$ mice presented decreased body weight compared to $SNX27^{+/+}$ or $SNX27^{+/-}$ animals and severe growth retardation, including multiple organ malformations (spleen, kidney, liver, heart, and intestine) during postnatal development (Cai, Loo, Atlashkin, Hanson, & Hong, 2011). Although most $SNX27^{-/-}$ mice survived at birth, they failed to thrive beyond P14 (Cai et al., 2011; X. Wang et al., 2013a) supporting the relevance of SNX27 for development and survival. Brain development during early postnatal period involves increases in dendritic branching and synapse formation, however in homozygous mice all these structures were severely compromised, as well as the total dendritic lengths of both cortical layer 5 and hippocampal CA1 neurons. Furthermore, histological examination of the same brains revealed neurodegeneration in the cortex at P14, reduced somal size, hyperchromicity and a marked decrease in dendritic branching (X. Wang et al., 2013a). While SNX27 was associated with epilepsy, patients with SNX27 variants display seizures, developmental delay, behavioral disturbance and subcortical brain abnormalities (Parente et al., 2020). Taken together, the present results indicate a role for sorting nexins in embryonic development, postnatal growth and neuronal function.

3.2. Sorting nexins in neurodegeneration

The prevalence of neurodegenerative disorders is increasing due in part to extensions in lifespan, with a profound impact in public health. Neurodegenerative diseases are debilitating conditions as a result of progressive degeneration of neuronal cells, impairing movement (e.g. ataxias) and superior cognitive functions (e.g. dementias). Dementias are responsible for the greatest burden of neurodegenerative diseases, with Alzheimer's representing approximately 60-70% of dementia cases.

Alzheimer's disease (AD) is characterized by memory loss and cognitive impairments (H. Zhang, Huang, Hong, Yang, & Zhang, 2018). Amyloid β (Aβ) deposition and hyperphosphorylation and aggregation of the cytoskeletal protein TAU are well-known hallmarks of this pathology (C. Li et al., 2016; Sotiropoulos et al., 2011; Takashima, Wolozin, & Buee, 2019). Aβ is generated via the amyloidogenic pathway through sequential proteolytic cleavage of amyloid precursor protein (APP) by two amyloidogenic proteases, the β- and γ-secretases. This pathway can be modulated by the retromer complex which transports APP to the cell surface and from endosomes to the Golgi complex where APP dissociates from β-secretase and therefore halts amyloidogenic processing. Interestingly, multiple SNXs are also involved in intracellular transport of APP and APP-cleavage secretases, thus affecting APP amyloidogenic and non-amyloidogenic pathways. SNX27, as previously described (C. Li et al., 2016), is a unique member of the SNXs family as it exclusively contains a PDZ (postsynaptic density 95/disc large/zona occludens) and a FERM domain, serving as an early-endosome-associated cargo adaptor for endosomal sorting of various transmembrane proteins, including β2-adrenergic receptor (Temkin et al., 2011), glucose transporter GLUT1 (Kvainickas et al., 2016) and AD-related proteins, such as γ-secretase and APP (Huang et al., 2016; X. Wang et al., 2014). A proteomic analysis indicated that cell surface APP levels are reduced in SNX27-depleted cells, suggesting that SNX27 is required for cell surface APP distribution (H. Zhang et al., 2018). In fact, a recent study in HEK293T cells shows that SNX7 decreases sAPPβ and Aβ production by modulating cell surface APP levels (Xu, Zhang, & Brodin, 2017).

Interestingly, SNX27 was proven to interact with AMPA (α-amino-3-hydrozy-5-methylisoxa-zole-4-propionic acid) receptors and to be a key regulator of cognitive processing. SNX27-PDZ domain makes it of particular interest for synaptic protein recycling since it is responsible for recognizing short amino acids motifs found at the C terminal of many synaptic targets (X. Wang et al., 2014) and allows SNX27 to interact with many neuronal receptors, such as NMDA (N-methyl-D-aspartate) and AMPA receptors, regulating their recycling to the plasma membrane. A study developed in a Down's syndrome mouse

model revealed that reduced expression of SNX27 causes redirection of NMDA and AMPA receptors for degradation that consequently affects long-term potentiation (LTP) and leads to impairments in learning and memory (X. Wang et al., 2013a). LTP and long-term depression (LTD) are two different forms of synaptic plasticity in the central nervous system. Recent studies indicate that LTP and LTD expression can be modulated by AMPA receptor function. The regulation of AMPA receptor function occurs through two distinct mechanisms: modulation of ion channel properties of the receptor and regulation of the synaptic targeting of the receptor (H. Lee et al., 2003).

Wang and collaborators have demonstrated a role for SNX27 as a major contributor to intellectual impairments in DS (X. Wang et al., 2013a). The study demonstrated revealed a decrease in the levels of SNX27 in both human DS brains and in Ts65Dn mouse brains, demonstrating that reduced levels of SNX27 contribute to synaptic dysfunction and cognitive deficits. Interestingly, SNX27 overexpression in Ts65Dn hippocampus rescued the cognitive and synaptic deficits. SNX27 is regulated by CCAAT/enhancer binding protein b (C/EBPb), a transcription factor downregulated in DS brains through transcriptional targeting by miR-155 encoded on triplicated chromosome 21 (X. Wang et al., 2013a). Taken together, dysregulation of a microRNA-155-C/EBPb-SNX27 pathway contributes to synaptic and cognitive impairments in DS brains. Down's syndrome pathology presents common pathological features with AD, namely amyloid plaques and tau tangles. The development of AD pathology in DS patients is probably due triplication of the APP gene that resides in chromosome 21 and results in elevated expression of APP and Aβ overproduction (Ness et al., 2012). Deficiencies in SNX27 expression is also a contributor of AD-like pathology in DS brains through directly regulating Aβ generation and inhibiting the γ-secretase complex. SNX27 depletion enhances Aβ production through modulating g-secretase activity (X. Wang et al., 2014) and APP recycling (Huang et al., 2016). Therefore, SNX27 deficiency, at least in part, contributes to Aβ accumulation and AD-like pathology in DS brains.

Besides SNX27, other SNXs have been associated with memory and neurodegenerative processes. A study realized using an APPswe/PSEN1dE9 mouse model demonstrated that overexpression of human SNX15 significantly reduces Aβ deposition in the hippocampus and improves short-term working memory (Feng, Niu, Ji, Gao, & Wen, 2015). Ablation of SNX6 was also demonstrated to cause a decrease in surface levels of AMPA receptors and lead to defects in synaptic function of CA1 pyramidal neurons and spatial memory (Niu et al., 2017). This protein was proved to be diminished in AD pathology. Furthermore, a study performed by Zhao and coworkers indicated a possible link between SNX12 and AD. They demonstrated that SNX12 is predominantly expressed in

brain tissues and SNX12 levels are significantly decreased in the human AD brains (Zhao et al., 2012). SNX3 was demonstrated to be disrupted in patients with microcephaly, microphthalmia, ectrodactyly, prognathism and mental retardation (Vervoort et al., 2002), while mutations in SNX14 were reported to be associated with intellectual disability and cerebral ataxia, indicating an essential role for SNX14 in neural development and function (Bacchelli et al., 2014).

At present, it is well-established and well-described the role of SNXs dysfunction in the pathogenesis of AD and DS. Nevertheless, many other neurodegenerative diseases, such as Parkinson's disease, Hereditary Spastic Paraplegia (HSP) or some lysosomal storage disorders, have implicated dysfunctional retromer complex and retromer-mediated trafficking (Jang, 2017; H. Zhang et al., 2018). Despite solid evidence associating SNXs with neurodegeneration, and the growing effort to functionally characterize this family, much is unknown about their precise functions in the nervous system and particularly on how they are modulated by stress and stress-related disorders.

In this thesis dissertation, using a multi-modal approach including the use of both rodent and *in vitro* models, we expect to contribute to elucidate new SNXs mechanism of action in the central nervous system and to survey the modulatory effects of stress in SNX function.

RESEARCH OBJECTIVES

Current evidence suggests a role for SNXs in nervous system regulation, being associated with distinct neurological conditions such as neurodegenerative disorders. However, the mechanisms behind SXNs impact in the CNS have not yet been fully understood. Moreover, how risk factors for neurodegenerative disorders, such as stress, modulate SNXs function at the behavioral and morphological levels remains still an unstated subject. Here, we aim to unravel the mechanisms of action of SNX27, a brain enriched protein tightly associated with nervous system regulation, as well as of other SNXs whose function is relevant for intracellular trafficking and to study the modulatory effects of stress on behavioral performance, neuronal morphology and in the subcellular localization of distinct regulators of synaptic plasticity. For such, we propose to:

1. Assess the impact of SNX27 reduced levels and/or stress exposure in the neuronal morphology of the dorsal DG region of the hippocampus, using a Golgi-Cox staining method.
2. Characterize the developmental landmarks of a $SNX27^{+/-}$ mouse model backcrossed to the C57BL/6J background.
3. Evaluate the behavioral performance of a $SNX27^{+/-}$ mouse model backcrossed to the C57BL/6J background, under control and chronic stress exposure conditions.
4. Characterize SNXs function and subcellular distribution and to study the modulatory effects of endosomal transport disruption and pharmacological stress on SNXs expression, using established neuronal-like cultures.

Overall, we aim to provide new insights of SNXs role in the CNS and pave the way to the identification of potential novel pathways of intervention to prevent/delay cognitive decline and to improve the treatment of distinct neurodegenerative diseases.

MATERIALS AND METHODS

1. Animals and housing conditions

SNX27 heterozygous ($SNX27^{+/-}$) mouse model was kindly provided by Dr. Wanjin Hong from the Institute of Molecular and Cell Biology, A*STAR, Singapore. The animals were generated by crossing heterozygous animals on a C57BL/6 and 129/SV mixed background (KO mice are not viable after P14 (X. Wang et al., 2013a)). Animals were backcrossed to the C57BL/6J background for 8 generations (bred in our animal facility) (figure 4). Mice were housed in the Life and Health Sciences Research Institute animal facility under standard environmental conditions (12h light/dark cycles (lights on from 8a.m. to 8p.m.); temperature of 22°C ± 1°C and relative humidity of 50-60%) with *ad libitum* access to food and water. All experimental procedures were carried out in accordance to EU directive 2010/63/EU and were approved by the local ethics committee (ORBEA) and the national authority for animal experimentation, Direção Geral de Alimentação e Veterinária (ID: 013051). Animals used in the developmental characterization received a toe tag at postnatal day (PND) 6 as previously described (Castelhano-Carlos, Sousa, Ohl, & Baumans, 2010), which remained unaltered throughout the experiment and allowed to evaluate each animals response in a blind manner. Animals used for the behavioral characterization received an ear tag at weaning age (P21) following the same purpose as previously mentioned.

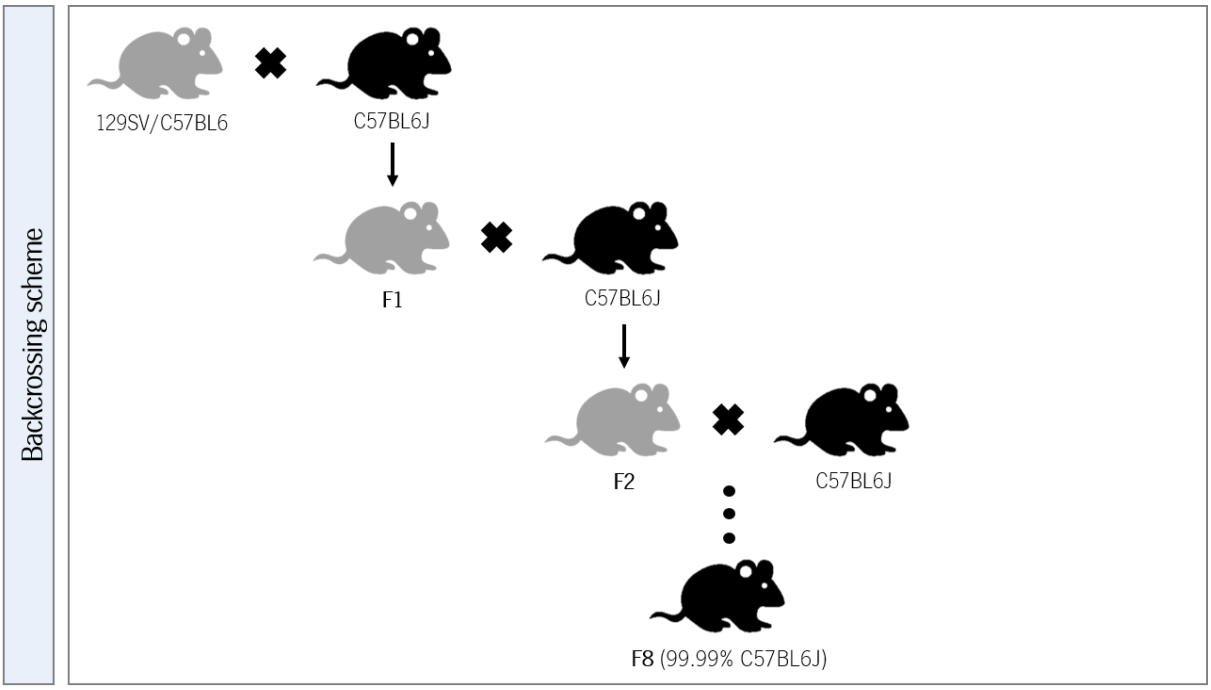

Figure 4 – Backcrossing scheme for the C57BL/6J background. Animals from a C57BL/6 and 129/SV mixed background were backcrossed to the C57BL/6J background for 8 generations following the represented schematics.

2. Animal genotyping

The collected tissue (ear/toe) was used for animal genotyping in order to distinguish wild-type (WT) and heterozygous (Het) animals. DNA was extracted from the animal tissue using the NaOH method. Briefly, animals' tissue sample was placed in 300 µL of 50mM NaOH solution and then placed at 98°C for 50 minutes. The samples were then homogenized in the vortex for 15 seconds and neutralized with 30 µL of 1M Tris solution (pH=8). Finally, samples were centrifuged for 6 minutes at 14 000 rpm and the supernatant was collected and stored at -20°C.

Polymerase chain reaction (PCR) was used to amplify DNA sequences using the following primers: KO1 – 5' AGAAATGAAGCATCGTTACCC 3'; KO2 – 5' GTTCCTGTCTCACCAGGTATAC 3'; KO3 (NEO) – 5' GGCCGCTTTTCTGGATTCATCG 3'. PCR master mix was prepared using 0,24 µL of dimethyl sulfoxide (DMSO); 7,36 µL of H_20; 1,2 µL of DreamTaq buffer 10x; 0,3 µL of each primer (KO1, KO2 and KO3) 20 µM; 0,06 µL of Dream Taq polymerase (5U/µL). 10 µL of the PCR mixture were added to 2 µL of the extracted DNA and samples were then incubated for 5 minutes at 95°C, followed by 5 cycles of 45 seconds at 95°C, 45 seconds at 56°C and 1 minute at 72°C, and then by 30 cycles of 45 seconds at 95°C, 45 seconds at 58°C and 1 minute at 72°C. Finally, samples were incubated at 72°C

for 10 minutes and left for hold at 4°C. PCR was performed using a thermal cycler (Mastercycler®, Eppendorf, Germany).

After DNA amplification, an electrophoresis was performed using a 1% (w/v) agarose gel in TAE buffer 1X (40 mM Tris, 20 mM acetic acid, 1 mM EDTA) for 30 minutes at 120mV. DNA intercalating agent Greensafe premium (Nzytech, Portugal) was used to visualize the DNA amplification products in the Bio-Rad Gel Doc EZ (Bio-Rad Laboratories, Ltd.). After gel polymerization, 6 µL of DNA loading dye (Fermentas, USA) was added to each sample and 10 µL of the samples were loaded in each well. The size of the amplified bands was determined by comparison with the molecular marker Generuler 100 bp Plus DNA Ladder (Thermo Fisher Scientific Inc.). WT animals presented a band at 229 bp whereas Het animals presented two bands at 229 and 300 bp.

3. Developmental characterization

Neonatal neurodevelopmental milestones assessment was performed according to a previously validated protocol in C57BL/6 mice (Castelhano-Carlos et al., 2010; Guerra-Gomes et al., 2020; Hill et al., 2008). Briefly, animals were evaluated for different developmental parameters on a daily basis during 21 days since the day of birth. Newborn animals were inspected for skin appearance, activity and presence of milk in the stomach, indicators of animals' wellbeing and adequate maternal care. On the day of birth, the number of pups in the litter was counted and since then animals were daily weighted and examined for the acquisition of developmental milestones throughout the neonatal period until the weaning age at PND21. This daily scoring included the assessment of maturity in different parameters such as: somatic parameters, reflexes, strength, coordination and spatial reference tests, which will be described in more detail bellow. At PND6, newborn mice were submitted to an identification procedure – the toe clipping. This procedure consists in clipping one of the toes at a portion (approximately 1/3) corresponding to the distal part of the toe (Castelhano-Carlos et al., 2010). The collected toe tissue was used for animals' genotyping.

Testing was performed at the same schedule every day, in the same experimental room, by the same researcher which was blind for animals' genotype during the execution of the protocol. Throughout the evaluation, the parameters were assessed according to the age of the pup and the score value was registered in an individual table for each animal.

3.1. Somatic Parameters

Animals body weight was registered every day from PND0 to PND21 (weight ± 0,01g), as a measure of morphological development. Anogenital distance (ANGD), corresponding to the distance between the opening of the anus and the opening of the genitalia, was registered daily since PND3 (distance ± 0,05mm). This parameter is an indicator for reproductive development and maturation. Eye opening was scored on a daily basis after an initial break in the membrane sealing was observed. The score was attributed according to the state of the eyes. Animals were continuously monitored and reached a score of 1 when one of the eyes was opened, or of 2 when both of the eyes were opened, and thus a mature response considered.

3.2. Neurological Reflexes

Neurological reflexes were evaluated since PND1 to PND21. Before the beginning of daily testing, the cages housing both the mother and the pups were taken from the housing room and moved to an experimental room. Tests were performed on a smooth foam pad, to ensure minimal disturbance of the pups, and after the evaluation, pups were immediately returned to their home cage and to the housing room. Daily score was attributed according to the absence/presence of a mature response (score 0 or 1, respectively) or according to a gradual evolution of the behavioral response. A score of 0 represented the absence of the mature response and when this was achieved a score of 3 was attributed. Neurological parameters were categorized according to the function analyzed and assessed as follows:

3.2.1. Labyrinthine reflex, coordination and strength

- Surface righting reflex – This parameter was evaluated from PND1 to PND13 and evaluates body righting and labyrinthine mechanisms. It consisted in putting the animal on its back, with its limbs pointing upwards, and the time the animal took to turn over onto its abdomen with all four paws touching the surface was scored. Complete acquisition of reflex was considered when the animal was able to get right and stand on all four limbs.

- Negative Geotaxis – This behavioral response was evaluated from PND1 to PND14 and it tests animals' labyrinth postural reaction. Animals were placed in a horizontal grid, tilted 45° to the plane,

with the head facing downwards. Time for the pup to turn 180° to the "head up" position was measured. A mature response was considered when the animal was able to turn immediately 180° and moved towards the top of the slope.

- Cliff Aversion – This parameter was evaluated from PND1 to PND14 and assesses spatial reflex and coordination. Animals were placed on the edge of a cliff, with the forepaws and face hanging over the edge, and their ability to turn and crawl away was observed.

- Postural Reflex – This reflex was assessed from PND5 until weaning age and allows for the evaluation of spatial and body righting responses. Newborns were placed in a small plastic box and gently shaken vertically and horizontally. Reflex was considered mature when the animal was able to maintain its original position in the box by extending all four limbs.

- Wire Suspension – This parameter was scored from PND5 to PND21 and assesses muscular strength. Animals were placed vertically holding a 2mm metal bar with its forelimbs. The mature response was achieved when the animal could hold its body weight alone, without falling.

- Grasping – This strength test was performed from PND5 until PND21 and assesses freeing reflex. The palm of the pups' forelimb was stimulated with a thin wire and a mature response was considered if the animal held the wire firmly.

- Air righting reflex – This response was evaluated from PND8 until weaning and it tests labyrinthine and body righting mechanisms and coordination. Mice were held on their back at approximately 13cm distance from the soft surface and released. The position upon landing on the surface was examined. The mature response was observed when the animal developed the reflex to turn his body during the fall and land on its four paws.

3.2.2. Tactile reflex

- Rooting – This test was performed from PND1 to PND12 and allows for the evaluation of mice tactile reflex and motor coordination. It consists in gently stroking a fine filament of cotton three times along the side of the head of the pup. The mature response is considered when the pup turns its head towards the filament.

- Ear Twitch – Animals' response to tactile and auditory reflex is assessed through this test. Animals' ear was stimulated by brushing the end of a cotton tip three times. If the newborn responded by flattening the ear against the side of the head, a score for mature response was attributed.

3.2.3. Auditory reflex

- Auditory startle – Newborn mice were tested for auditory reflex from PND7 to PND18. The reaction of the pup to a handclap was observed. If the animal reacts with a quick involuntary jump, a mature response was considered and a score of 1 was attributed.

3.2.4. Motor

- Walking – The development of locomotive coordination and muscular strength was evaluated by observing animals freely moving, since PND5 until weaning age. Mature walking was considered when animals were able to walk straight with the body supported completely by the four limbs, without dragging the belly over the surface.

- Open Field Traversal – This test allows the evaluation of locomotion and the extinguishing of pivoting behavior. From PND8 to PND21, the pup was placed in the center of a plastic sheet containing a circle with 13 cm of diameter. The length of time the animal takes to move out of the circle was recorded. A mature response was considered when the mouse was able to respond in less than 30 seconds.

3.2.5. Homing Test

At PND11 newborn mice were transferred to a cage containing 1/3 of shaving from their home cage and the remaining 2/3 of the cage with clean shavings (figure 5). The pups were placed in the center of the cage, facing away from the home cage shavings. The time taken to reach the home litter sawdust was recorded (3 trials). A successful trial was considered when animal's four paws effectively crossed onto the home cage shavings and each trial lasted a maximum of 150 seconds with an inter-

trial interval of approximately 10s. Here, the locomotor and olfactory capability of the pups was assessed.

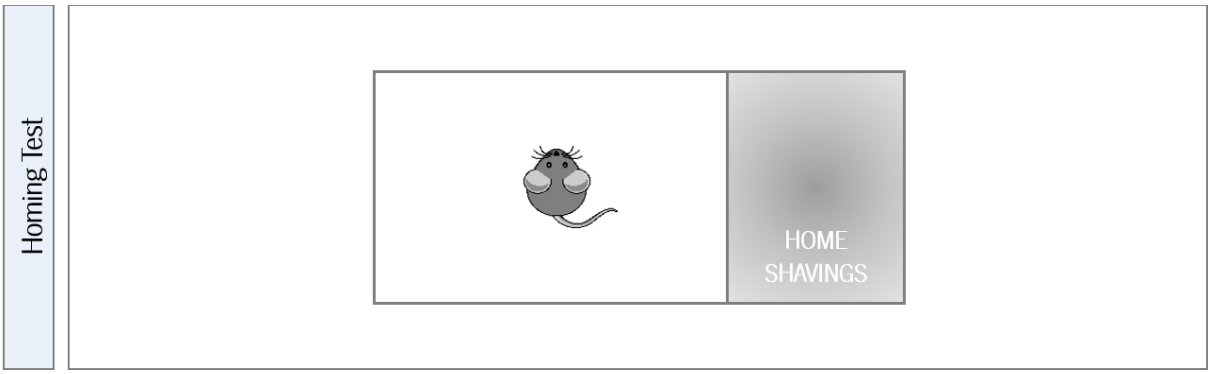

Figure 5 – Schematic representation of the laboratory apparatus used for the Homing test. 1/3 of shavings from the pups home cage (represented in grey) was added to a cage containing 2/3 of clean shavings (represented in white). The pups were placed in the center of the cage, facing away from the home cage shavings. The time taken to reach the home litter sawdust was recorded (3 trials – maximum of 150 seconds with an inter-trial interval of approximately 10s).

4. unpredictable Chronic Mild Stress (uCMS) protocol

SNX27$^{+/-}$ and WT littermate controls male mice with 3,4 months of age were subdivided in two groups: a control group (CON) and a stress-exposed group (uCMS). Approximately half of the animals were exposed to a previously validated unpredictable Chronic Mild Stress (uCMS) paradigm (Alves et al., 2017; Bessa et al., 2009; Mateus-Pinheiro et al., 2013) known to induce depressive-like behavior, an anxiety- and anhedonic-like phenotype and cognitive deficits (Willner, 2017b). This stress paradigm consists in a random, continuous and unpredictable exposure to a wide range of different mild stressors. Briefly, the uCMS protocol consisted in a daily exposure of distinct stressors (up to 3 stressors per day), such as confinement to a restricted space (50 mL falcon), shaking in a container (plastic box container), placement in a tilted cage (30º), placement in an overcrowded environment, housing on a damp bedding, exposure to stroboscopic lights, exposure to a dark room, reversed light/dark cycle for 48 hours, every 7 days for a period of 6 weeks (table 1). Animals were periodically monitored for health markers such as significant weight loss (more than 20% of the initial weight), barbering or the presence of wounds. Control animals were handled every day for a period of 2 weeks before the beginning of the behavioral characterization.

Table 1 - Representation of weekly stressors exposure during the uCMS protocol. Intensity, duration and stressors exposure were randomly assigned over the 6 weeks of the protocol. Body weight was monitored on a weekly basis at the same time period of the day.

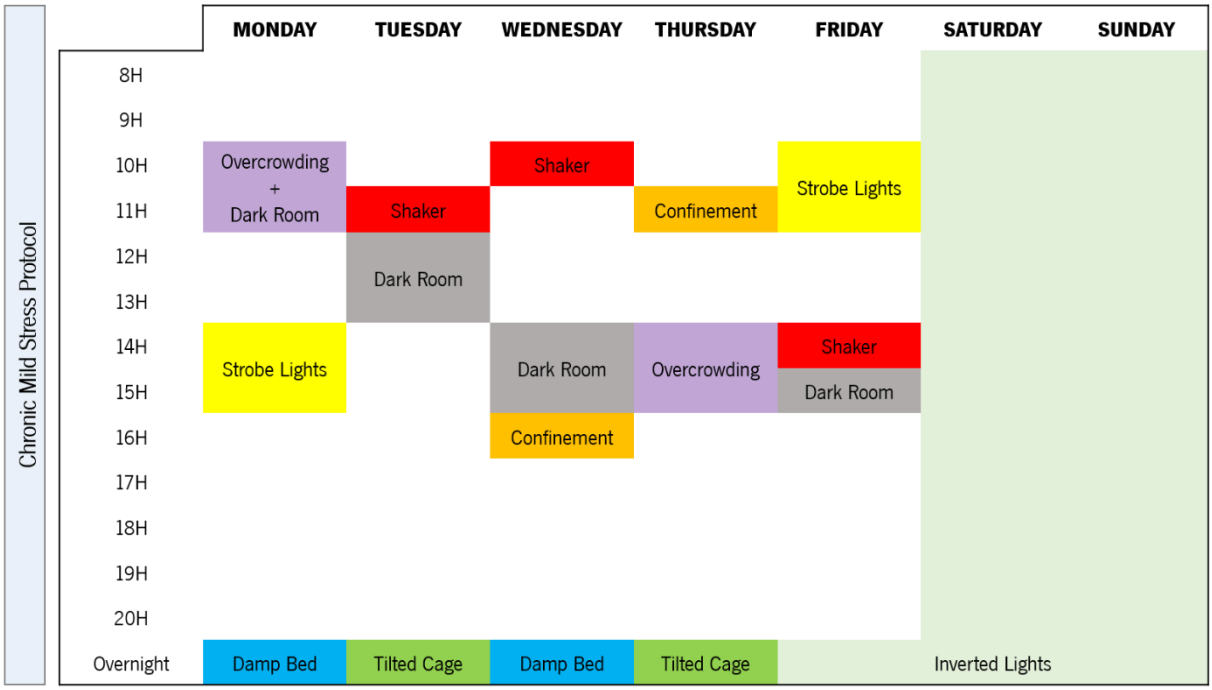

5. Corticosterone measurements

Blood serum corticosterone levels were assessed in WT and SNX27$^{+/-}$ animals, from both control and stress exposed groups, a week prior to the beginning of the uCMS protocol and after the behavioral characterization at the nadir (8a.m.) and zenith (8p.m.) phases. Blood sampling was obtained by tail tipping within a maximum of 120 seconds after the mouse was removed from its home cage. Samples were allowed to clot and the clot was then removed using a needle. Samples were then centrifuged at 14.000 rpm for 5 minutes and the supernatant (blood serum) was collected and stored at -80°C for further analysis (figure 6).

Blood serum corticosterone levels were assessed using a Corticosterone ELISA kit (ADI-901-097, Enzo Life Sciences, USA), following the manufacturer's instructions. Briefly, 5µL of each sample was added to a 96-well plate followed by 5µL of the Steroid Displacement Reagent (SDR) 1:100. Samples were then homogenized and diluted in 190µL of ELISA buffer to a final dilution of 1:40. In the meantime, corticosterone standard solutions were prepared in the same buffer (two replicas of each) and added into the appropriate wells. All samples (100µL) were plated, and then, 50µL of blue

conjugate and yellow antibody were added to each well, cover it with sealing tape and left incubate at room temperature on a plate shaker for 2 hours at ≈300rpm. After the incubation, the wells were washed three times by adding 200µL of wash solution. Between washes, the plate was tapped 4/5 times on absorbent paper towel to remove the content of the wells completely. After the final wash, 200µL of the pNpp Substrate solution was added to each well and left for incubation at room temperature for 1 hour without shaking. Immediately before reading the plate in a microplate reader at 405nm, 50µL of Stop solution was added to each well.

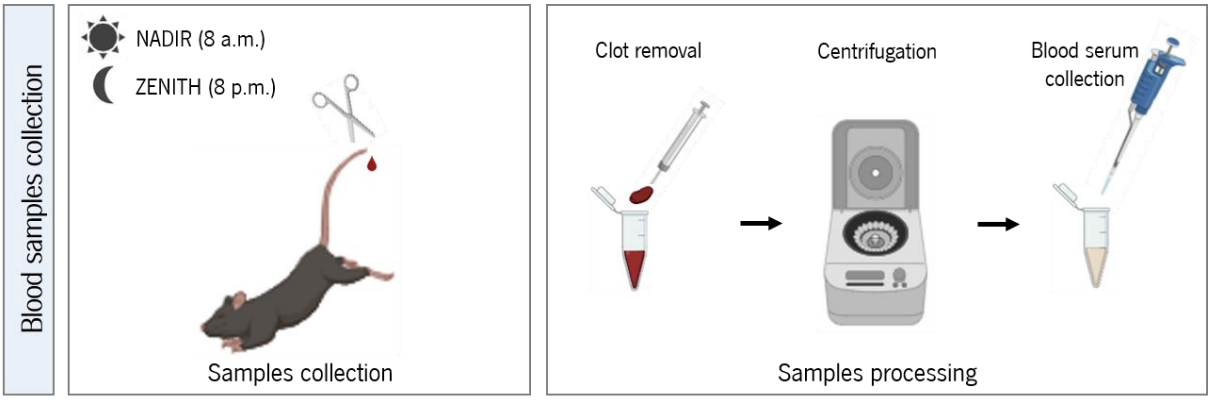

Figure 6 – Blood serum collection for measurement of corticosterone levels. Blood sampling was obtained by tail tipping within a maximum of 120 seconds after the mouse was removed from its home cage at the nadir (8 a.m.) and zenith (8 p.m.) phases. Samples were allowed to clot and the clot removed using a needle. Samples were centrifuged at 14.000 rpm for 5 minutes and the supernatant (blood serum) was collected and stored for further processing.

6. Behavioral characterization

After chronic stress exposure for a period of 6 weeks, the behavioral characterization was performed in order to evaluate different behavioral dimensions. Elevated Plus Maze (EPM), Open Field (OF), Novelty Suppressed Feeding (NSF) and Light/Dark Box Test (L/D Box) were performed to assess anxiety-like phenotypes. Forced Swim Test (FST) was conducted to assess depressive-like behavior. Novel Object Recognition Test (NORT), Two-Trial Place Recognition Test (Y-Maze) and Contextual Fear Conditioning were performed to measure cognitive behavior. All behavioral experiments were performed according to previous validated protocols and followed the order represented below. The experimental layout is represented below (figure 9).

6.1. Elevated Plus Maze

The EPM is a commonly used behavioral assay to assess anxious-like behavior in rodents (Pellow, Chopin, File, & Briley, 1985). This test relies on rodents' proclivity towards dark and enclosed spaces and their natural aversion for heights/open spaces (Walf & Frye, 2007). The EPM consists in an elevated, plus-shaped apparatus with two opposite open arms (50,8 cm x 10,2 cm) and two closed arms (50,8 cm x 10,2 cm x 40,6 cm) elevated 72,4 cm above the floor with an intersection area of 100 cm^2. Animals were placed individually in the center of the intersection area, facing an open arm and then were allowed to freely explore the maze for 5 minutes. The maze was cleaned with 10% ethanol between trials to remove any trace odors. Behavioral activity was recorded using a suspended video camera and analyzed using EthoVision XT 13.0 (Noldus Information Technology, Netherlands). The time animals spent in the open arms was taken as a measure for anxious-like behavior (Pellow et al., 1985).

6.2. Open Field

The Open Field test is a behavioral paradigm based upon the exposure of subjects to unfamiliar aversive places (Belzung & Griebel, 2001) that allows the evaluation of locomotor, anxious-like behavior and exploratory activity (Prut, Belzung, Rabelias, & Psychobiologie, 2003). The OF test uses a closed apparatus of 30,5 cm height with a highly illuminated square arena of 43,2 cm x 43,2 cm. Animals were placed individually in the center of the arena and allowed to explore it freely for 5 minutes and their movement was traced using a two 16-beam infrared system. The arena was cleaned with 10% ethanol between trials. Data was extracted using the Activity Monitor software (Med Associates, Inc., Vermont, USA), considering a central and an outer zone. Distance travelled in the arena (locomotor behavior), activity in the center of the arena (anxious-like behavior) and the vertical counts of the animals (exploratory-like behavior) were assessed.

6.3. Novelty Suppressed Feeding

The NSF test is also a conventional test used to assess anxious-like behaviors (Samuels & Hen, 2011). For the NSF test, animals were kept food deprived for 18 hours before the beginning of the trial.

For the test trial a single food pellet was placed in the center of the OF arena and the time the animal took to reach the pellet was measured, as well as the time for the first bite. The trial was concluded when the animal bit the pellet, or after 10 minutes, regardless of the absence of action. The arenas were cleaned with 10% ethanol between trials. After test completion, in order to assess appetite drive, animals were placed on a single cage with a pre-weighted food pellet. The pellet was weighted after 5, 15 and 30 minutes to measure the amount of food consumed.

6.4. Light/Dark Box

The Light/Dark Box test is one the most widely used tests to measure anxious-like behavior in mice (Serchov, Calker, & Biber, 2016). This test is based on the innate aversion of mice to brightly illuminated areas and on their spontaneous exploratory behavior in response to mild stressors as novel environments and light (Bourin & Hascoe, 2003). For this test the OF arena is equally divided into light and dark compartments connected by an entrance. Animals were placed at the center of the arena facing towards the dark compartment and were allowed to freely move between the two chambers for 10 minutes. The arenas were cleaned with 10% ethanol between trials. Data was extracted using the Activity Monitor software (Med Associates, Inc., Vermont, USA), considering a light zone and a dark zone. The distance and time animals spent in each compartment were quantified.

6.5. Forced Swim Test

The FST is a predictive validated behavioral paradigm used as a measure of depressive-like behavior (Petit-Demouliere, Chenu, & Bourin, 2005). Animals were placed in individual cylinders filled with water (24°C, 50 cm of depth) separated by a piece of paper, for 6 minutes. After 6 minutes, the animals were removed from the cylinder and placed in a warmed environment to avoid risk of hypothermia. Behavior was recorded using a video camera and immobility times analyzed using EthoVision XT 13.0 (Noldus Information Technology, Netherlands). Latency to immobility and immobility time were analyzed during the last 4 minutes of testing since the animals show more stable levels of immobility during this period (Petit-Demouliere et al., 2005). An animal was considered to be immobile when it made only necessary movements to keep its head above water (Castagn, Moser, Roux, & Porsolt, 2010).

6.6. Two-Trial Place Recognition Test

The Two-Trial Place Recognition Test in the Y-Maze was designed to evaluate spatial recognition memory, a form of episodic-like memory based on mice innate propensity to explore novel environments (Kraeuter, Guest, & Sarnyai, 2019). The apparatus was composed by three identical arms (29,5 cm x 7,5 cm x 15,5 cm) which are randomly designated starter arm, familiar arm and novel arm. Each arm contained visual cues placed in the top of the walls to increase spatial recognition and navigation. The test is divided in two trials. For the first trial, mice were allowed to explore two arms (starter arm and familiar arm) during 10 minutes. On the second trial (retrieve trial), for a period of 5 minutes, mice were allowed to freely explore the 3 arms. The two trials were separated by an inter trial interval of 1 hour in which the animals returned to their home cages (figure 7). The test was performed in dimmed light conditions and the maze was cleaned with 10% ethanol between trials. Behavioral activity was recorded with a video camera and analyzed using EthoVision XT 13.0 software (Noldus Information Technology, Netherlands). The time spent in the novel arm was analyzed and expressed as the percentage of total experiment time. The discrimination index was also calculated following the represented equation (Equation 1).

Equation 1:

$$\frac{Time\ in\ the\ novel\ arm - \frac{Time\ in\ the\ start\ arm + Time\ in\ the\ familiar\ arm}{2}}{Time\ in\ the\ novel\ arm + \frac{Time\ in\ the\ start\ arm + Time\ in\ the\ familiar\ arm}{2}}$$

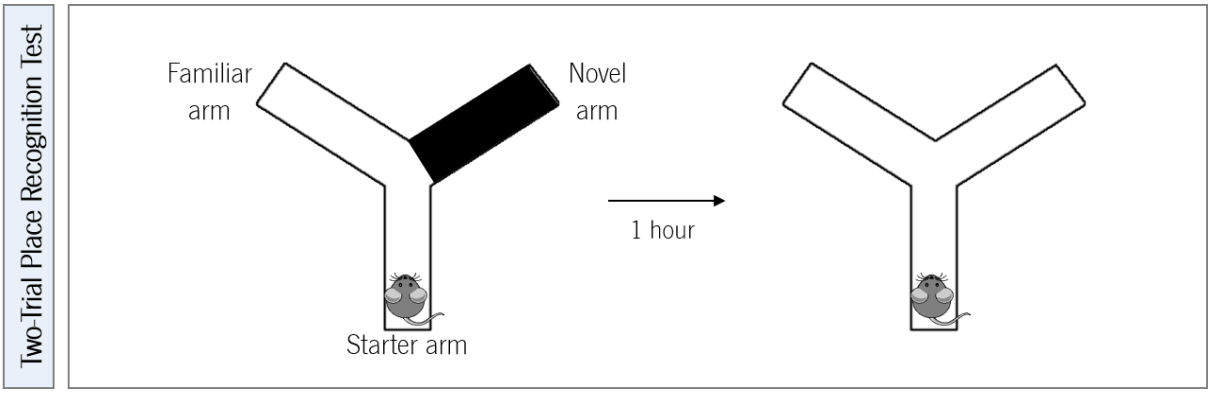

Figure 7 – Schematic representation of the Two-Trial Place Recognition Test in the Y-Maze paradigm. On the first trial (on the left), mice were allowed to explore the starter and the familiar arm for 10 minutes. One hour later, on the retrieve trial (on the right), mice were allowed to explore the 3 arms and the time animal spent in the novel arm of the maze was analyzed.

6.7. Contextual Fear Conditioning

The CFC was performed to assess associative learning using two white acrylic chambers (20 cm x 16 cm x 20.5 cm (MedAssociates)). Animals were exposed to two different probes, a context and a cue probe (sound) where the chamber where animals received a foot shock was equipped with a steel shock grid at the bottom, as previously described (Gu et al., 2012) (figure 8). The arenas were always cleaned with 10% ethanol between trials. Mouse freezing behavior was recorded using video cameras and manually scored using a behavioral scoring program (Observer). CFC was conducted for three consecutive days and performed according to the following:

Day 1 – Training session

One the first testing day, animals were placed inside the white chamber containing a shock grid on the floor (Context A). For 5 minutes and 30 seconds, mice received three consecutive sound-shock pairings. During the first 2 minutes and 40 seconds, mice were allowed to freely explore the chamber without any associated cue. After that, a cue (sound) was introduced. More specifically, 18s before the application of a foot shock a sound was turned on and this period co-terminated with a 2 second shock of 0.5 mA. This procedure was repeated 3 times until the test was over. Animals returned to their home cages 30 seconds after the last shock. During this day, the testing room was only illuminated with a red light and a dimly- white light in the corner of the room. For the analysis of baseline and post-shock freezing behavior, the first 2 minutes and 40 seconds and the last 30 seconds were analyzed, respectively. Freezing behavior was considered when a complete privation of movement, for a minimum of 1 second, was observed (Gu et al., 2012).

Day 2 – Context Probe

On day 2 (24 hours after the training session), animals were re-exposed to the familiar (white) chamber and freezing behavior was measured for 3 minutes. Two hours later, animals were placed in a new context (Context B). In this context, room conditions were changed in order to alter both spatial and odor references: room light was turned on, chambers were covered with black plastic cardboards, shock grid was covered, a vanilla extract scent was added to the chambers and the researcher wore different gloves and lab coat colors. This period session lasted for 3 minutes and freezing behavior was measured. Freezing behavior was considered when a complete privation of movement, for a minimum of 1 second, was observed (Gu et al., 2012).

Day 3 – Cue Probe

On the last day, animals were placed in the new context (Context B) for 3 minutes. In the final 20 seconds the sound was turned on and their freezing behavior was measured for 1 minute. Freezing behavior was considered when a complete privation of movement, for a minimum of 1 second, was observed (Gu et al., 2012). The percentage of freezing behavior was calculated as well as the discrimination index (difference of freezing in Context A and B/ total freezing in both contexts) (Gu et al., 2012).

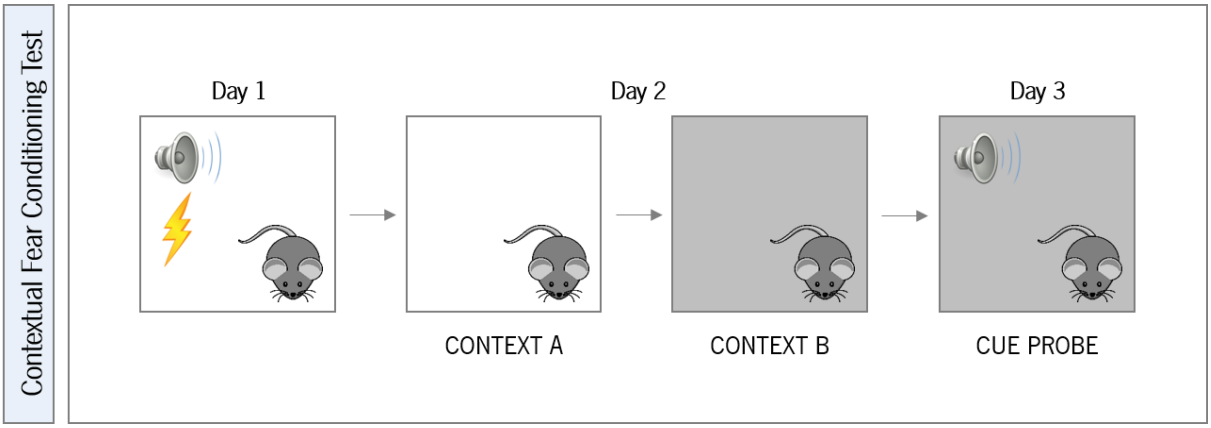

Figure 8 – Schematic representation of the CFC paradigm. During day 1 (Training session), the animal was exposed to a white chamber (Context A) and conditioned with 3 sound-shock pairs. At day 2, animals were exposed to the same context (Context A) without the aversive stimuli. 2 hours later, animals were exposed to a new context (Context B). At day 3 (Cue Probe), animals were re-exposed to the novel context (context B) and the cue (sound) was turned on. Freezing behavior was analyzed in all contexts.

6.8. Burrowing Test

The burrowing test is a widely non-invasive method used to detect behavioral dysfunction in rodents and it is based on rodents' natural ability for burrowing (R M J Deacon, 2009). The burrowing test was performed before, during and after the behavioral characterization, in order to infer about animals well-being during the characterization. Briefly, a full burrow filled with approximately 200g of food pellets was placed on a clean cage with bedding. The burrow was carefully placed against the longer wall of the cage with its closed end against the back wall of the cage. The test started 3 hours before the dark cycle and each animal was placed into each cage-burrow setup for 2 hours. Animals returned to their home cage after the testing session with food and water *ad libitum*. The amount of material displaced from the burrow was measure, defined as the total weight before the burrowing

activity minus the weight left in the tube (Robert M J Deacon, 2006). The percentage of material displaced was calculated based on the initial weight of material in the burrow and the weight left in the tube after the test.

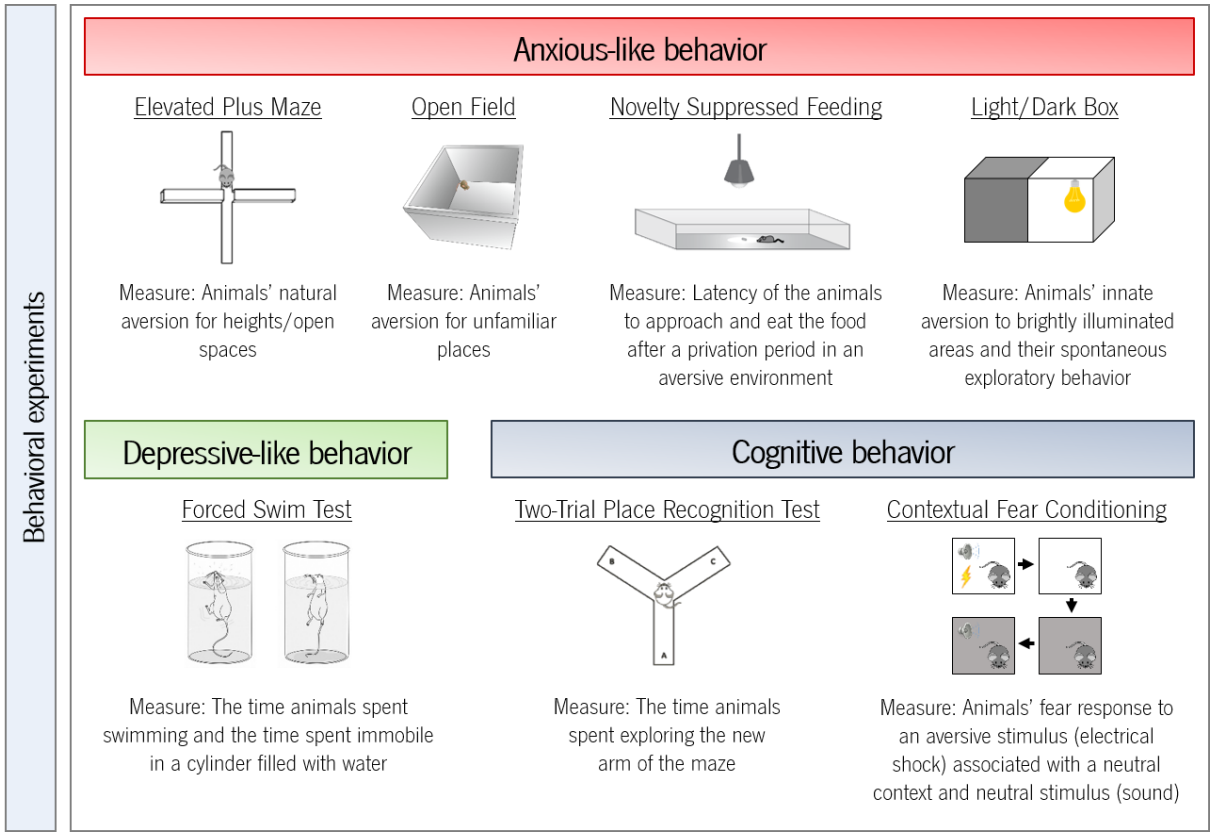

Figure 9 – Representation of the behavioral paradigms performed for the behavioral characterization of the SNX27$^{+/-}$ C57BL6/J mice after stress expsoure. Six weeks after the Chronic Mild Stress protocol the behavioral characterization was performed to assess anxious-like behaviors through the EPM, Open Field, NSF and L/D Box test; depressive-like behavior through the FST; and cognitive behavior through the Two-Trial Place Recognition Test and CFC.

7. Tissue processing

Animals were anesthetized with a mixture of ketamine (75 mg/Kg; Imalgene, USA) and metedomidine (1 mg/Kg; Syba, USA) solution and then transcardiacally perfused with 0.9% of NaCl solution. The brains were then extracted from the skull and the following areas were macrodissected for molecular analysis: prefrontal cortex and dorsal and ventral hippocampus. Distinct tissues such as spleen, liver and tail were also collected. All tissue samples were stored in RNase free tubes at -80°C.

8. Morphological analysis

Three dimensional (3D) morphological analysis of neurons was performed on Golgi-Cox stained neurons at the dentate gyrus (DG) region of the hippocampus, as well as of the amygdala and the bed nucleus of the stria terminalis (BNST) regions. The mouse brain subregions were identified according to Paxinos mouse brain atlas (Paxinos & Franklin, 2004). The brain samples used for the morphological analysis are resultant from animals generated by crossing heterozygotes on a C57BL/6 and 129/SV mixed background and divided in two groups: a control group (CON) and a stress-exposed group, submitted to a modified chronic unpredictable stress (CUS) protocol (Monteiro et al., 2015). These mice were also subjected to an extensive behavioral characterization performed with my contribution during my final degree internship. Mice were deeply anesthetized with a mixture of ketamine (75 mg/Kg; Imalgene, USA) and metedomidine (1 mg/Kg; Syba, USA) solution and then transcardiacally perfused with 0.9% of NaCl solution. Tissue processing was performed as described below:

Golgi-Cox staining and 3D-reconstrucution of hippocampal neurons

Brains were removed from the skull and impregnated in a Golgi-Cox solution (5 parts of 5% potassium dichromate solution, 5 parts of 5% mercury chloride solution, and 4 parts of 5% potassium chromite solution) for 14 days in the dark at room temperature (RT). After this period, brains were transferred to a 30% (w/v) sucrose solution in PBS and kept at 4°C until further processing. A vibratome (MicroHM-650V) was used to section the brains in slices of 200 µM thickness. Brains were then blotted onto gelatin-coated microscope slides and alkalinized in 18.7% ammonia. Slices were developed in Dektol (Kodak, Rochester, NY, USA), fixed in Kodak Rapid Fix, dehydrated and xylene cleared before mounted in Entellan and coverslipped (Zaqout & Kaindl, 2016).

The hippocampus was divided into dorsal and ventral regions following the bregma coordinates as described in the Paxinos mouse brain atlas (Paxinos & Franklin, 2004). Neurons from WT and SNX27$^{+/-}$ mice were analyzed and a minimum of 7 neurons were studied per area. Each selected neuron was evaluated using a motorized microscope (Axioplan-2, Zeiss) with a coupled camera (CMA-D2, Sony) controlled by the Neurolucida software (MBF Bioscience, USA) under 100x (oil) magnification. 3D analysis of the reconstructed neurons were conducted using the NeuroExplorer software (MBF Bioscience, USA). Data was analyzed following distinct parameters such as total length and Sholl analysis (Binley, Ng, Tribble, Song, & Morgan, 2014).

9. Cell culture

9.1. Murine neuroblastoma N2a cell line culture

Murine neuroblastoma N2a cells were maintained at 37°C in a humidified 5% CO_2 atmosphere in DMEM supplemented with GlutaMAX (ThermoFisher Scientific), 10% fetal bovine serum (FBS) (Merck), penicillin (100 U/mL) (ThermoFisher Scientific) and streptomycin (100 µg/mL) (Alfagene). Cells were negative for mycoplasma contamination.

DMEM is a widely used basal medium for supporting the growth of many different mammalian cells and contains no proteins or growth promoting agents. Therefore, it requires supplementation to be a "complete" growth medium. FBS is the most used serum-supplement for *in vitro* cell culture due to having very low levels of antibodies and containing growth factors. The antibiotics Pen-Strep were used to prevent contamination from Gram positive and Gram negative bacteria.

9.2. Cell thawing

In order to maintain cells for experimental procedures, cells were thawed in complete growth medium. Cryogenic vials containing cells were placed in a heat bath at 37°C until partially defrosted. Cells were then transferred to a 50 mL falcon with complete growth medium and centrifuged for 3 minutes at 900 rpm at 4°C. The medium was removed and the pellet was resuspended in 10 mL of complete growth medium. Cells were plated in a T-75 flask and medium was changed every 2 to 3 days (figure 10).

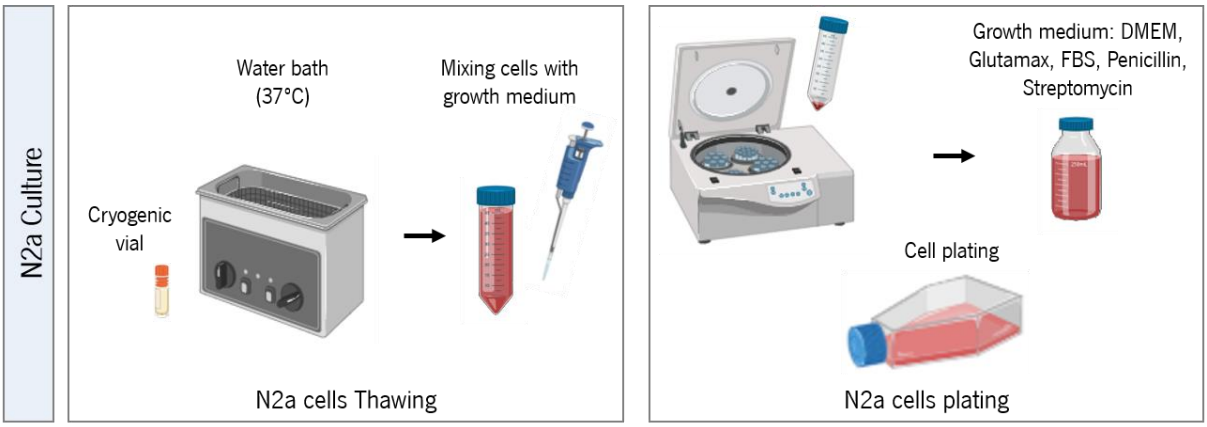

Figure 10 – Culture of a murine neuroblastoma cell line N2a. Cells were thawed in a water bath at 37°C, mixed with growth medium and centrifuged at 4°C. Cells were seeded at a T-75 flask with growth medium and maintained at 37°C in a humidified 5% CO_2 atmosphere. Medium was changed every 2 to 3 days.

9.3. Pharmacological Treatments

N2a cells were plated in 6-well (for WB) or 24-well (for IF) plates at 30-40% confluence and maintained at 37°C in humidified 5% CO_2 atmosphere prior to pharmacological manipulation. Pharmacological treatments were performed using the following agents in the indicated concentrations and time courses: dexamethasone (10 µM, 48 hours, Jenapharm), VPS34 inhibitor (VPS34IN1, 1µM, 24 hours, Dundee University). Dexamethasone was prepared using DMEM medium and added to the plates, while VPS34IN1 was prepared in DMEM supplemented with GlutaMAX, 10% fetal bovine serum, penicillin (100 U/mL) and streptomycin (100 µg/mL) (Alfagene). Cells were allowed to grow at 37°C in humidified 5% CO_2 atmosphere to 80-90% confluence before further processing.

9.4. Freezing cells

In order to store the cells for other procedures, cells were frozen in a ratio of 90% FBS and 10% DMSO (Sigma Aldrich). After medium removal, cells were washed with PBS and added 0.05% Trypsin-EDTA (ThermoFisher Scientific) and left incubating at 37°C for 3 minutes. Once in suspension, complete growth medium was added and cells were centrifuged for 3 minutes at 900 rpm at 4°C. For cell counting, cells were diluted in Trypan Blue (ThermoFisher Scientific) and mounted on a Neubauer chamber. Total number was estimated and cells aliquoted in a final concentration of 5,0 x 10^6 cells/mL/vial. Then, vials were stored at -80°C for 24 hours and later moved to cryogenic freezing.

10. RNA isolation

Total RNA was extracted from animal tissues (PFC, dorsal and ventral DG) using TripleXtractor (Grisp, Portugal). Briefly, samples were homogenized in TripleXtractor buffer using a 1mL syringe and incubate at room temperature for 5 minutes. Lysates were added 0.2 mL of chloroform per 1mL of TripleXtractor used (Sigma Aldrich) for phase separation and vortex for 5 to 6 seconds. Subsequently, samples were incubated at room temperature for 2 to 3 minutes and centrifuged for 10 minutes at 14,000g at 4°C. This results in the separation into a lower red phenol-chloroform phase, an interphase, and a colorless upper aqueous phase containing the RNA. The aqueous phase was then transferred to a new RNase free tube and RNA was precipitated by adding 1 volume of isopropanol (Sigma Aldrich) per 1 volume of TripleXtractor used together with glycogen (Roche). The tubes containing the RNA were inverted 5 to 10 times by hand and samples incubated for 10 minutes at room temperature. Samples were then centrifuged for 10 minutes at 15,000g at 4°C. Supernatants were discarded and pellets were washed with 70% ethanol (CarloErba Reagents) prepared with RNase-free water. Microtubes were carefully inverted a few times and centrifuged for 8 minutes at 15,000g at 4°C. After the washing step, ethanol was discarded and tubes were air-dry for 5 to 10 minutes in order to remove trace amounts of ethanol. RNA pellet was resuspended in RNase-free water (Invitrogen) and stored at -80°C for later use.

11. cDNA synthesis and real-time quantitative PCR analysis

Total RNA was converted using the iScript Advanced cDNA Kit for RT-qPCR (Bio-Rad, USA). Quantifications were performed in a Fast Real-Time PCR System (Applied Biosystems, USA) using the SsoFast EvaGreen Supermix (Bio-Rad, USA). The housekeeping gene HPRT was used as an internal control and the relative expression was calculated using the ΔC_T method.

12. Protein biochemistry and immunoblotting

Cells and tissues were washed in PBS and scraped in radioimmunoprecipitation assay buffer (RIPA) (Pierce) supplemented with protease and phosphatase inhibitor cocktails (Sigma Aldrich) at 4°C. Homogenates were centrifuged for 10 minutes at 16,000g at 4°C. Supernatants were processed for protein dosage using the Pierce BCA Protein Assay kit (ThermoFisher Scientific) and samples diluted to

equal concentration with supplemented RIPA buffer. Lysates were denatured in 2x Laemmli Buffer (Bio-Rad, USA) by heating samples at 98°C for 5 minutes. Then, 30 µg of total protein were loaded onto an SDS-PAGE gel (10%) and electrophoresed for 1h15min at 150V. Reference molecular weight markers from Grisp (Grisp, Portugal) were used. Samples were transferred (semi-dry transfer) to a nitrocellulose membrane (Bio-Rad, USA) in a blotting system (Bio-Rad, USA) for 7 minutes at 25V/2,5A. Membranes were blocked for 1 hour with 5% non-fat milk/2.5% BSA in TBS solution (50mM Tris-Cl, 150mM NaCl, pH7.5), to prevent non-specific background binding of the primary and/or secondary antibodies. After blocking, membranes were incubated overnight with primary antibodies SNX27 (1:1000 Anti-SNX27 rabbit, Novus Biologicals), SNX25 (1:1000 Anti-SNX25 rabbit, Citomed), SNX12 (1:1000 Anti-SNX12 rabbit), SNX3 (1:1000 Anti-SNX3 rabbit), p62 (1:1000 Anti-p62 rabbit, Abcam), GR (1:1000, Anti-GR rabbit, ProteinTech) overnight. Membranes were then washed (3 x 10min) with TBS-Tween (0.1% Tween) and incubated, at room temperature with agitation, for 2 hours with conjugated secondary antibodies (Bio-Rad, USA). A final wash in TBS-T (3 x 10 min) was performed followed by revelation with chemiluminescent signal using the Clarity Western ECL substrate kit (Bio-Rad, USA) with the gel blotting imaging system (Chemidoc, Bio-Rad, USA). Relative protein quantification was performed by densitometry using the Image Lab software (Bio-Rad, USA). All samples were normalized for a loading control protein (1:2000, Actin, Abcam).

13. Immunofluorescence and confocal microscopy

N2a cultured cells were washed with PBS and fixed with 4% paraformaldehyde (PFA, ITW Reagents) for 15 minutes at room temperature. Cells were washed (3 x 5min) in phosphate-buffered saline (PBS, Merck) and incubated during 30 minutes with a blocking solution containing PBS supplemented with 1% bovine serum albumin (BSA, Sigma-Aldrich) and 0.05% saponin (Sigma-Aldrich) for permeabilization. Subsequently, coverslips were incubated with the primary antibody EEA1 (1:150, Santa Cruz Biotechnology), SQSTM1 (1:100, Abnova), SNX27 (1:150, Santa Cruz Biotechnology), SNX25 (1:150, Citomed), SNX12 (1:150, Santa Cruz Biotechnology) and SNX3 (1:150, Santa Cruz Biotechnology) diluted in blocking buffer for 1 hour at room temperature. Cells were washed (3 x 5min) in the same buffer and incubated with Alexa-488 or -594 goat secondary antibodies: anti-mouse IgG (1:300, Santa Cruz Biotechnology) and anti-rat IgG (1:300, ThermoFisher Scientific) for 1 hour in the dark, at room temperature. Finally, cells were washed in blocking buffer (2 x 5min) and PBS (2 x 5min), mounted in DAPI Fluoromount-G (SouthernBiotech) and let drying overnight in the dark. Confocal stacks

and super-resolution images were acquired using an Olympus Fluoview FV100 confocal microscope (Olympus, Germany). Fluorescence was collected with 100x plan immersion oil objective. Extraction of single z-frame and maximum intensity projections were performed with ImageJ software (ImageJ, USA).

14. Statistical analysis

The sample size for each task was calculated using G*Power 3.1.9.4 software, fixing significance level (α)=0.05, effect size=0.45 and power (1-β)=0.7. Effect size used was inferred according to the available literature on similar animal studies. Statistical analysis and graphic's representation were carried out using GraphPad Prism 7 (GraphPad Software, La Jolla, USA) and IBM SPSS Statistics 25 (IBM Com, USA). All data assuming a Gaussian distribution by the Kolmogorov-Smirnov normality test followed parametric tests while non-parametric tests were used for discrete variables. Two-way analysis of variance (ANOVA) with Tukey *post-hoc* test was applied to analyze behavioral data (EPM, OF, NSF, L/D Box, FST, NORT, Y-Maze, and CFC), considering the factors: condition (control vs. uCMS) and genotype. Two-way repeated measures ANOVA was used to analyze animals' weight, anogenital distance and behavioral data (NSF – appetite drive curve, Burrowing), followed by Tukey *post-hoc* analysis for multiple comparisons. Two-tailed independent sample t-test was applied in analysis of developmental parameters and for comparison of two experimental conditions of *in vitro* assays. Two-way ANOVA was conducted to analyze neuronal morphological data, considering two groups: young animals and old animals. Data is expressed as mean ± SEM (standard error of the mean). Statistical significance was considered for $p<0.05$ and is indicated by an asterisk (*).

RESULTS

1. The SNX27$^{+/-}$ mixed background mouse model

The animals used for the morphological characterization were not from the herein described set and are resultant from animals generated by crossing heterozygotes on a C57BL/6 and 129/SV mixed background. Previously to the development of this thesis, male animals were divided in two groups with different ages (Young – 6 to 9 months old; Old – more than14 months) and each group was subdivided in two groups: a control group (CON) and a stress-exposed group (CUS), submitted to a modified chronic unpredictable stress (CUS) protocol (Monteiro et al., 2015). Briefly, this protocol consisted in a daily exposure to one of the stressors: Restraint – animals were placed inside a 50 mL falcon; Social defeat – animals were placed in the cage of an aggressive mice (CD1) until being defeated, after that mice stayed in a transparent plastic glass (to avoid further physical contact) inside the CD1 mice resident cage; Shaking – animals from one cage were placed in a plastic box container and placed in a shaker at 150 rpm; Hot air stream – animals were exposed to a hot air stream from a hairdryer; Tilted cage – home cages were tilted overnight in a 45° angle; Inverted light cycle – regular room light was OFF during day and ON during the night for 2 consecutive days. The animals used for this study were previously behaviorally characterized during my final degree internship and master rotation, and the obtained data suggests that reduction of SNX27 levels induces anxious-like behavior in young animals, while validating SNX27 association with memory impairments.

1.1. Neuronal 3D morphology of the SNX27$^{+/-}$ mouse model during aging and stress exposure

Chronic stress, a suggested precipitant of brain pathologies, has been reported to impact on brain plasticity by causing neuronal remodeling, related to alterations in dendritic length and arborization, as well as neurogenesis suppression in the adult hippocampus. In fact, several studies described that stress-exposure causes adverse consequences on neuronal morphology, particularly inducing shrinkage of the apical dendrites of hippocampal CA3 and dentate gyrus neurons and loss of spines in CA1 neurons (Mcewen, Nasca, & Gray, 2015). Moreover, age was also described to be associated with a decrease in dendritic length in areas related with cognitive abilities. Studies using a rat model observed that old animals displayed shorter dendritic tress in the granular neurons in the DG area of the hippocampus comparing with young animals (Mota et al., 2019).

In order to evaluate the morphological alterations promoted by stress-exposure , aging, and decreased levels of SNX27, total length and branching of Golgi-Cox stained neurons were assessed at the dorsal part of the dentate gyrus (DG) region of the hippocampus in animals generated by crossing heterozygotes on a C57BL/6 and 129/SV background, the published animal model. Two-way ANOVA analysis indicated no statistically significant differences in the total dendritic length between control and stress exposed groups regardless of genotype for young animals (figure 11A, table 2). The same was observed for old animals where neuronal length was similar regardless of genotype or stress exposure (figure 11B, table 3). Regarding neuronal branching analysis, no statistical significant differences were observed regardless of genotype or exposure to the stress protocol in young and old animals (figure 12, table 4 and 5) indicating that reduction in SNX27 levels does not impact on the neuronal morphology of the dorsal part of the DG region of the hippocampus.

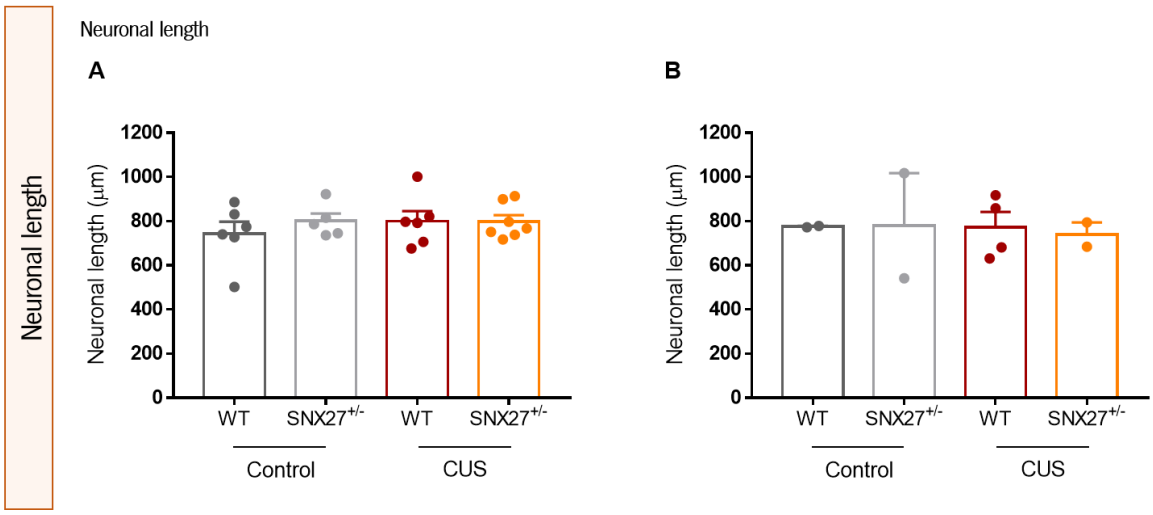

Figure 11 – SNX27 reduction does not impact on neuronal length in the dorsal region of the hippocampus. Dendritic length of dorsal hippocampal neurons of WT and SNX27$^{+/-}$ mice in control and chronic stress conditions. (A) Total dendritic length of young animals. (B) Total dendritic length of old animals. Data is represented as mean ± SEM; Young: n= 5-7 animals per group; Old: n=2-4 animals per group (6-7 neurons per animal). Significance level was considered for $p<0.05$.

Table 2 – Total dendritic length of young animals (μm). Data is represented as mean ± SEM; n represents the number of animals per group.

	WT	**SNX27$^{+/-}$**	**Statistical test, significance, effect size**
Control	743.90 ± 53.94 n=6	801.30 ± 33.58 n=5	Interaction F(1,20)=0.4845 p=0.4944 Condition F(1,20)=0.3752 p=0.5471 Genotype F(1,20)=0.4344 p=0.5174
CUS	799.30 ± 46.61 n=6	797.70 ± 29.56 n=7	

Table 3 – Total dendritic length of old animals (μm). Data is represented as mean ± SEM; n represents the number of animals per group.

	WT	**SNX27$^{+/-}$**	**Statistical test, significance, effect size**
Control	775.70 ± 2.821 n=2	779.50 ± 238.1 n=2	Interaction F(1,6)=0.026 p=0.8767 Condition F(1,6)=0.037 p=0.8542 Genotype F(1,6)=0.017 p=0.9019
CUS	772.30 ± 68.69 n=4	739.40 ± 54.84 n=2	

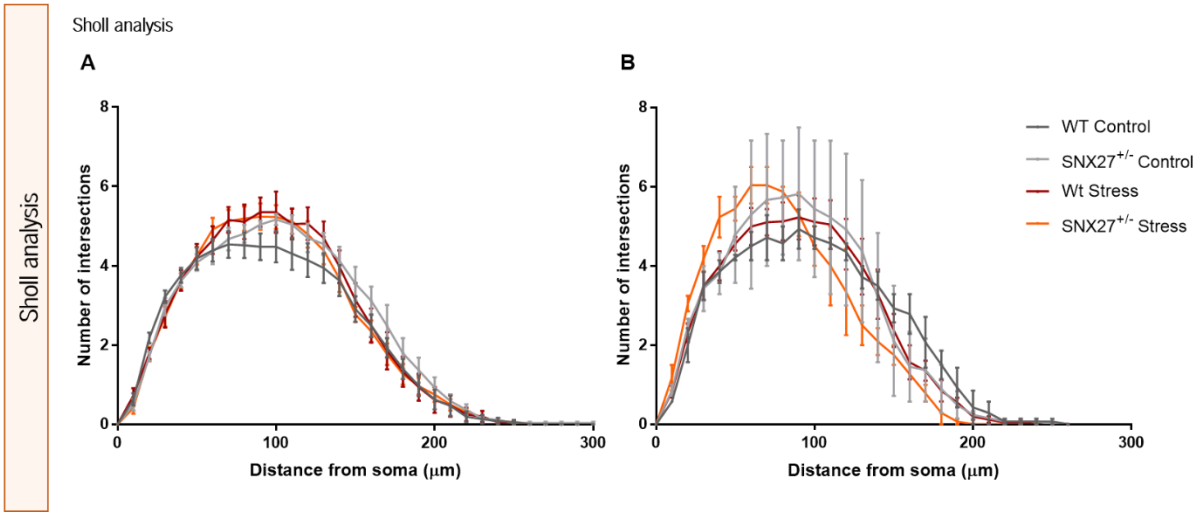

Figure 12 – SNX27 reduction does not impact on neuronal complexity in the dorsal region of the hippocampus. Neuronal complexity of dorsal hippocampal neurons of WT and SNX27+/- mice in control and chronic stress conditions. (A) Neuronal branching of young animals. (B) Neuronal branching of old animals. Data is represented as mean ± SEM; n=6-7 neurons per animal. Significance level was considered for $p<0.05$.

Table 4 – Neuronal branching of young animals. Data is represented as mean ± SEM; n represents the number of animals per group.

	WT	**SNX27$^{+/-}$**	**Statistical test, significance, effect size**
Control	1.591 ± 0.2915 n=6	1.765 ± 0.3147 n=5	Interaction F(117,780)=0.8153 p=0.9169 Distance from soma F(39,780)=250.80 p<0.0001 Genotype/Condition F(3,20)=0.6295 p=0.6044
CUS	1.722 ± 0.3273 n=6	1.686 ± 0.3223 n=7	

Table 5 – Neuronal branching of old animals. Data is represented as mean ± SEM; n represents the number of animals per group.

	WT	**SNX27$^{+/-}$**	**Statistical test, significance, effect size**
Control	2.405 ± 0.3638 n=2	2.516 ± 0.4335 n=2	Interaction F(78,156)=0.9239 p=0.6477 Distance from soma F(26,156)=83.67 p<0.0001 Genotype/Condition F(3,6)=0.0374 p=0.9893
CUS	2.396 ± 0.4038 n=4	2.331± 0.4425 n=2	

2. The SNX27$^{+/-}$ C57BL/6J mouse model

C57BL/6J WT (SNX27$^{+/+}$) and Het (SNX27$^{+/-}$) animals were obtained by performing several backcrossing from the mixed - C57BL/6 and 129/SV background - to the C57BL/6J pure background. All the obtained animals used throughout the experimental procedures were genotyped in order to identify WT and Het animals. After DNA extraction using the NaOH method, DNA sequences were amplified by PCR taking advantage of the K01, K02 and K03 primers. The K01-forward and K02-reverse primers match the SNX27 gene sequence present in animals from both genotypes, while the K03-neo-reverse primer hybridizes the allele of the gene that contains the deletion cassette present in heterozygous animals (SNX27$^{+/-}$), amplifying with the K01-forward primer and giving rise to two bands of different molecular weights in heterozygous animals. Therefore, the presence of a unique band at 229 bp is indicative of a WT animal, whereas Het animals presented two bands at 229 and 300 bp (figure 13).

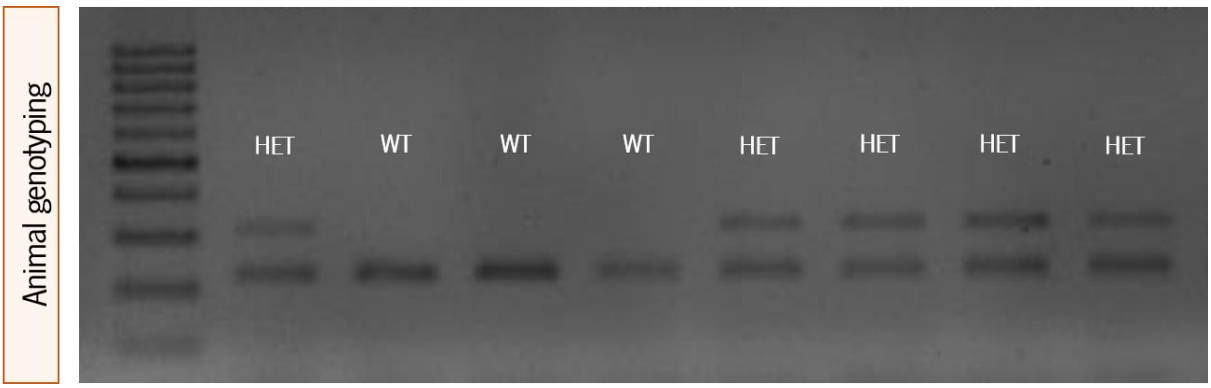

Figure 13 – Genotyping of WT and SNX27$^{+/-}$ animals. Representative image of the agarose gel. After DNA extraction and amplification of DNA sequences by PCR, samples were separated by their molecular weight on a 1% (w/v) agarose gel. The presence of a band at 229 bp is indicative of a WT animal, whereas the presence of two bands at 229 e 300 bp is indicative of a Het animal.

2.1. Evaluation of the degree of purity of the SNX27$^{+/-}$ C57BL/6J mouse line

Animals generated from a heterozygous crossing on a C57BL/6 and 129/SV background were backcrossed for 8 generations to a C57BL/6J background in order to eliminate interfering genetic determinants resulting from genetic drifting. A mutant line is considered fully congenic when 99.9% of its genome is from the recipient inbred strain to which it is being backcrossed. To confirm the presence

of a pure C57BL/6J background, a 384 single nucleotide polymorphism (SNP) panel was employed to generate allelic profiles of the tested mice for comparison with the profile of the reference strain (C57BL/6J). Each SNP contains 2 alleles. One allele is identified with a complementary oligonucleotide (TaqMan) probe labeled with the fluorescent dye FAM, while the complementary probe to the other allele is labeled with the fluorescent dye VIC. Therefore, the genotypes for homozygotes are reported FF or VV and VF for heterozygotes. It is expected that an inbred strain is homozygous to the recipient C57BL/6J strain at each SNP marker.

Results demonstrate that the generated experimental strain is 98.93% homozygous for the C57BL/6J strain (figure 14). The Percent Match was determined by comparing the genotype of the animals with the reference strain at each marker. Furthermore, when chromosome 3 is excluded from the analysis, attending on the location of the SNX27 donor mutation in this region, the degree of purity reaches approximately 99.5%.

Percent Match to Alleic Profile of Recipient/Reference Strain

LTM # - Sample ID	Sex	Gen	DOB	Donor Parent (% Match)	Assays Called Number	Assays Called Rate	Percent Match	w/o Chr 3
001-A	M	F7	24-Jul-2019	HET (SNX27+/-)	373	100.0%	99.20%	99.72%
002-B	M	F7	28-Aug-2019	HET (SNX27+/-)	371	99.5%	99.06%	99.57%
003-C	M	F7	27-Aug-2019	HET (SNX27+/-)	373	100.0%	98.53%	99.15%
					1117	99.8%	98.93%	99.48%

Figure 14 – Results obtained with the 384-SNP panel to assess the presence of a fully congenic line to the C57BL6/J background. The Percent Match was determined by comparing the genotype of the animals with the reference strain at each marker. Chromosome 3 was excluded because it contains the donor mutation. Each line on the table represents a unique sample obtained from different mice.

This generated mouse model is referred from now on as the SNX27$^{+/-}$ C57BL/6J mouse model (in opposition to the SNX27$^{+/-}$ mixed background).

In order to confirm the reduction of SNX27 levels in this newly generated heterozygous animals, the expression levels of the SNX27 gene in distinct brain regions were quantified through qRT-PCR analysis. The expression of SNX27 in the PFC and dorsal and ventral DG were analyzed and compared between Het animals and WT littermate controls. In all the tested brain regions, SNX27 levels are significantly reduced approximately at 50% in the Het mice (figure 15, table 6).

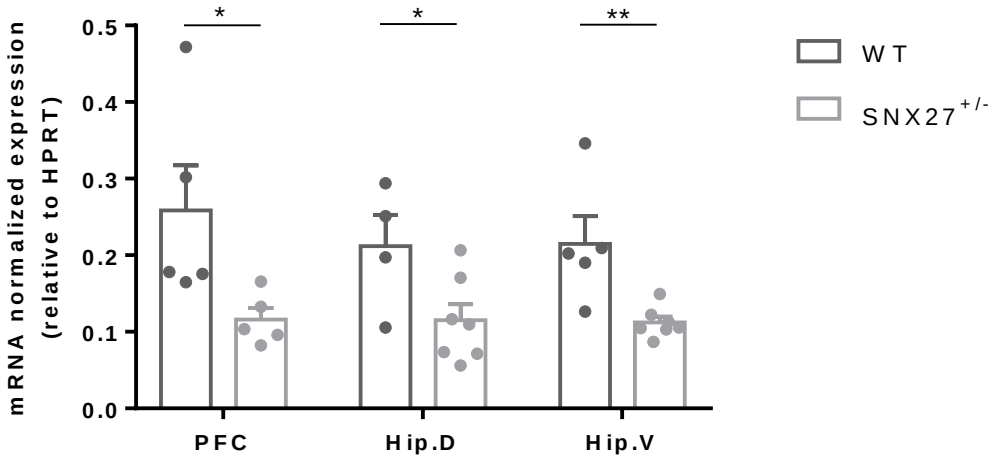

Figure 15 – Expression of SNX27 is reduced in Het mice in the PFC, and the dorsal and ventral DG regions. Quantification of SNX27 in the PFC, and dorsal and ventral DG regions by qRT-PCR. WT animals are represented by dark grey bars/dots whereas Het animals are represented by light grey bars/dots. Data is represented as mean ± SEM; n=4-7 per group. Significance level is represented by * $p<0.05$; ** $p<0.01$.

Table 6 – Quantification of SNX27 expression levels in the PFC, and the dorsal and ventral DG regions of WT and SNX27$^{+/-}$ animals. Data is represented as mean ± SEM; n represents the number of animals per group.

	WT	**SNX27$^{+/-}$**	**Statistical test, significance, effect size**
PFC	0.285 ± 0.05899 n=5	0.116 ± 0.01491 n=5	t(2.341)=8 p=0.0473 Cohen's d=3.9280
Dorsal DG	0.212 ± 0.04060 n=4	0.115 ± 0.02102 n=7	t(2.371)=9 p=0.0418 Cohen's d=3.0005
Ventral DG	0.2149 ± 0.03598 n=5	0.1122 ± 0.00741 n=7	t(3.304)=10 p=0.0080 Cohen's d=3.9537

3. Developmental characterization of the SNX27$^{+/-}$ C57BL/6J mouse model

Attending on SNX27 role in development and survival, as SNX27$^{+/-}$ KO animals are not viable after P14 and present severe growth deficits, we assessed the impact of SNX27 reduction during post-natal development. In the postnatal days that precede weaning, from PND0 to PND21, WT and SNX27$^{+/-}$ newborn mice were evaluated for the acquisition of several somatic and neurological responses using a developmental milestones protocol (figure 16). The milestones protocol is widely used for assessment of neuro-dependent behavior during neonatal development and allows for a fast screening of all litters to be examined daily within a short relative period of time (Guerra-Gomes et al., 2020).

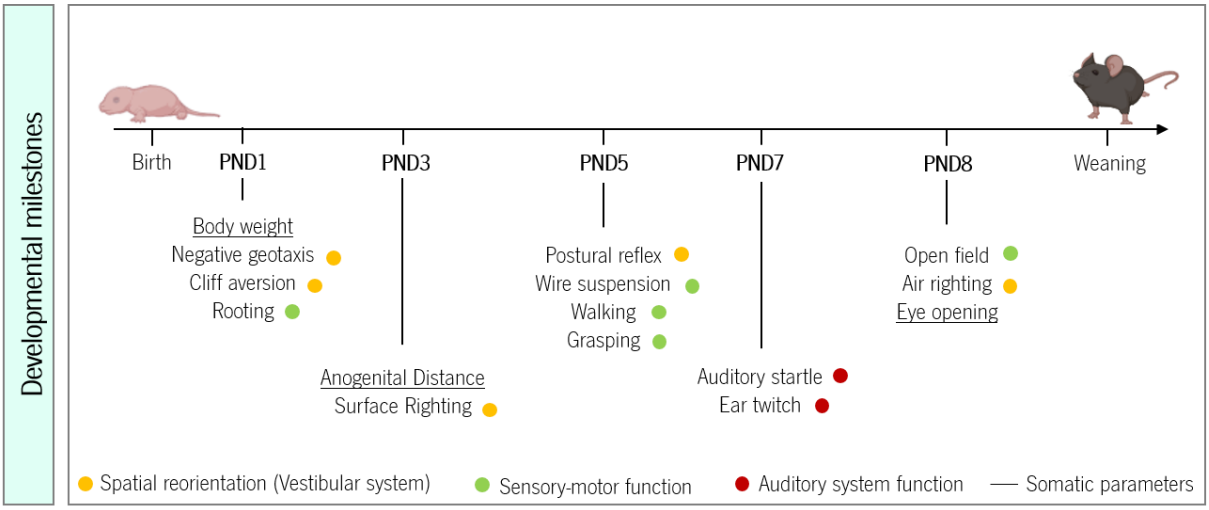

Figure 16 – Representative scheme of the experimental timeline used for assessment of developmental milestones from birth to weaning age. Each developmental parameter was assembled according to the tested function (in yellow – parameters that rely in spatial reorientation dependent on the vestibular system; in green – parameters dependent on sensory-motor function; in red – parameters dependent on the auditory system function; in underline – somatic parameters).

3.1. Somatic parameters

Somatic parameters were assessed during the first 21 days of life of WT and SNX27$^{+/-}$ C57BL/6J mice. Body weight and anogenital distance were evaluated as somatic monitoring parameters to infer about mice normal growth and physical health. Regarding body weight assessment, results show that WT and SNX27$^{+/-}$ C57BL/6J mice display increased body weight along time, which was similar between genotypes and gender (figure 17A, table 7). Anogenital distance in male WT and SNX27$^{+/-}$ C57BL/6J

animals equivalently increased along the time and no differences were found between genotype (figure 17B, table 8). Similarly, female WT and SNX27$^{+/-}$ C57BL/6J mice also display a daily increase anogenital distance, which was not significantly different between genotypes (figure 17B, table 8). Overall, our results indicate that reduced expression of SNX27 does not interfere with general growth during the development of male and female newborn mice.

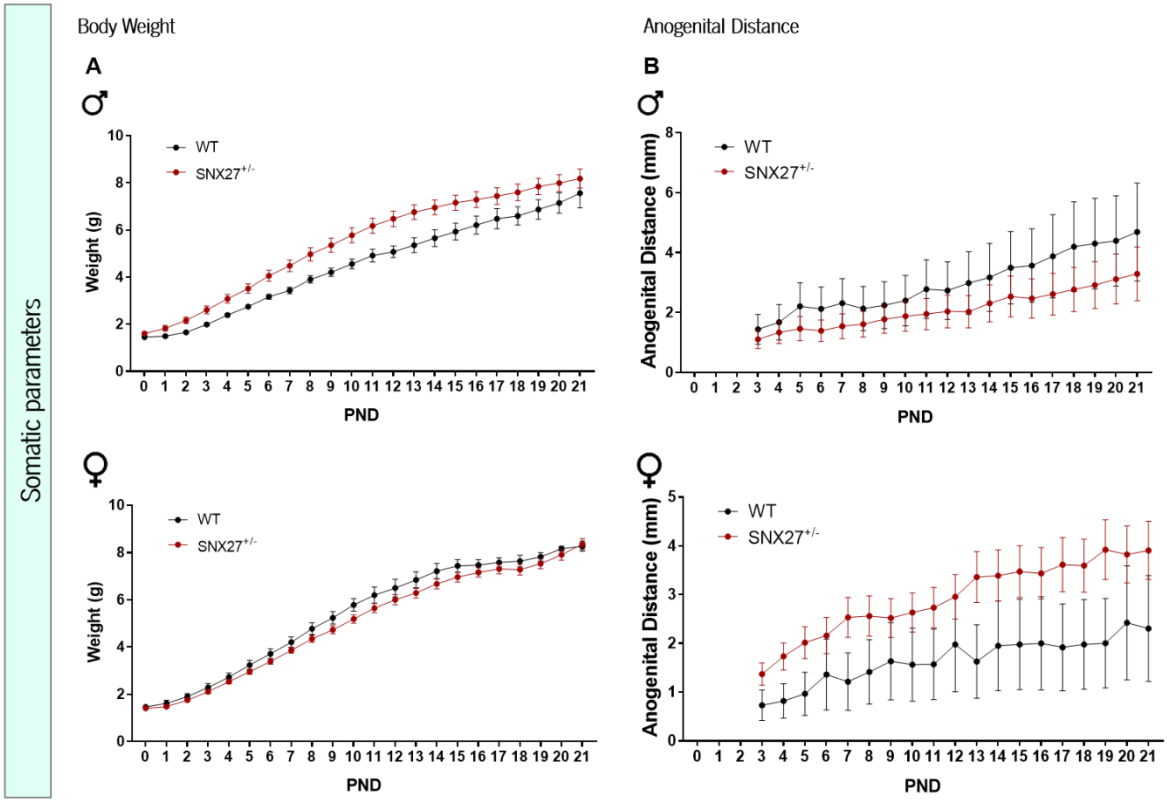

Figure 17 – Reduced levels of SNX27 does not impact on somatic parameters during postnatal evaluation. Assessment of somatic parameters during the first 21 days of life. (A) Body weight evolution from PND0 to PND21 of WT and SNX27$^{+/-}$ newborn mice (male and female). (B) Anogenital distance measurement from PND3 to PND21 of WT and SNX27$^{+/-}$ newborn mice (male and female). WT animals are represented in black and SNX27$^{+/-}$ animals are represented in red. Data is represented as mean ± SEM. Significance level is considered for $p<0.05$.

Table 7 – Assessment of body weight during the first 21 days of life (g). Data is represented as mean ± SEM; n represents the number of animals per group.

	WT	SNX27$^{+/-}$	Statistical test, significance, effect size
Males	4.491 ± 0.4195 n=5	5.413 ± 0.4672 n=18	Interaction F(21,441)=2.004 p=0.0055 Time F(21,441)=270.4 p<0.001 Genotype F(1,21)=3.186 p=0.0887
Females	5.35 ± 0.5053 n=5	5.031 ± 0.4895 n=12	Interaction F(21,315)=1.014 p=0.4454 Time F(21,315)=585.7 p<0.001 Genotype F(1,15)=1.601 p=0.2251

Table 8 - Assessment of anogenital distance from PND3 to PND21 (mm). Data is represented as mean ± SEM; n represents the number of animals per group.

	WT	SNX27$^{+/-}$	Statistical test, significance, effect size
Males	2.985 ± 0.2237 n=5	2.112 ± 0.1471 n=18	Interaction F(18,378)=0.7337 p=0.7762 Time F(18,378)=14.98 p<0.0001 Genotype F(1,21)=0.5358 p=0.4723
Females	1.655 ± 0.1095 n=5	2.933 ± 0.175 n=12	Interaction F(18,270)=1.5 p=0.0891 Time F(18,270)=17.8 p<0.0001 Genotype F(1,15)=2.268 p=0.1528

3.2. Neurological reflexes

Neurodevelopmental evaluation also included the acquisition of several neurological parameters related to sensorial and motor functions, labyrinthine reflex, coordination and strength, auditory system function and tactile reflex development in male and female WT and SNX27$^{+/-}$ mice.

The correct formation of the vestibular system was assessed through a battery of behavioral tests, namely surface righting reflex, negative geotaxis, cliff aversion, postural reflex and air righting reflex. In the surface righting reflex no significant differences were found between male WT and SNX27$^{+/-}$ mice. A similar mature response was also found for female mice regardless of genotype. In the negative geotaxis test the acquisition of the mature response was similar for males and females WT and SNX27$^{+/-}$ mice. Results obtained for the cliff aversion test showed that male WT and Het mice present a mature response approximately at the same postnatal day, which was also confirmed for female mice. Moreover, we found that reduction of SNX27 expression levels did not alter postural reflex acquisition in males and females mice. Finally, in the air righting test male and female WT and SNX27$^{+/-}$ mice displayed an analogous mature response.

Another important parameter of neurological development is strength, which was evaluated in the wire suspension and grasping test. Our results indicated that male WT and SNX27$^{+/-}$ mice acquired the mature response approximately at the same postnatal day, which was also observed for females regardless of genotype in the wire suspension test. In the grasping test, a similar mature response was also observed for male and female WT and SNX27$^{+/-}$ mice. Tactile reflex development was evaluated in rooting and ear twitch tests. Our results show that male WT and SNX27$^{+/-}$ mice display a similar mature response in the rooting test, which was also observed for females. Furthermore, ear twitch test showed no significant differences between WT and SNX27$^{+/-}$ mice from both genders. Auditory system reflex was assessed by the auditory startle test where we observed that male and female WT and SNX27$^{+/-}$ mice equally acquired this milestone. Motor function was evaluated through the open field traversal and walking tests. Our data show an equal acquisition of the mature response in the open field traversal test for male and female mice from both genotypes. The same was observed for the acquisition of the mature walking ability for male and female mice from both genotypes (figure 18, table 9 and 10).

Altogether, our data indicate that reduction of SNX27 levels caused no delay in the developmental parameters assessed suggesting that maturation of somatic and neurological reflexes occurs in the normal and expected time window.

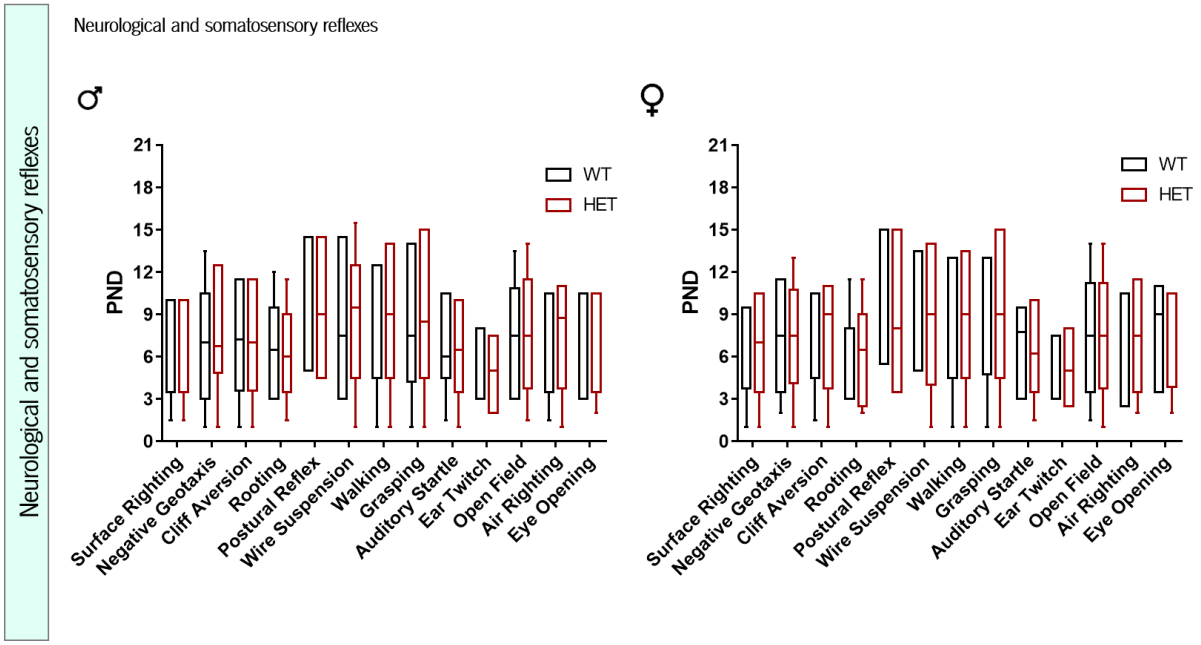

Figure 18 – Reduced levels of SNX27 does not impair the acquisition of neurological and somatosensory reflexes during postnatal evaluation. Assessment of neurological and somatosensory reflexes during the first 21 days of life. WT animals are represented in black and SNX27$^{+/-}$ animals are represented in red. Data is represented as mean ± SEM. Significance level is considered for $p<0.05$.

Table 9 – Neurological and somatosensory reflexes development for male WT and SNX27$^{+/-}$ mice. Data is represented as mean ± SEM.

	Neurological test	Statistical test	Significance
LABYRINTHINE, COORDINATION AND STRENGTH	Surface righting reflex	F(1,12)=0	p>0.9999
	Negative geotaxis	F(1,13)=0	p>0.9999
	Cliff aversion	F(1,13)=0	p>0.9999
	Postural reflex	F(1,16)=0	p>0.9999
	Wire suspension	F(1,16)=0	p>0.9999
	Grasping	F(1,16)=0	p>0.9999
	Air righting reflex	F(1,13)=0	p>0.9999
TACTILE REFLEX	Rooting	F(1,11)=0	p>0.9999
	Ear twitch	F(1,8)=0	p>0.9999
AUDITORY REFLEX	Auditory startle	F(1,11)=0	p>0.9999
MOTOR	Walking	F(1,16)=0	p>0.9999
	Open Field traversal	F(1,13)=0	p>0.9999

Table 10 – Neurological and somatosensory reflexes development for female WT and SNX27$^{+/-}$ mice. Data is represented as mean ± SEM.

	Neurological test	Statistical test	Significance
LABYRINTHINE, COORDINATION AND STRENGTH	Surface righting reflex	F(1,12)=0	p>0.9999
	Negative geotaxis	F(1,13)=0	p>0.9999
	Cliff aversion	F(1,13)=0	p>0.9999
	Postural reflex	F(1,16)=0	p>0.9999
	Wire suspension	F(1,16)=0	p>0.9999
	Grasping	F(1,16)=0	p>0.9999
	Air righting reflex	F(1,13)=0	p>0.9999
TACTILE REFLEX	Rooting	F(1,11)=0	p>0.9999
	Ear twitch	F(1,8)=0	p>0.9999
AUDITORY REFLEX	Auditory startle	F(1,11)=0	p>0.9999
MOTOR	Walking	F(1,16)=0	p>0.9999
	Open Field traversal	F(1,13)=0	p>0.9999

4. Multidimensional behavioral characterization of SNX27$^{+/-}$ C57BL/6J mouse model under exposure to a chronic mild stress protocol

4.1. Biometric parameters

To explore the impact of SNX27 modulation on behavioral performance, we generated a SNX27$^{+/-}$ mouse model in a pure background (C57BL/6J). For such, 21 WT animas and 23 Het animals were behaviorally characterized, where approximately half of the animals were submitted to the CMS protocol. To assess animals' distress during the execution of the CMS protocol and the behavioral characterization, animals' weight was registered on a weekly basis. Body weight loss exceeding 20% of the initial weight was considered a critical endpoint. Of notice, the uCMS paradigm was maintained during the behavioral characterization.

The biometrical assessment highlighted a significant impact of time on body weight during the extent of the experiments. Additionally, the repeated measures ANOVA analysis showed an interaction between time and genotype and stress-exposure along with significant differences between genotype and condition (figure 19A, table 11). Interestingly, results show that weight gain is abrogated or reduced in animals exposed to the uCMS paradigm, regardless of genotype. Regarding body weight variation, results show a significant impact of stress on body weight gain as well as a significant impact of genotype (figure 19B, table 12). Tukey's *post hoc* multiple comparison test demonstrated that SNX27$^{+/-}$-stress-exposed animals significantly lost weight, while this was not observed for SNX27$^{+/-}$-control mice ($p=0.0139$).

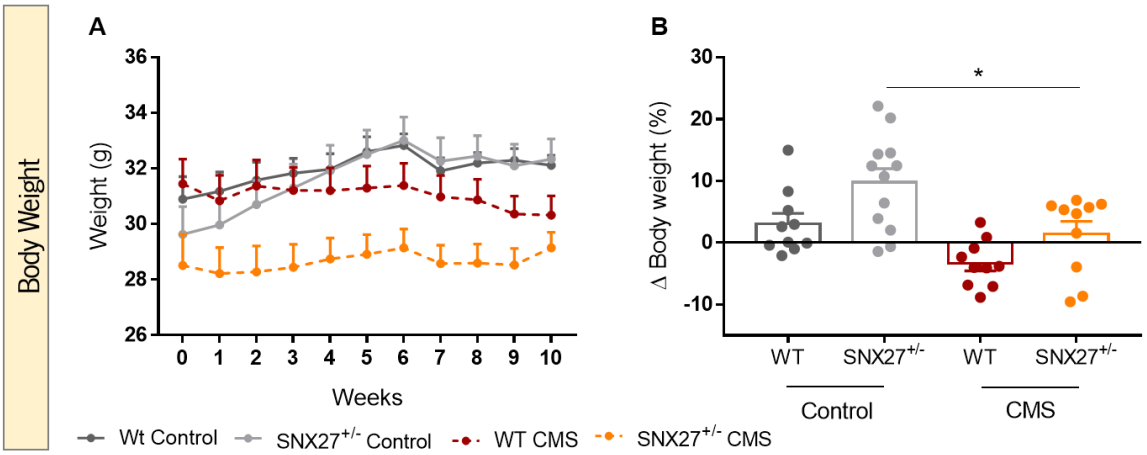

Figure 19 – Body weight gain is abrogated or reduced in uCMS-exposed animals. Assessment of body weight in WT and SNX27$^{+/-}$ animals from control and stress-exposed (uCMS) groups. (A) Body weight measures along the weeks. (B) Body weight alteration in comparison to the first week of measure. Control animals are represented in grey (dark grey – WT; light grey – SNX27$^{+/-}$) and stress-exposed groups are represented in color (dark red – WT; orange – SNX27$^{+/-}$). Data is represented as mean ± SEM. Significance level is considered for $p<0.05$.

Table 11 – Body weight assessment in WT and SNX27$^{+/-}$ animals from control and stress-exposed (uCMS) groups (g). Data is represented as mean ± SEM; n represents the number of animals per group.

	WT	**SNX27$^{+/-}$**	**Statistical test, significance, effect size**
Control	31.95 ± 0.1725 n=11	31.65 ± 0.3339 n=12	Interaction F(30,390)=6.992 p<0.0001 Time F(10,390)=18.24 p<0.0001 Genotype/Condition F(3,39)=3.216 p=0.0331
CMS	31.03 ± 0.1193 n=10	29.01 ± 0.0754 n=11	

Table 12 – Body weight alteration assessment (in comparison to the first week) in WT and SNX27$^{+/-}$ animals from control and stress-exposed (uCMS) groups. Data is represented as mean ± SEM; n represents the number of animals per group.

	WT	SNX27$^{+/-}$	Statistical test, significance, effect size
Control	3.072 ± 1.659 n=10	9.764 ± 2.231 n=12	Interaction F(1,38)=0.260 p=0.6160 Condition F(1,38)=15.440 p=0.0003 Genotype F(1,38)=9.342 p=0.0041
uCMS	-3.36 ± 1.184 n=10	1.432 ± 2.023 n=10	

Additionally, in order to assess animal distress and discomfort, the burrowing test was performed, which is based on rodent's natural ability for burrowing. This test was performed at three different time points after 6 weeks of the uCMS protocol: before, during and after the behavioral characterization. The repeated measures ANOVA demonstrated an interaction between time and genotype and stress-exposure, highlighting an effect of time and genotype and stress-exposure condition (figure 20, table 13). Tukey's *post hoc* multiple comparison test showed that WT-stress-exposed animals have increased burrowing activity compared to their WT controls (p=0.0003) in the first time point assessed. This was also observed in Het animals (p<0.0001). Regarding the second time assessed, *post hoc* analysis showed that the previous effect was maintained in Het animals (p=0.0091).

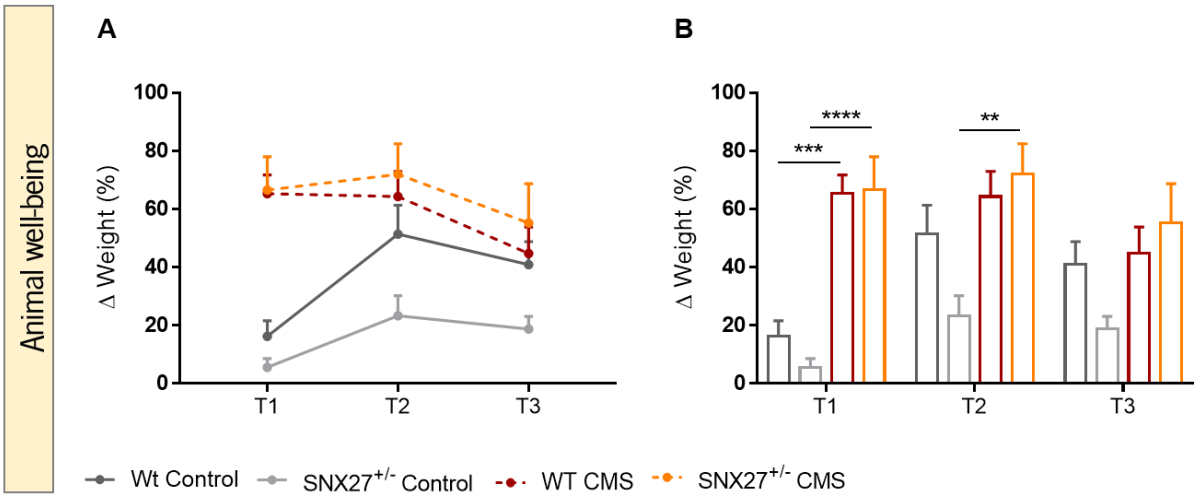

Figure 20 – uCMS-exposed animals display decreased burrowing activity over the weeks. Assessment of animals' well-being through the Burrowing Test. Percentage of pellets burrowed was measured at the beginning and ending of the test at each time point (T1 – prior to behavior; T2 – during behavior; T3 – after behavior). Control animals are represented in grey (dark grey – WT; light grey – SNX27$^{+/-}$) and stress-exposed groups are represented in color (dark red – WT; orange – SNX27$^{+/-}$). Data is represented as mean ± SEM. Significance level is considered for $p<0.05$.

Table 13 - Percentage of pellets burrowed measured at the beginning and ending of the test at each time point. Data is represented as mean ± SEM; n represents the number of animals per group.

		WT	SNX27$^{+/-}$	Statistical test, significance, effect size
T1	**Control**	16.17 ± 5.335 n=10	5.561 ± 2.963 n=11	
	uCMS	65.31 ± 6.396 n=10	66.53 ± 11.390 n=10	
T2	**Control**	51.34 ± 9.932 n=11	23.33 ± 6.899 n=12	Interaction F(6,80)=4.125 p=0.0012 Time F(2,80)=7.776 p=0.0008 Genotype/Condition F(3,40)=6.642 p=0.0010
	uCMS	64.32 ± 8.626 n=10	71.93 ± 10.510 n=10	
T3	**Control**	40.90 ± 7.877 n=11	18.74 ± 4.267 n=11	
	uCMS	44.68 ± 9.099 n=10	55.23 ± 13.45 n=10	

To evaluate the efficiency of the uCMS protocol, serum corticosterone levels were measured a week prior to the beginning of the uCMS protocol and after the behavioral characterization at the nadir (8a.m.) and zenith (8p.m.) phases. The present data is concerned to the measurements performed after the behavioral characterization.

At the nadir phase, results showed a significant impact of stress-exposure and genotype in corticosterone concentration (figure 21, table 14). Tukey's *post hoc* multiple comparisons showed that WT-stress-exposed animals have increased corticosterone levels comparing to WT-controls (p=0.0232). Surprisingly, multiple comparisons test demonstrated that SNX27$^{+/-}$-stress-exposed have decreased concentration of corticosterone in the blood serum comparing to the WT-stress-exposed (p=0.0137).

Regarding the zenith phase, the two-way ANOVA analysis demonstrated a significant effect of stress-exposure in corticosterone concentration regardless of genotype (figure 19, table 10).

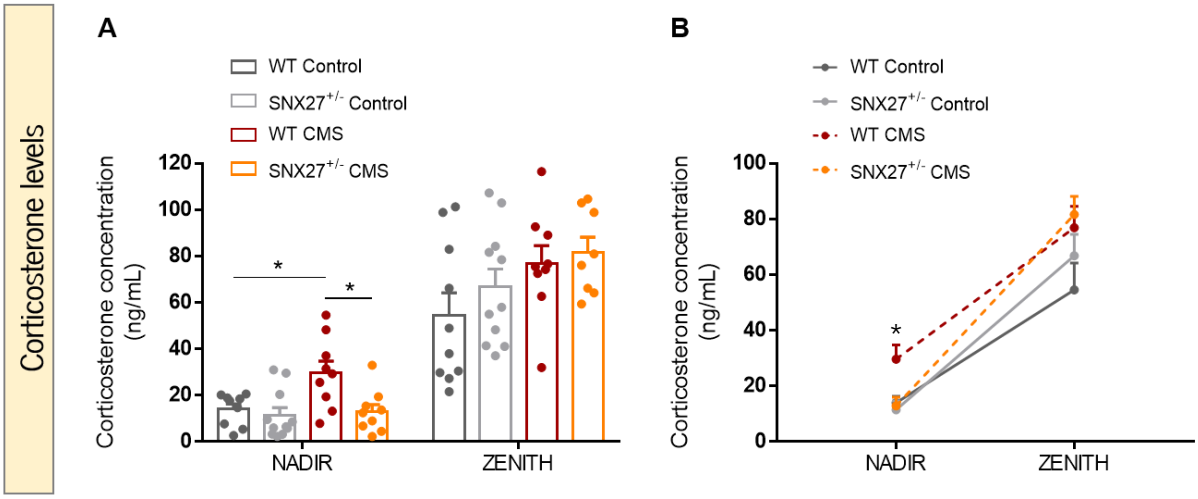

Figure 21 – uCMS-exposed animals present increased levels of corticosterone in the blood. Quantification of blood serum corticosterone levels in control and stress-exposed groups after the behavioral characterization. (A) Corticosterone concentration in the blood serum of WT and SNX27$^{+/-}$ mice from control and uCMS-exposed groups after the behavioral characterization. (B) Variation of corticosterone concentration at the nadir and zenith phases in the blood serum of WT and SNX27$^{+/-}$ mice from control and uCMS-exposed groups after the behavioral characterization. Control animals are represented in grey (dark grey – WT; light grey – SNX27$^{+/-}$) and stress-exposed groups are represented in color (dark red – WT; orange – SNX27$^{+/-}$). Data is represented as mean ± SEM. Significance level is considered for $p<0.05$.

Table 14 – Quantification of blood serum corticosterone levels at the nadir and zenith phases in control and stress exposed groups after the behavioral characterization (ng/mL). Data is represented as mean ± SEM; n represents the number of animals per group.

		WT	SNX27$^{+/-}$	Statistical test, significance, effect size
NADIR	**Control**	14.00 ± 2.303 n=9	11.44 ± 3.168 n=11	Interaction F(1,34)=3.934 p=0.0555 Condition F(1,34)=5,738 p=0.0222 Genotype F(1,34)=7.295 p=0.0107
	uCMS	29.60 ± 5.13 n=9	12.91 ± 3.091 n=9	
ZENITH	**Control**	54.51 ± 9.673 n=10	66.83 ± 7.604 n=11	Interaction F(1,34)=0.2128 p=0.6475 Condition F(1,34)=5.147 p=0.0298 Genotype F(1,34)=1.089 p=0.3042
	uCMS	76.86 ± 7.652 n=9	81.63 ± 6.486 n=8	

4.2. Locomotor and exploratory behavior

To assess for locomotor and exploratory behaviors the OF test was performed. Locomotor and exploratory behaviors are required for all the behavioral experiments, therefore, significant alterations in these behaviors could influence the performance of the animals in the remaining behavioral tests.

Regarding total distance assessment, indicator of locomotor behavior, the two-way ANOVA analysis demonstrated a stress-exposure effect (figure 22A, table 15) where it can be observed that animals exposed to the uCMS paradigm display increased travelled distances, thus increased locomotor behavior. Accordingly, Tukey's *post hoc* multiple comparisons showed that WT-stress-exposed animals travel longer distances comparing to their WT-control ($p<0.0001$) and, as previously, SNX27$^{+/-}$-stress exposed animals have increased travelled distance comparing to their controls ($p<0.0001$). The same result was also observed for the number of vertical counts, indicator of exploratory behavior, where statistical analysis showed a stress-exposure effect (figure 22B, table 16). *Post hoc* multiple comparisons test showed that WT-stress-exposed animals performed more vertical counts during the OF

test comparing to their WT-controls ($p<0.0001$) and this was also observed for SNX27$^{+/-}$-stress exposed animals which have increased number of vertical counts comparing to their controls ($p<0.0001$).

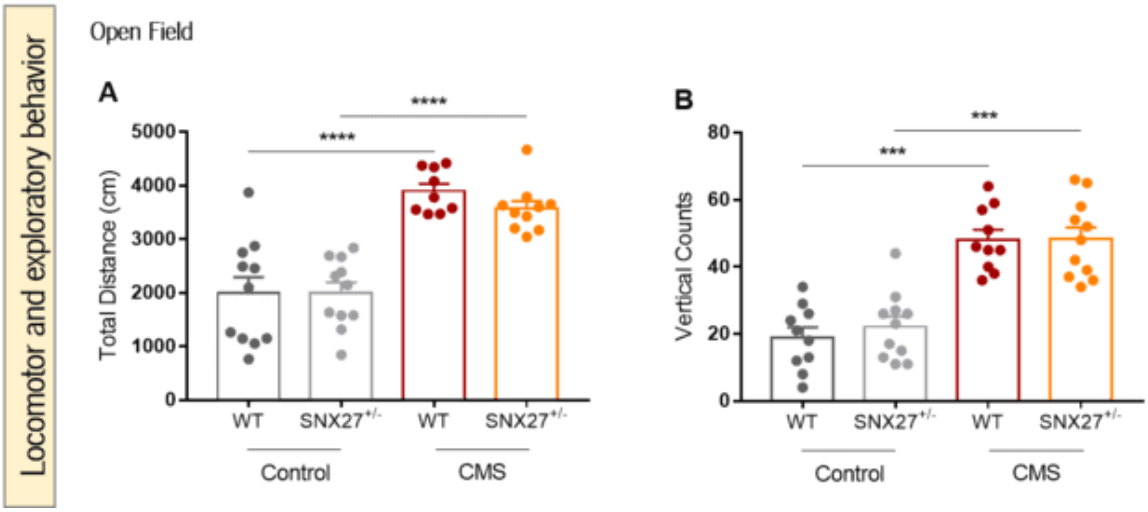

Figure 22 – uCMS-exposed animals display increased locomotor and exploratory behaviors. Evaluation of locomotor and exploratory behaviors by the Open Field test. (A) Total distance travelled by the animals during the test. (B) Number of vertical counts performed by the animals. Control animals are represented in grey (dark grey – WT; light grey – SNX27$^{+/-}$) and stress-exposed groups are represented in color (dark red – WT; orange – SNX27$^{+/-}$).Data is represented as mean ± SEM. Significance level is considered for $p<0.05$.

Table 15 – Total distance travelled by the animals during the OF test (cm). Data is represented as mean ± SEM; n represents the number of animals per group.

	WT	**SNX27$^{+/-}$**	**Statistical test, significance, effect size**
Control	1994.0 ± 297.0 n=11	2000.0 ± 195.3 n=11	<u>Interaction</u> F(1,37)=0.6201 p=0.4360 <u>Condition</u> F(1,37)=66.3500 p<0.0001 <u>Genotype</u> F(1,37)=0.5711 p=0.4546
uCMS	3896.0 ± 135.7 n=9	3568.0 ± 144.0 n=10	

Table 16 - Number of vertical counts performed during the OF test. Data is represented as mean ± SEM; n represents the number of animals per group.

	WT	SNX27$^{+/-}$	Statistical test, significance, effect size
Control	23.73 ± 5.558 n=11	22.18 ± 3.045 n=11	Interaction F(1,38)=0.2409 p=0.6264 Condition F(1,38)=76.18 p<0.0001 Genotype F(1,38)=0.2974 p=0.5887
uCMS	48.10 ± 2.976 n=10	48.27 ± 3.493 n=11	

4.3. Anxious-like behavior

The OF and EPM tests are a measure of anxious-like behavior. In the OF anxious-like behavior indirectly correlates with increased time spent in the center of the arena, while in the EPM test it associates with reduced time spent in the open arms of the maze. Statistical analysis did not reveal any significant differences between groups in the time spent in the center of the arena in the OF or in the time spent in the open arms of the EPM, although a stress-exposure effect was observed in the time spent in the center of the open filed arena, where uCMS-exposed animals spent a higher time in this area comparing to their controls (figure 23A and B, table 17 and 18).

The Light/Dark Box test is another measure of anxiety-like behavior, which correlates with increased time spent in the light zone of the arena. The two-way ANOVA analysis highlighted a stress-exposure effect with uCMS-exposed groups spending less time in the illuminated zone of the arena, thus more anxiogenic (figure 23C, table 19). Moreover, in SNX27$^{+/-}$ stress-exposed animals, Tukey's *post hoc* multiple comparisons showed decreased time spent in the lighter area of the arena when exposed to the uCMS protocol comparing to SNX27$^{+/-}$ control animals (p=0.0069).

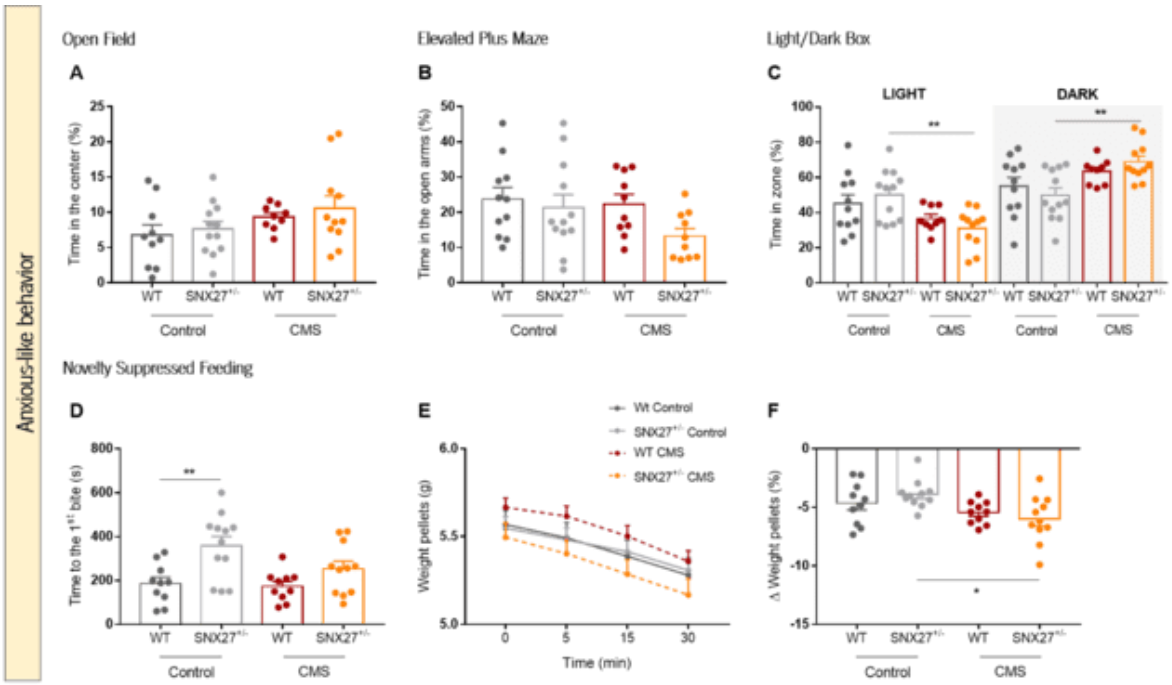

Figure 23 – Reduction of SNX27 increased anxious-like behavior in the L/D Box. Assessment of anxious-like behavior by the Open Field Test, Elevated Plus Maze test, Light/Dark Box test and Novelty Suppressed Feeding Test. (A) Time spent in the center of the arena during the OF test. (B) Time spent in the open arms of the apparatus of the EPM test. (C) Time spent in the light and dark zones of the arena during the L/D Box test. (D) Time for the first bite in the NSF test. (E) Weight of the pellets along the time in the NSF test. (F) Weight variation of the pellets in the NSF test. Control animals are represented in grey (dark grey – WT; light grey – SNX27$^{+/-}$) and stress-exposed groups are represented in color (dark red – WT; orange – SNX27$^{+/-}$).Data is represented as mean ± SEM. Significance level is considered for $p<0.05$.

Table 17 – Time spent in the center of the arena in the OF. Data is represented as mean ± SEM; n represents the number of animals per group.

	WT	**SNX27$^{+/-}$**	**Statistical test, significance, effect size**
Control	6.757 ± 1.4770 n=10	7.653 ± 1.096 n=12	<u>Interaction</u> F(1,38)=0.0206 p=0.8865 <u>Condition</u> F(1,38)=4.263 p=0.0458 <u>Genotype</u> F(1,38)=0.6567 p=0.4228
uCMS	9.339 ± 0.5827 n=9	10.620 ± 1.741 n=11	

Table 18 - Time spent in the open arms of EPM apparatus. Data is represented as mean ± SEM; n represents the number of animals per group.

	WT	SNX27$^{+/-}$	Statistical test, significance, effect size
Control	23.73 ± 3.333 n=11	21.32 ± 3.743 n=12	Interaction F(1,39)=1.108 p=0.2989 Condition F(1,39)=2.216 p=0.1446 Genotype F(1,39)=3.287 p=0.0775
uCMS	22.35 ± 2.786 n=10	13.28 ± 2.112 n=10	

Table 19 - Time spent in the light and dark zones of the arena during the L/D Box Test. Data is represented as mean ± SEM; n represents the number of animals per group.

		WT	SNX27$^{+/-}$	Statistical test, significance, effect size
LIGHT ZONE	**Control**	45.04 ± 5.090 n=11	50.14 ± 4.157 n=12	Interaction F(1,39)=1.7310 p=0.1960 Condition F(1,39)=11.5400 p=0.0016 Genotype F(1,39)=0.0026 p=0.9593
	uCMS	36.65 ± 2.367 n=9	31.14 ± 3.307 n=11	
DARK ZONE	**Control**	54.96 ± 5.090 n=11	49.86 ± 4.157 n=12	Interaction F(1,39)=1.7310 p=0.1960 Condition F(1,39)=11.5400 p=0.0016 Genotype F(1,39)=0.0026 p=0.9593
	uCMS	63.35 ± 2.367 n=9	68.86 ± 3.307 n=11	

The NSF test was also performed as a measure of anxiety-like behavior, which indirectly correlates with an increased latency to feed when in an anxiogenic environment. For the test trial, statistical analysis demonstrated a genotype along with a stress-exposure effect in the time took by the animals to perform the first bite to the pellet in the center of the arena (figure 23D, table 20).

Accordingly, *post hoc* multiple comparisons test showed that Het control animals display increased time to the first bite to the pellet comparing to WT control mice (p=0.0052), thus indicative of increased anxious-like behavior in the Het animals. Regarding appetite drive assessment, it was observed a time effect on the weight of the pellets eaten by all the animals during the test (figure 23E, table 20). Moreover, weight variation of the pellets at the final and initial time points was also assessed as a measure of appetite drive. The two-way ANOVA analysis showed an effect of stress-exposure in the variation of the weight of the pellets, where stressed animals seem to have increased appetite drive. Interestingly, in Het mice, exposure to the uCMS protocol increased appetite drive comparing to Het control animals (p=0.0159) (figure 23F, table 20).

Table 20 – Time to the 1st bite, Weight of the pellets along time and Variation of the weight of the pellets in the NSF Test. Data is represented as mean ± SEM; n represents the number of animals per group.

		WT	SNX27$^{+/-}$	Statistical test, significance, effect size
TIME TO THE 1ST BITE	**Control**	186.5 ± 28.68 n=10	358.5 ± 42.67 n=12	Interaction F(1,39)=1.834 p=0.1835 Condition F(1,39)=2.928 p=0.0950 Genotype F(1,39)=13.23 p=0.0008
	uCMS	174.2 ± 21.80 n=10	252.9 ± 35.40 n=11	
WEIGHT PELLETS	**Control**	5.433 ± 0.0629 n=11	5.438 ± 0.0513 n=12	Interaction F(9,120)=1.66 p=0.1062 Time F(3,120)=259.00 p<0.0001 Genotype/Condition F(3,40)=1.099 p=0.3608
	uCMS	5.536 ± 0.0683 n=10	5.338 ± 0.0712 n=11	
Δ WEIGHT PELLETS	**Control**	-4.642 ± 0.5744 n=10	-3.883 ± 0.3672 n=11	Interaction F(1,38)=1.816 p=0.1858 Condition F(1,38)=9.038 p=0.0047 Genotype F(1,38)=0.0482 p=0.8275
	uCMS	-5.446 ± 0.3086 n=10	-5.993 ± 0.6060 n=11	

4.4. Depressive-like behavior

Depressive-like behavior was assessed through the FST. In this behavioral test depressive-like phenotype directly correlates with increased immobility time and learned helplessness. Statistical analysis did not find any significant differences between groups regarding latency to immobility time, or the immobility time (figure 24, table 21 and 22). Therefore, reduced levels of SNX27 and exposure to the uCMS protocol did not induce depressive-like behavior in the assayed animals.

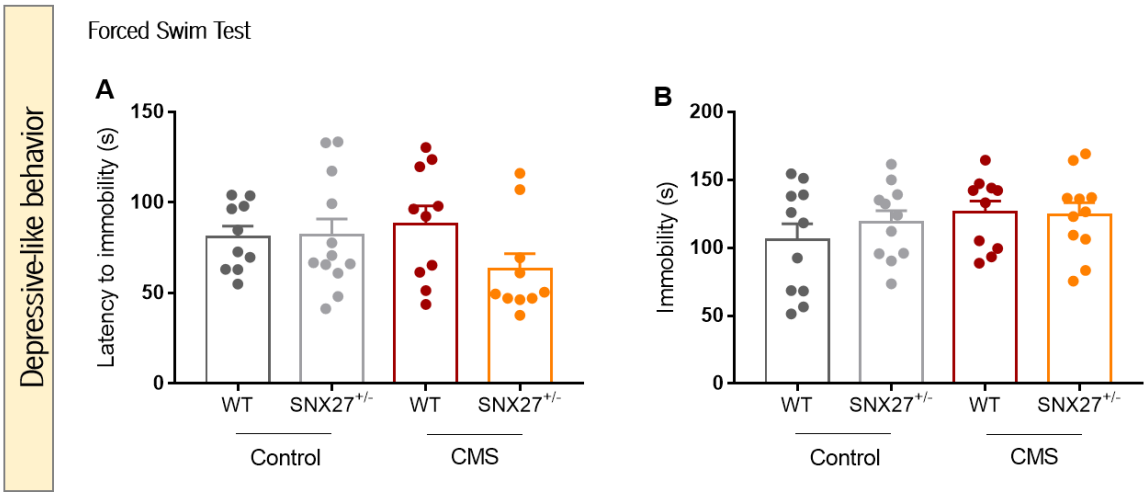

Figure 24 – uCMS-exposed animals do not display depressive-like behavior. Analysis of depressive-like behavior by the Forced Swim Test. (A) Latency to immobility during the FST. (B) Immobility time in the last 4 minutes of the FST. Control animals are represented in grey (dark grey – WT; light grey – SNX27$^{+/-}$) and stress-exposed groups are represented in color (dark red – WT; orange – SNX27$^{+/-}$).Data is represented as mean ± SEM. Significance level is considered for $p<0.05$.

Table 21 – Latency to immobility in the Forced Swim Test. Data is represented as mean ± SEM; n represents the number of animals per group.

	WT	**SNX27$^{+/-}$**	**Statistical test, significance, effect size**
Control	81.12 ± 5.882 n=10	81.78 ± 9.102 n=12	Interaction F(1,38)=2.22 p=0.1445 Condition F(1,38)=0.4307 p=0.5156 Genotype F(1,38)=1.997 p=0.1658
uCMS	88.30 ± 9.877 n=10	63.30 ± 8.546 n=10	

Table 22 – Immobility time in the last 4 minutes of the Forced Swim Test. Data is represented as mean ± SEM; n represents the number of animals per group.

	WT	**SNX27$^{+/-}$**	**Statistical test, significance, effect size**
Control	105.90 ± 11.87 n=11	119.10 ± 8.34 n=11	Interaction F(1,39)=0.6132 p=0.4383 Condition F(1,39)=1.7610 p=0.1922 Genotype F(1,39)=0.3646 p=0.5494
uCMS	126.00 ± 8.44 n=10	124.30 ± 8.88 n=11	

4.5. Cognitive behavior

Cognitive behavior was assessed through the Y-Maze Two-Trial Place Recognition Test and the Contextual Fear Conditioning Test. The Y-Maze test evaluates spatial recognition memory by taking advantage of mice natural drive to explore novel environments, as already mentioned. Statistical analysis showed an interaction between genotype and stress-exposure in the time spent in the novel arm of the Y-Maze (figure 25A, table 23) and in the discrimination index (figure 25B, table 24). Our results show that uCMS-exposed WT mice display deficits in recognition memory, since they spend less time in the novel arm of the maze (p=0.0104) and fail to discriminate the novel arm (p=0.0078) when compared to their WT controls. On opposite, SNX27$^{+/-}$-stress-exposed mice display higher recognition memory comparing to WT-stress-exposed animals demonstrated by increased time spent in the novel arm of the maze (p=0.0466) and higher discrimination indexes (p=0.0446) when compared to WT-stress-exposed mice.

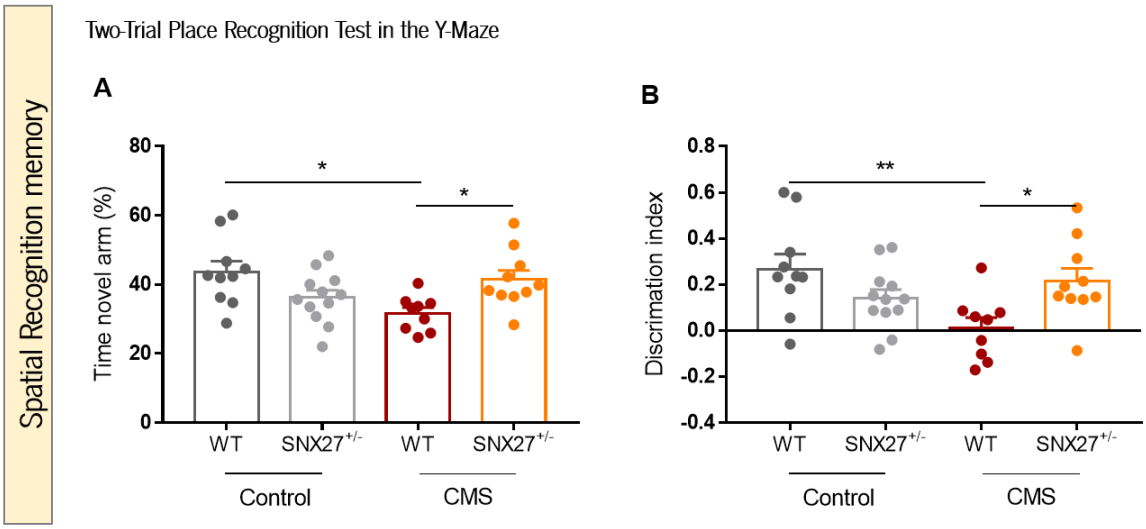

Figure 25 – WT uCMS-exposed animals display memory impairments. Evaluation of spatial recognition memory by the Y-Maze Test. (A) Time spent by the animals in the novel arm of the Y-Maze. (B) Discrimination index in the Y-Maze test. Control animals are represented in grey (dark grey – WT; light grey – SNX27$^{+/-}$) and stress-exposed groups are represented in color (dark red – WT; orange – SNX27$^{+/-}$). Data is represented as mean ± SEM. Significance level is considered for $p<0.05$.

Table 23 – Time spent in the novel arm of the Y-Maze. Data is represented as mean ± SEM; n represents the number of animals per group.

	WT	**SNX27$^{+/-}$**	**Statistical test, significance, effect size**
Control	43.65 ± 3.088 n=10	36.25 ± 2.124 n=12	Interaction F(1,37)=12.19 p=0.0013 Condition F(1,37)=1.874 p=0.1792 Genotype F(1,37)=0.2389 p=0.6279
uCMS	31.66 ± 1.686 n=9	41.48 ± 2.639 n=10	

Table 24 – Discrimination index in the Y-Maze Two-Trial Place Recognition Test. Data is represented as mean ± SEM; n represents the number of animals per group.

	WT	**SNX27$^{+/-}$**	**Statistical test, significance, effect size**
Control	0.2679 ± 0.0646 n=10	0.1399 ± 0.0383 n=12	Interaction F(1,37)=10.57 p=0.0025 Condition F(1,37)=3.12 p=0.0856 Genotype F(1,37)=0.5724 p=0.4541
uCMS	0.0104 ± 0.0461 n=9	0.2161 ± 0.0544 n=10	

The CFC test was also performed as a measure of cognitive behavior. In this test, animals were submitted to a context probe, intended to evaluate hippocampal-dependent memory and a cue probe intended to assess the integrity of amygdala-dependent processes. Concerning the percentage of immobility displayed in the CFC test, statistical analysis demonstrated a stress-exposure effect in the basal context and in the new context (Context B) (figure 26A, table 25). Accordingly, it was observed that SNX27$^{+/-}$ control animals displayed increased freezing behavior in the new context when comparing to SNX27$^{+/-}$ stress-exposed group (p=0.0120). Data regarding discrimination index highlighted a stress-exposure effect where stressed animals present increased discrimination indexes (figure 26B, table 26). In fact, the *post hoc* multiple comparisons test showed that SNX27$^{+/-}$-stress-exposed mice presented higher discrimination index comparing to their controls (p=0.0111).

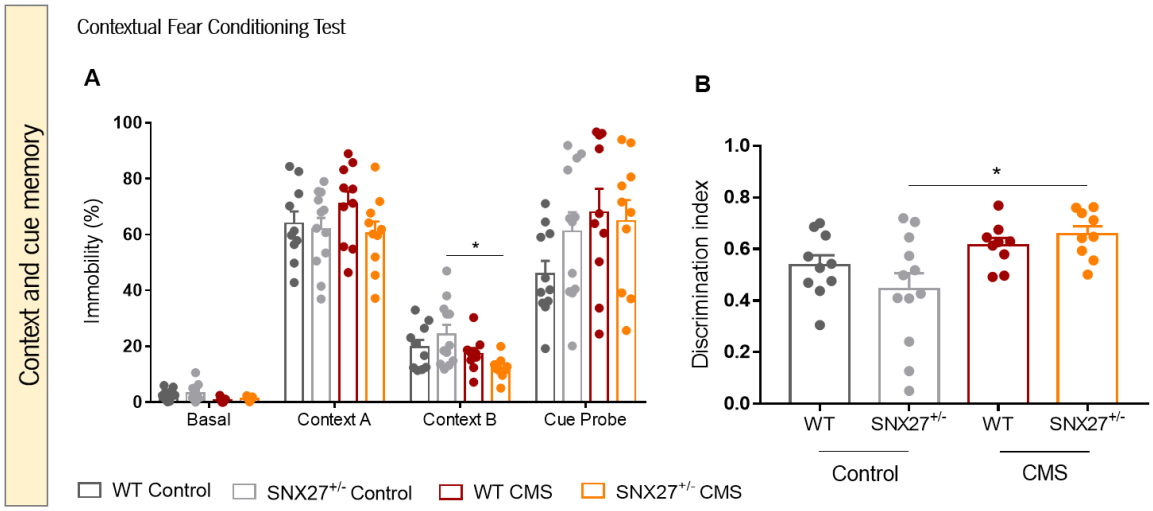

Figure 26 – SNX27$^{+/-}$ uCMS-exposure animals display different freezing time on the new context. Analysis of context and cue memory by the CFC test. (A) Percentage of immobility in the different contexts during the CFC test. (B) Discrimination index in the CFC test. Control animals are represented in grey (dark grey – WT; light grey – SNX27$^{+/-}$) and stress-exposed groups are represented in color (dark red – WT; orange – SNX27$^{+/-}$).Data is represented as mean ± SEM. Significance level is considered for $p<0.05$ and represented by an asterisk (*).

Table 25 – Percentage of immobility in the different contexts during the CFC test. Data is represented as mean ± SEM; n represents the number of animals per group.

		WT	SNX27$^{+/-}$	Statistical test, significance, effect size
Basal	**Control**	2.771 ± 0.6318 n=10	3.172 ± 0.9541 n=11	Interaction F(1,35)=0.00031 p=0.9859 Condition F(1,35)=9.1930 p=0.0046 Genotype F(1,35)=0.3964 p=0.5331
	uCMS	0.775 ± 0.2650 n=9	1.198 ± 0.2385 n=9	
Context A	**Control**	63.96 ± 4.321 n=10	61.99 ± 3.972 n=12	Interaction F(1,38)=0.9917 p=0.3256 Condition F(1,38)=0.3944 p=0.5337 Genotype F(1,38)=2.127 p=0.1529
	uCMS	70.89 ± 4.538 n=10	60.42 ± 4.216 n=10	
Context B	**Control**	19.74 ± 2.525 n=10	24.30 ± 3.336 n=12	Interaction F(1,36)=3.2240 p=0.0810 Condition F(1,36)=7.5090 p=0.0095 Genotype F(1,36)=0.0053 p=0.9422
	uCMS	17.24 ± 2.091 n=9	12.29 ± 1.334 n=9	
Cue Probe	**Control**	45.81 ± 4.759 n=11	61.10 ± 6.871 n=12	Interaction F(1,39)=1.755 p=0.1930 Condition F(1,39)=3.462 p=0.0704 Genotype F(1,39)=0.7639 p=0.3874
	uCMS	67.96 ± 8.408 n=10	64.82 ± 7.504 n=10	

Table 26 – Discrimination index in the Contextual Fear Conditioning Test. Data is represented as mean ± SEM; n represents the number of animals per group.

	WT	**SNX27$^{+/-}$**	**Statistical test, significance, effect size**
Control	0.5371 ± 0.0388 n=10	0.4438 ± 0.0621 n=12	Interaction F(1,36)=2.137 p=0.1524 Condition F(1,36)=9.697 p=0.0036 Genotype F(1,36)=0.288 p=0.5948
uCMS	0.6143 ± 0.0286 n=9	0.6575 ± 0.0313 n=9	

5. *In vitro* characterization of SNXs function and distribution

Mounting evidence supports SNXs as key regulators of protein trafficking given their association with elements of the endocytic network, particularly through interaction with PIP enriched membranes, such as in early and late endosomes. Still, SNXs association with known endocytic markers in neuronal, or neuronal-like cells, has been poorly described and mostly relies from overexpression models with fluorescently tagged SNXs, which can interfere with SNXs distribution and association with protein and/or lipid interaction partners. In here, we used recently developed commercial antibodies towards distinct SNXs to explore the subcellular localization of endogenous SNX27, as well as other SNXs relevant for nervous system homeostasis regulation, such as SNX3, SNX12 and SNX25. Initially, we performed immunofluorescence analysis in a murine neuroblastoma cell line under control conditions. Due to technical limitations, only association with lysosomal-associated membrane protein (LAMP1) marker was employed. LAMP1 is an endosomal protein canonically used as a marker of late endocytic compartments, being required for fusion of phagosomes with lysosomes. LAMP1 extended post-translational glycation confers protection of late endosomal membranes from the action of active lipases found in their acidic lumen (J. Li & Pfeffer, 2016). Immunofluorescence analysis did not show any obvious co-localization of the various SNXs with the late endosomal marker LAMP1 (figure 27). Nonetheless, a detailed and objective quantification of co-localization parameters is required to further confirm these findings, as the evaluation of SNXs co-localization with additional endocytic markers, which could also be complemented biochemically by blotting these markers after subcellular fractionation and gradient separation, to assure the separation between distinct organelles.

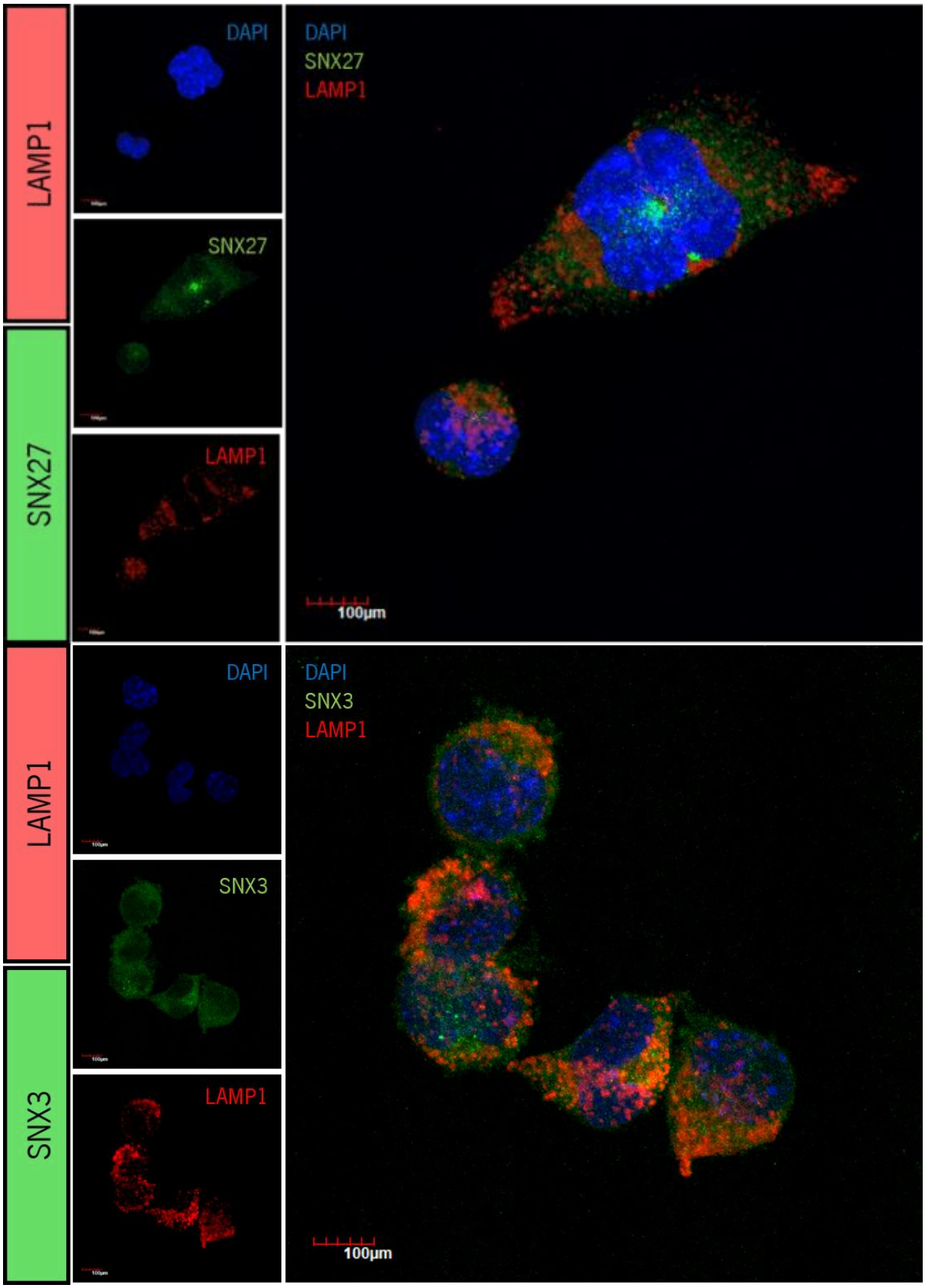
LAMP1
DAPI
SNX27
LAMP1
DAPI
SNX27
LAMP1
100µm
LAMP1
DAPI
SNX3
LAMP1
DAPI
SNX3
LAMP1
100µm

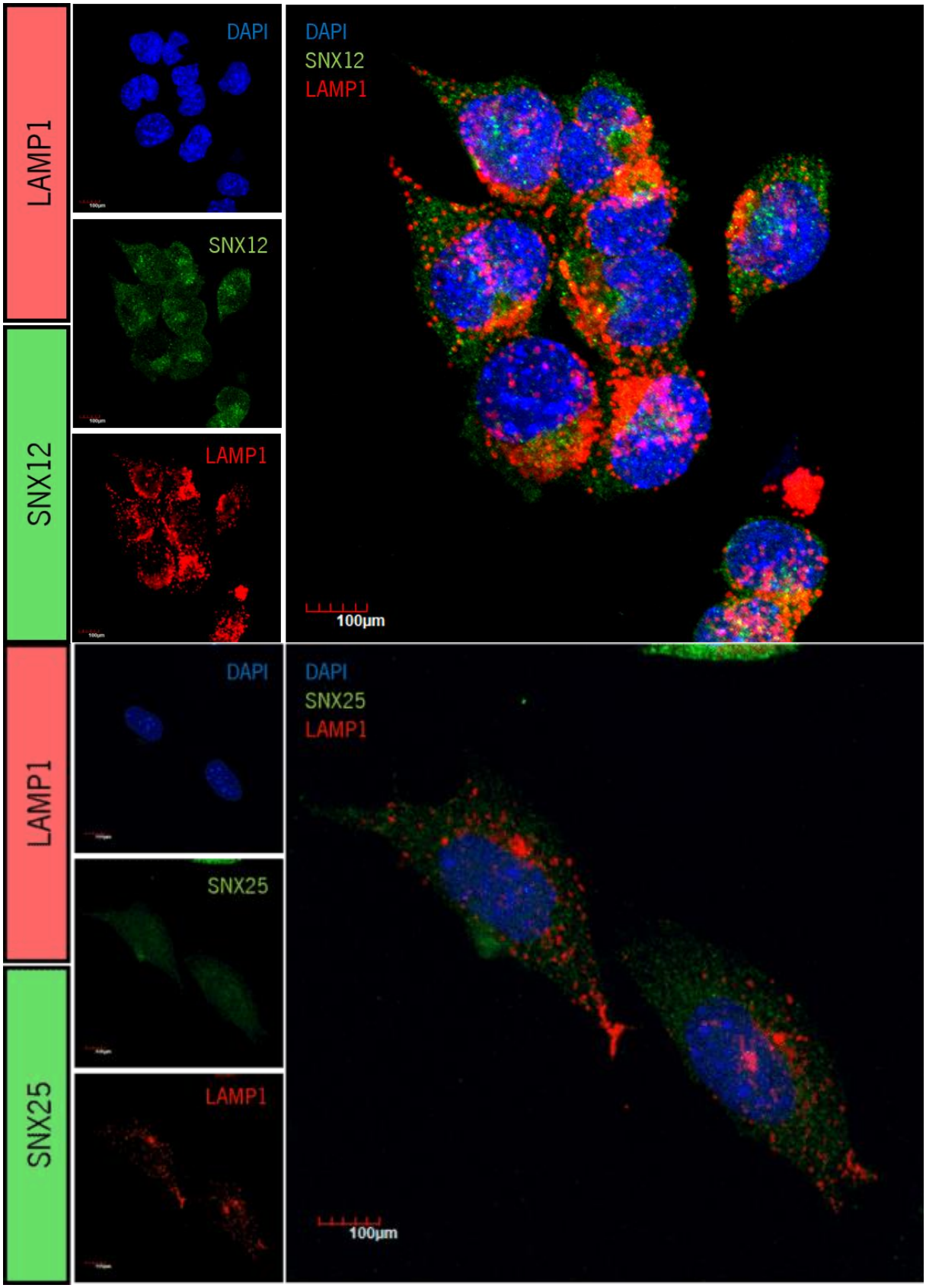

Figure 27 – Co-localization study for SNXs and LAMP1. Immunostaining of N2a cells for SNX27, SNX3, SNX12, SNX25 and LAMP1 markers. Representative confocal microscope images of N2a cells. n=1 experiment, 2 replicas per condition. Scale=100 µm.

5.1. Modulatory effects of pharmacological manipulation in SNXs expression

SNXs are characterized by the presence of a PX-domain, which interacts with PIPs, most commonly with PtdIns3P (PI3P). Hence, most SNXs are associatd with PtdIns3P-enriched elements, particularly in the early endocytic network. To assess whether pharmacological inhibition of PI3P could impact on SNXs expression, we used a potent and highly selective Vps34 kinase inhibitor 1 (VPS34IN1) (Bago et al., 2014), which inhibits the generation of PI3P and modulates autophagy. This synthetic inhibitor was described to selectively decrease the levels of PI3P by ≈50% after 24 hours in the murine neuroblastoma cell line N2a (Miranda et al., 2018). Our findings demonstrated that after pharmacological inhibition with VPS34IN1 for 24 hours the levels of SNX27 were increased while the levels of SNX3 were decreased. As previously demonstrated, after Vps34 inhibition the levels of p62, an autophagy substrate, were increased (figure 28, table 27). In fact, p62 is an autophagy receptor that is involved in the recruitment of ubiquitinated cargo to growing autophagosomes. As such, when autophagy is inhibited, p62 accumulates in punctate structures together with ubiquitin-positive aggregates and thus is a useful reporter of autophagy clearance (Miranda et al., 2018).

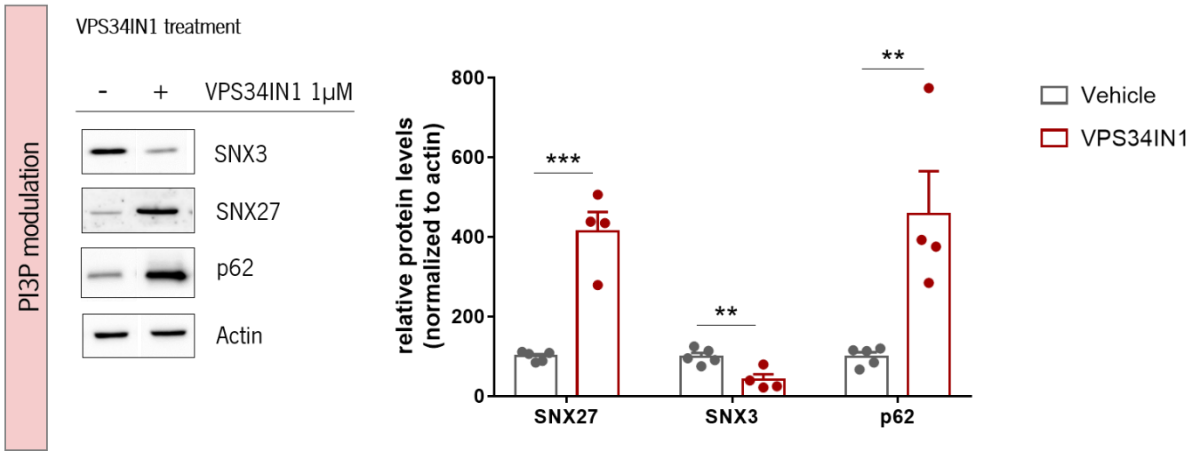

Figure 28 – VPS34 inhibition impacts SNXs expression levels. Quantification of SNXs expression levels related to vehicle in control and PI3P modulating (VPS34IN1) conditions. Vehicles are represented by grey bars/dots whereas VPS34IN1 treatment is represented by dark red bars/dots. Data is represented as mean ± SEM; n=3 per group, from 2 independent experiments. Significance level was considered for $p<0.05$.

Table 27 - Relative protein levels of the analyzed markers. Data is represented as mean ± SEM; n represents the number of replicates.

	Vehicle	VPS34IN1 1 μM	Statistical test, significance, effect size
SNX27	100.0 ± 5.429 n=5	414.7 ± 48.080 n=4	t(7.374)=7 p=0.0002 Cohen's d=9.198
SNX3	100.0 ± 8.682 n=5	41.6 ± 13.340 n=4	t(3.819)=7 p=0.0065 Cohen's d=5.189
p62	100.0 ± 10.360 n=5	456.8 ± 108.300 n=4	t(3.722)=7 p=0.0074 Cohen's d=4.638

Attending on the role of stress exposure on endosomal dysregulation and SNX modulation, (unpublished data; (Vieira et al., 2017)) we set to investigate if stress exposure affected SNXs expression. For such, we treated a murine neuroblastoma cell line N2a with a synthetic glucocorticoid Dexamethasone (DEX) for 48 hours. Interestingly, SNX27 expression was significantly higher in the cells exposed to the synthetic GC, dexamethasone, whereas that was not observed for SNX3 and SNX12. As an internal control, the expression of the glucocorticoid receptor GR was also monitored, and shown to be increased after DEX treatment (figure 29, table 28). As previously described, after GC treatment we observed that p62 levels were higher in cells treated with DEX (figure 29, table 28). Altogether, our results show that SNX27 expression levels are similarly modulated by either Vps34 inhibition, or GC treatment, since SNX27 levels are significantly higher in N2a cells exposed to these pharmacological treatments. In addition, we also observe higher levels of the autophagy receptor p62 in both pharmacological treatments, suggesting a common impairment of autophagy, either at autophagosome biogenesis or autophagosome clearance. While further studies will be required to dissect how SNX27 relates to several aspects of endosomal and lysosomal dysfunction, namely morphology, trafficking and degradation of potentially toxic substrates via autophagy, including tau and Aβ, we highlight SNX27 upregulation as a common observation between decreased PI3P levels and exposure to increased GCs, both of which are associated with increased susceptibility of AD related pathology and neurodegeneration (Miranda et al., 2018; Silva et al., 2018). Interestingly, the AD-associated SNX3 seems to be modulated in the opposite direction following the above-mentioned pharmacological treatments.

In parallel, N2a treated cells and controls were also analyzed by IF staining. As observed in protein blotting, SNX27 and p62 fluorescence intensity was higher in the DEX treated-cells, namely in punctate structures, whereas no alterations were observed in SNX3 and SNX12 fluorescence intensity (figure 30). We also found that intensity of fluorescence of SNX25 is increased with DEX treatment. Moreover, SNX25 appear to co-localize with the LAMP1 marker but not with the EEA1 marker. The autophagy receptor p62 appear to co-localize with the LAMP1 marker while this is not observed for any of the remaining SNXs. (figure 30).

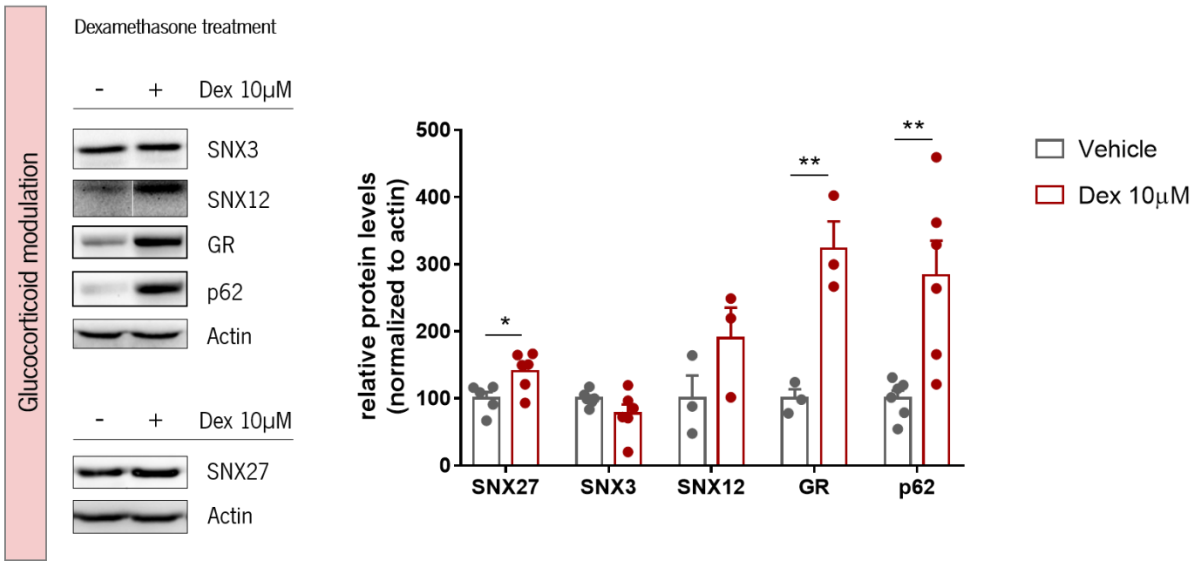

Figure 29 – Dexamethasone treatment influences the expression levels of SNXs and glucocorticoid receptors. Quantification of SNXs levels and GR related to vehicle in control and glucocorticoid modulation (dexamethasone) conditions. Vehicles are represented by grey bars/dots whereas dexamethasone treatment is represented by dark red bars/dots. Data is represented as mean ± SEM; n=3 per group, from 2 independent experiments (except for SNX12 and GR, where n=3 replicas per group, from 1 experiment). Significance level was considered for $p<0.05$ and represented by an asterisk (*).

Table 28 – Relative protein levels of the analyzed markers. Data is represented as mean ± SEM; n represents the number of replicates.

	Vehicle	DEX 10 μM	Statistical test, significance, effect size
SNX27	100.00 ± 9.50 n=5	140.90 ± 11.64 n=6	t(2.647)=9 p=0.0266 Cohen's d=4.369
SNX3	100.00 ± 4.58 n=6	77.52 ± 13.58 n=6	t(1.569)=10 p=0.1478 Cohen's d=2.218
SNX12	100.00 ± 34.05 n=3	190.00 ± 44.98 n=3	t(1.596)=4 p=0.1858 Cohen's d=2.256
GR	100.00 ± 13.44 n=3	322.90 ± 40.84 n=3	t(5.184)=4 p=0.0066 Cohen's d=7.332
p62	100.00 ± 11.72 n=6	283.50 ± 51.62 n=6	t(3.467)=10 p=0.0061 Cohen's d=4.903

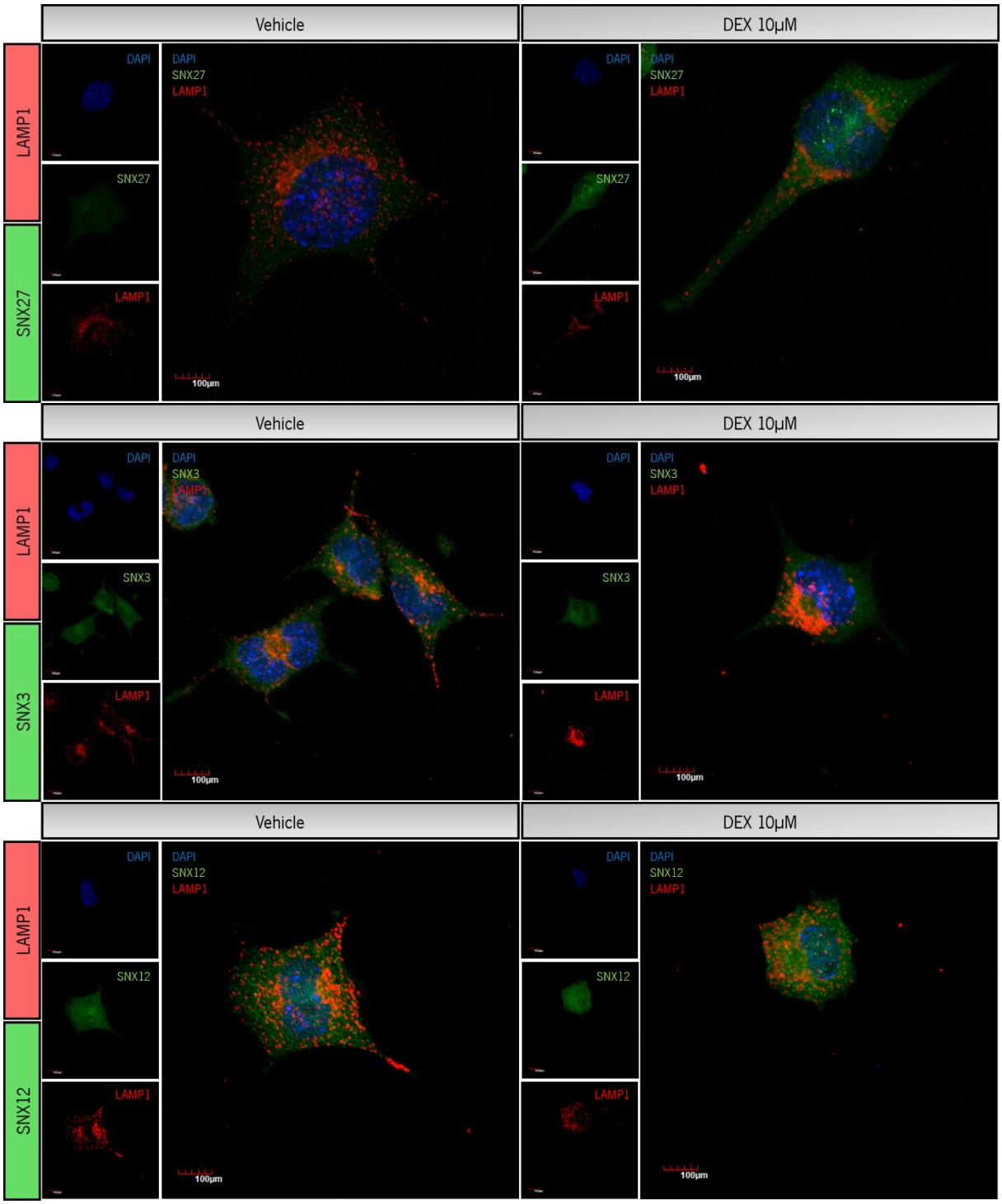
Vehicle
DEX 10μM
LAMP1
SNX27
DAPI
SNX27
LAMP1
100μm
Vehicle
DEX 10μM
LAMP1
SNX3
DAPI
SNX3
LAMP1
100μm
Vehicle
DEX 10μM
LAMP1
SNX12
DAPI
SNX12
LAMP1
100μm

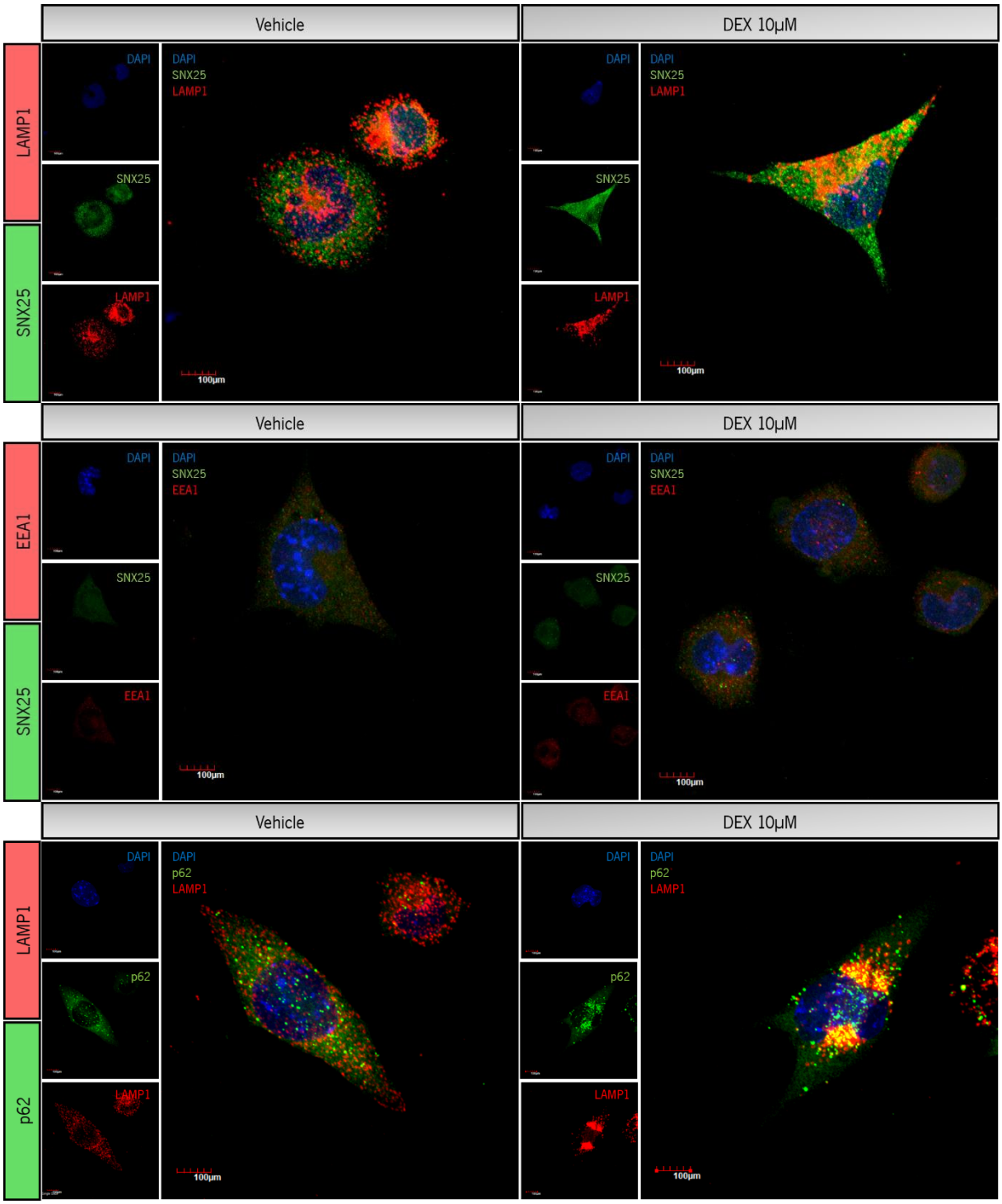

Figure 30 – Co-localization study of different SNXs and LAMP1 in control and stress-mimicking conditions. Immunostaining of N2a cells for SNX27, SNX3, SNX12, SNX25, p62, EEA1 and LAMP1 markers. Representative confocal microscope images of N2a cells. n=1 experiment, 2 replicas per condition. Scale=100 µm.

DISCUSSION

1. The SNX27$^{+/-}$ mixed background

1.1. The impact of reduced levels of SNX27 expression in the neuronal morphology in the mixed background in aging and chronic stress-exposure

Previous studies addressing neuronal morphology in the hippocampus and cerebral cortex of SNX27 knockout animals at early postnatal ages from the mixed background demonstrated that these areas are severely compromised, displaying reduced total dendritic length in CA1 and cortical layer 5 neurons. Behavioral characterization of SNX27$^{+/-}$ animals performed in the host lab, in control and upon stress exposure in young and aged animals, indicated that SNX27$^{+/-}$ mice displayed memory impairments and a possible anxious-like phenotype. In consideration of this evidence, we characterized the neuronal morphology of HET animals in control and stress-exposure conditions at different ages focusing on the hippocampus. Initially we set out to analyze the DG region of the dorsal hippocampus, attending on its association with cognitive performance. Several authors reported that the dorsal hippocampus is crucial for memory encoding and spatial learning and play a role in information processing (Fanselow & Dong, 2010; Kheirbek et al., 2013; Strange, Witter, Lein, & Moser, 2014).

Our results on the morphological analysis of the dorsal DG neurons showed that reduced levels of SNX27 did not impact on the total dendritic length and neuron complexity, regardless of age. Supporting our findings, Wang and collaborators reported that Het animals presented “grossly” normal neuroanatomy (X. Wang et al., 2013a). While we used the Golgi-Cox staining method to evaluate neuronal morphology, this study used Nissl staining, which labels both neuronal and glial cells, thus not being the most adequate method to study neuronal morphology in detail. Moreover, we did not find any significant differences concerning the effects of stress-exposure in the neuronal morphology, in either WT or SNX27$^{+/-}$ animals. According to the literature, exposure to chronic stress modulates neuronal morphology in several brain regions. Particularly, neuronal atrophy was reported in the DG region of animals exposed to the CUS protocol, displaying a decrease in the dendritic length (Lopes et al., 2016) and reduced number of dendritic branch points (Bessa et al., 2009). Moreover, in the PFC region, chronic stress-exposure induces neuronal atrophy resulting in reduced total dendritic length and apical dendritic shrinkage (Teplytska et al., 2016). The discrepancy in our results regarding the effects of stress-exposure on neuronal morphology of WT animals could be due to the small sample size for each

group, since others studies have used a sample size of 6 or more animals per group comparing to our study, in which we used sample size equal or lower than the reported, and also due to user subjectivity. Moreover, we also didn't find an age effect in the neuronal morphology of our animals. Previous reports indicate that aged animals present shorter dendritic trees compared to younger animals in the DG region (Mota et al., 2019), which is not in accordance with our findings. In the future, we would like to increase the number of animals analyzed and, attending on the behavioral data obtained, extend the neuronal morphological characterization to other brain areas, such as the ventral DG region of the hippocampus, the PFC and the amygdala, which were demonstrated to be related with anxiety and emotional regulation (Fanselow & Dong, 2010).

2. The SNX27$^{+/-}$ C57BL/6J pure background

2.1. SNX27 expression reduction does not impair the acquisition of somatic and neurological developmental milestones

Rodent models have been progressively used as research tools to study early life alterations that influence disease outcomes in later stages of adulthood (Nathanielsz & Diehl-Rabadán, 2013) and as a result, comprehension of the developmental processes occurring during prenatal and postnatal stages of development in these models is essential. In the SNX27$^{+/-}$ model the study of postnatal development is particularly important since the SNX27 knockout model is not viable after P14 and there is no evidence suggesting if reduced levels of SNX27 could delay development. For the first time, we provided a comprehensive analysis of how SNX27 partial deletion in a pure genetic background can influence mice postnatal development through a detailed evaluation of neurodevelopmental milestones. Our evaluation consisted of a thorough examination of several somatic and neurological parameters. Of notice, it is important to mention that by backcrossing the original mouse line to the C57BL/6J background we have reduced the possibility that the observed defects (if any) could arise from the existence of a mixed genetic background. Although not fully congenic, the generated experimental strain is 98.93% homozygous for the C57BL/6J strain, particularly when the chromosome where the SNX27 donor mutation is located is exclude where the degree of purity reaches approximately 99.5%.

Our results indicate that SNX27$^{+/-}$ mice display body weight increase similar to their controls, both in males and females. These results are in accordance with previous studies (Cai et al., 2011) and also unpublished data from our laboratory showing that adult WT and SNX27$^{+/-}$ mice display similar body weight. Interestingly, in male mice, Het animals show a tendency to increased body weight. Supporting our findings, a recent study in a patient with heterozygous SNX27 variant observed that this patient displayed developmental delays, seizures, behavioral disturbance and truncal obesity (Parente et al., 2020). Moreover, Cai and coworkers have demonstrated that homozygous knockout mice for SNX27 (SNX27$^{-/-}$) have impaired body weight gain and display growth retardation in multiple organs, namely, spleen, kidney, liver, heart and intestine (Cai et al., 2011). Moreover, it was demonstrated that the SNX27-knockout model exhibits skeletal growth deficits, reflected by shortening of limbs and tail and a smaller skull size, and reduced bone mass (Chan et al., 2016). Survival of newborn homozygous knockout mice was also compromised. From a SNX27 double-heterozygous cross, only 16% of the newborn pups were homozygotes comparing to the expected 25% by Mendelian cross, suggesting an

important role for SNX27 in embryonic development (Cai et al., 2011). In fact, from our double-heterozygous cross, we did not observe the born of any homozygous animals. Regarding reproductive assessment, SNX27$^{+/-}$ mice presented a normal sexual differentiation as we did not find any differences in anogenital distance in males and females SNX27$^{+/-}$ mice. Regarding eye opening, our results indicate that heterozygotes acquire this developmental milestone at the typical described age (PND13) (Heyser, 2003). Altogether, the presented evidence indicates that SNX27$^{+/-}$ mice display a normal physical maturation.

In addition to a correct physical development, development of neurological reflexes is also crucial during postnatal periods. In mice this period comprises important steps of brain growth and malformations occurring during early life stages are associated to the appearance of several neurodevelopmental pathologies (Berger-sweeney et al., 2003). To assess correct maturation of neurological reflexes during postnatal period, we performed a battery of tests related with sensory-motor functions, auditory reflexes, locomotion, coordination and strength in males and females WT and SNX27$^{+/-}$ mice. In our study, we demonstrate that WT and SNX27$^{+/-}$ mice acquire a similar mature response for sensory-motor and auditory reflexes. The same was observed for the acquisition of motor-related responses evaluated in the walking and open field traversal tests in which WT and SNX27$^{+/-}$ displayed the mature response approximately at the same postnatal day. From this data, we expect SNX27$^{+/-}$ mice to be able to perform behavioral tests that depend on the tactile, auditory and motor abilities without major impairments. During the developmental characterization, we have also assessed progressive maturation of sensory and motor skills depending on the vestibular system. In mammals, the vestibular system is responsible for the sense of balance and spatial orientation, coordinating movement with balance (Day & Fitzpatrick, 2005). In vestibular system-dependent tests, such as surface righting reflex, negative geotaxis, cliff aversion, postural reflex and air righting reflex no significant differences were observed between WT and SNX27$^{+/-}$ mice from both genders. Accordingly, in the grasping and wire suspension test we observed that male and females mice, regardless of genotype, equally performed this tests within the normal range for the appearance of the mature response for this milestones (Heyser, 2003). A previous study has demonstrated that SNX27$^{-/-}$ mice failed to thrive beyond 4 weeks of life and displayed severe brain atrophy. Histological analysis of SNX27$^{-/-}$ brains showed neuronal degeneration occurring in the cortex as well as decreased total dendritic length and branching of cortical layer 5 and hippocampal CA1 neurons, suggesting that brain development is severely compromised during the early postnatal development of these mice (X. Wang et al., 2013a). Overall, our data provides strong evidence for a normal somatic and neurological

development of the SNX27$^{+/-}$ mice, discarding the possibility that developmental alterations could be occurring during SNX27$^{+/-}$ mice development and that could be interfering with the behavioral assessment of this animal model during adulthood.

2.2. The effects of SNX27 reduction in a rodent model of chronic stress exposure

Growing evidence has implicated SNXs in endocytic events underlying neurodegenerative processes, cognitive decline and synaptic plasticity. Particularly, SNX27 was demonstrated to be important for learning and memory (X. Wang et al., 2013a) and to be involved in Aβ levels regulation. However, how this protein is modulated by chronic stress-exposure, a known risk factor for the development of neurodegenerative disorders such as AD (Justice, 2018), has not been addressed yet. Interestingly, preliminary data from the host lab indicates that SNX27 expression is reduced in rodents exposed to a CMS protocol. In this work, we performed an extensive behavioral characterization of the SNX27$^{+/-}$ C57BL/6J mouse model under chronic stress-exposure in a question to elucidate the role of SNX27 in behavioral performance, namely in the emotional dimension (attending on preliminary behavioral data from the mixed background), under stress conditions, where synaptic function is challenged and emotional dysfunction is potentiated. Attending on the resilience of C57BL/6 animals to stress (Farley et al., 2012) and to preliminary data obtained with the mixed background mouse model, we decided to perform the uCMS paradigm instead, as this is described has more aggressive and more effective in inducing emotional distress (Willner, 2017b). This protocol is a previous validated stress paradigm that mimics the behavioral response of depressive-, anxiety- and anhedonic-like phenotypes and cognitive deficits (Alves et al., 2017; Bessa et al., 2009; Mateus-Pinheiro et al., 2013). Our data indicates that we were able to induce a stress-response in animals subjected to the uCMS paradigm, regardless of genotype. Body weight alterations is a commonly used measure of stress protocol efficacy in rodents (Nollet et al., 2013). According to the guidelines for animal welfare provided by the national authority for animal experimentation, a decrease of 20% in animal's initial body weight during the execution of the experimental protocol should be considered as a humane endpoint and an indicator to terminate the experiment. This condition was not verified in any of the animals tested. Body weight was assessed on a weekly basis and our results demonstrated that body weight gain was abrogated or reduced in uCMS-exposed animals in opposition to body weight increase of control groups, as previously demonstrated by others (Schweizer, Henniger, & Sillaber, 2009), and this was independent of genotype. In this manner differences between WT and SNX27$^{+/-}$ animals were not observed, both in

control or stress-exposure conditions, suggesting that SNX27 expression reduction does not significantly impact on body weight gain under constitutive (see figure 17A) or stressful conditions.

Chronic stress causes dysregulation of the HPA axis reflected by elevation in the levels of glucocorticoids. As a result, different models of chronic stress exposure often describe disturbed corticosterone (CORT) levels in mice and rat models (Alves et al., 2017; Monteiro et al., 2015; Silva et al., 2018). Our results showed that uCMS-exposed animals present an alteration in CORT production in response to the stress protocol. This was particularly evident in WT animals, where we observed that the uCMS-exposed group presented a markedly increase in the levels of CORT in the blood serum at the nadir phase. Interestingly, these increase was not observed in Het animals suggesting that SNX27$^{+/-}$ mice may have a decrease HPA response to chronic stress in the nadir phase. At the zenith phase, we observed an effect of the uCMS protocol, where stress-exposed animals presented increased levels of CORT in the blood.

Animals' health status was also evaluated by measuring burrowing activity of control and stress-exposed groups. The burrowing test is a sensitive method to detect behavioral dysfunction and relies on rodents natural burrowing abilities (Robert M J Deacon, 2006). Burrowing behavior has also been used as an accessible tool to monitor disease progression and sickness behavior in models of psychiatric and neurodegenerative disorders. This behavior was demonstrated to be reduced by stress exposure where anhedonic mice showed disrupted burrowing behavior (Strekalova et al., 2011; Strekalova & Steinbusch, 2010). Our data shows that over the weeks of the behavioral assessment uCMS-exposed animals decreased their burrowing activity while control groups increased, suggesting that the uCMS paradigm has an effect on well-being of our mice. Interestingly, at the beginning of the behavioral assessment stressed-exposed animals present increased burrowing behavior comparing to their controls, suggesting that these animals were more active after the uCMS protocol, which might be due to the fact that they were more handled and also exposed to distinct stressors for several weeks, whereas control groups were not. These findings are supported by our data on the OF test, where stress-exposed animals display increased locomotor and exploratory activities. Interestingly, in the non-exposed group, WT animals seem to progressively increase their burrowing behavior over the time. Of notice that in control Het animals the burrowing behavior is comparative lower. These findings open the possibility for SNX27 to play a role in mice well-being since in control conditions loss of SNX27 decreases burrowing activity. Alternatively to the burrowing test, the nest building test could have also been performed to explore these questions (Nollet et al., 2013).

2.2.1. The effects of SNX27 reduction and uCMS-exposure on locomotor behavior

Locomotor behavior was assessed by the OF test. This test is crucial to discard any locomotor defects that could influence other behavioral paradigms since they all rely on mice capability to walk. Our results demonstrated that reduced levels of SNX27 did not influence locomotor and exploratory activities. Supporting our data, a previous study by Wang and collaborators reported that SNX27$^{+/-}$ animals do not present any locomotor defects (X. Wang et al., 2013a). Regarding the effects of the CMS paradigm on this type of behavior, our data indicate that uCMS-exposed animals have increased locomotor and exploratory behavior, given by increased total distances and vertical counts. These results are in accordance with the literature, where several authors report that CMS-exposure increased locomotor activity in C57BL/6 mice (Mineur, Belzung, & Crusio, 2006; Zhu et al., 2019) and are also corroborated by data obtained in the burrowing test where CMS-exposed animals are more active and display increased burrowing activity at the first assessed time-point. This is interestingly observed in T2 and T3 (during behavioral analysis) where control animals also increase their burrowing activity.

2.2.2. The effects of SNX27 reduction and stress-exposure on emotional-related behaviors

Attending on preliminary data concerning the behavioral analysis of the SNX27$^{+/-}$ animals on the mixed background, which indicated a role for SNX27 in anxious-like behavior, we performed an extensive characterization of the emotional dimension through the execution of several tests that assess anxious-like behavior, namely, the OF test, the EPM test, the L/D Box test and the NSF test. In fact, in the NSF our data demonstrated that in control conditions SNX27$^{+/-}$ animals display increased anxious-like behavior given by increased time to take the first bite in the pellet placed in the more anxiogenic region of the arena (center) in the NSF test in starvation conditions. However, these trait was not evident in the remaining performed behavioral tests that assess anxious-like behaviors. In control conditions SNX27$^{+/-}$ animals did not present significant differences in the time spent in the center of the arena of the OF, nor in the open arms of the EPM or in the light zone of the arena of the L/D Box, comparing to their WT controls. Moreover, concerning the effects of uCMS paradigm on anxious-like phenotypes, our results demonstrate that SNX27$^{+/-}$ uCMS-exposed animals spend less time in the lighter zone of the arena of the L/D Box test, which is demonstrative of an evident anxious-like behavior. Interestingly, in this behavioral test, SNX27$^{+/-}$ animals when exposed to the uCMS protocol spend less time in the light region of the L/D Box and thus display increased anxious-like behaviors comparing to

their controls. Accordingly, in the EPM test, there was also a tendency for SNX27$^{+/-}$ animals to present increased anxious-like behavior in the presence of stress-exposure conditions. These findings suggest that in this stress-resilient mouse background, the reduction of SNX27 seems to facilitate the appearance of emotional-associated deficits, whenever they are both observed in control conditions. Nevertheless, another experimental animal set needs to be characterized to further confirm phenotypes concerning anxious-like behaviors.

The impact of SNX27 reduced levels and stress-exposure on behavioral despair was also explored during this work. For such, we performed the FST to evaluate depressive-like behavior and we found out that SNX27 reduction nor CMS-exposure impact on animals immobility time, which is not in accordance with the available literature (Gao, Chen, Su, Marshall, & Xiao, 2017; Mineur et al., 2006). Several studies have demonstrated that exposure to stress paradigms increased behavioral despair. Animals submitted to the uCMS paradigm display increased immobility time in the FST test (Gao et al., 2017; C. Hu et al., 2017). The fact that we did not find any differences in behavioral despair of uCMS-exposed animals could be due the genetic background of our mice. In fact, several studies have reported strain-related differences regarding stress-exposure on behavioral performance showing that BALB/c mice are more susceptible to uCMS and social defeat stress than C57BL/6 mice (Farley et al., 2012; Palumbo, Zubilete, Cremaschi, & Mari, 2009; Savignac, Finger, & Pizzo, 2011). Interestingly, SNX27$^{+/-}$ animals when exposed to the stress protocol have a tendency to display increased latency to immobility during the FST indicative of depressive-like behavior. This was also observed when assessing anxious-like behavior, where reduction of SNX27 levels seems to promoted phenotype appearance in stress-exposed animals.

2.2.3. The effects of reduced levels of SNX27 and stress-exposure on cognitive behavior

In consideration of SNX27 described role in learning and memory processes (X. Wang et al., 2013a) we performed an evaluation of cognitive behaviors in our mouse model using the Y-Maze and Contextual Fear Conditioning tests, by our interest in exploring anxiety associated traits. In the Y-Maze test we assessed spatial recognition memory and our data demonstrated that WT animals when exposed to the uCMS paradigm display cognitive impairments given by less time exploring the novel arm of the maze and decreased discrimination index. Accordingly, previous studies using the uCMS paradigm have demonstrated that stress-exposed animals display reduced exploration of novel objects and reduced discrimination index (Moreira, Almeida, Leite-almeida, & Sousa, 2016). Interestingly, Het

animals when exposed to the uCMS protocol spend more time in the novel arm of the maze and display increased discrimination index. These evidences were also observed in the CFC test that evaluates context and cue memory. SNX27$^{+/-}$ uCMS-exposed animals display decreased freezing percentages in the new context, and discriminate better the new context in comparison with SNX27$^{+/-}$ control animals. Nonetheless, our results are not in accordance with the available literature. Wang and coworkers have demonstrated that SNX27$^{+/-}$ mice display cognitive impairments in the Novel Object Recognition test (NORT) and in the Barnes Maze test (X. Wang et al., 2013a). Moreover, unpublished data from the host lab demonstrated that SNX27$^{+/-}$ animals on a mixed background display cognitive impairments in the Morris Water Maze test (MWM), as well as in the NORT and in the Y-Maze. A more extensive cognitive characterization of a new set of animals is necessary to confirm these results, namely by performing other cognitive assessment paradigms, such as the NORT, MWM test or the Barnes Maze test.

3. The effects of pharmacological modulation on SNXs expression and distribution

The major function of the SNX family is reported to be associated with endosomal sorting and signaling, thus, in this work, we started by performing a co-localization study between different SNXs and the lysosomal-associated membrane protein 1 (LAMP1). Our findings suggest that none of the SNXs analyzed, except for SNX25, co-localize with the late endosomal marker LAMP1. Supporting our findings, in hippocampal neurons, SNX27 was demonstrated to co-localize with the early endosome marker Rab5 (Tang, Al-haddawi, Dawe, Hong, & Loo, 2014). Moreover, a previous study on HeLa cells transfected with SNX12-EGFP demonstrated that SNX12 co-localized with the early endosome marker EEA1 but not with a tetraspanin CD63, which is predominantly found in multivesicular bodies, an intermediate compartment in the early to late endosome transition, also positive for LAMP1 (Zhao et al., 2012). In the future, we would like to extend our co-localization studies to additional markers of endocytic compartments, particularly using early endosome markers such as EEA1, APPL1 and Rab5, as well as with other recycling and retrieval markers, such as those that form sorting complexes like ESCRT, retromer and retriever, considering the close interaction between SNX27 in cargo retrieval from degradation. In parallel the use of reporters of late endosomes-lysosomes may unravel novel associations of SNXs with the endocytic network.

Several authors have reported SNXs association with PI3P-enriched elements of the early endocytic network, due to the presence of the PX domain which interacts with phosphatidylinositols and most commonly with PI3P. In this work, we addressed whether inhibition of PI3P could modulate SNXs

expression using a Vps34 kinase inhibitor (VPS34IN1). VPS34IN1 is a potent and highly selective inhibitor that inhibits the generation of PI3P and modulates autophagy. Interestingly, recent evidence has associated Vps34 to neurodegenerative pathologies, such as AD. A study conducted in primary neuronal cultures demonstrated that silencing of Vps34 caused endosomal abnormalities and altered amyloidogenic processing of APP, know pathological features of AD. Our results indicate that after pharmacological inhibition of PI3P kinase with VPS34IN1, the levels of SNX27 are significantly increased while the opposite is observed for SNX3, where its levels are decreased. The mechanisms by which these SNXs are modulated need to be further explored, however it is described that SNX27 is associated with the recycling pathway while SNX3 seems to be involved both in degradation, by regulating intraluminal vesicles formation and also in cargo retrieval from the degradative pathway, by aiding in retromer complex recruitment and function. Moreover, as previously reported Vps34 inhibition caused autophagy impairments by increasing the levels of p62. Recent findings suggest that autophagy inhibition and consequent accumulation of p62 is associated with activation of the mTOR pathway (Silva et al., 2018) and many studies describe an essential role for mTOR in protein homeostasis (Wullschleger, Loewith, & Hall, 2006). Interestingly, our findings with VPS34IN1 were partially demonstrated with the synthetic glucocorticoid DEX. In cells treated with DEX the levels of SNX27 were also increased, suggesting that SNX27 is similarly modulated by Vps34 inhibition and GC treatment. In addition, in both conditions we observed an increase of the autophagic receptor p62, suggesting impairments in autophagy. Previous studies have also reported that GC treatment induces blockage of autophagic clearance accumulating the autophagic marker p62 (Silva et al., 2018). Our immunofluorescence studies also support an accumulation of p62 in cells treated with DEX, namely in punctate form, suggesting the accumulation of autophagy substrates that may have been labeled for degradation, namely though ubiquitination, but have failed to be cleared. Overall, our findings suggest that decreased PI3P levels and increased GC have a common effect on the upregulation of SNX27, however further studies will be performed to clarify how elevated SNX27 expression relates to dysfunction of the endocytic pathway in these conditions which associate with neurodegeneration. As future work, we wish to determine its subcellular localization biochemically. We propose the application of subcellular fractionation, namely segregation of soluble and membrane-bound/particulate fractions, to determine the membrane recruitment of SNX27 and whether it is functionally relevant to endocytic processing, namely using animal tissues, such as distinct brain regions, in parallel to N2a cell lysates. Buoyant and floatation gradient separation strategies could be performed to evaluate co-migration with canonical endocytic markers to further support immunohistochemical analysis. Depending on the

degree of co-localization, experiments will be conducted to functionally evaluate those compartments. If major findings are in early compartments, ligand induced signaling and receptor internalization will be assessed, namely the EGR and EGFR receptor (Miranda et al., 2018). If early to late compartments, we can evaluate cargo sorting to intraluminal vesicles (ILVs) of multivesicular bodies and/or exosome formation. These intermediate compartments can be identified with rab7, CD63 or the atypical phospholipid IBPA, which is exclusively found in ILVS. If co-localization is seen with autophagosomes, autophagy flux, this is, determination of autophagosome biogenesis and autophagosome clearance, can be determined by measuring the degree of lipidation of autophasome marker LC3 in the presence of lysosomal neutralizers, namely bafilomycin a1 or chloroquine. To better understand the role of SNX27 in the CNS, it is thus important to characterize all compartments it may associate with and further understand the effect of SNX27 modulation and the processing of disease related proteins, namely TAU and Amyloid β in the context of AD specifically, or alternatively, the levels of relevant synaptic proteins with implication in cognition and memory formation.

FUTURE PERSPECTIVES

In this thesis we opened new insights on SNXs role in neuronal physiology and neurodegeneration associated with endolysosomal dysfunction. Attending on the data obtained regarding SNX27 role in behavioral performance and how different SNXs are modulated in context of disease, several research questions were raised and need to be further explored, particularly, the mechanisms of action of distinct SNXs in the central nervous system. In the future, we aim to explore in more detail molecular changes at the RNA and protein levels in different brain regions, such as the dorsal and ventral DG, amygdala and bed nucleus of the stria terminalis (BNST). The amygdala and BNST are regions intrinsically related with pathophysiological states such as fear, anxiety and addiction. Therefore, anxiety-related genes as corticotropin-releasing factor (CRF) and glucocorticoid receptors are crucial to better understand molecular changes related with this phenotypes. Additionally, it would also be important to address the expression of several molecules related with synaptic plasticity due to SNX27 role in neuronal plasticity. For example, BDNF and NCAM molecules have been implicated in neurite outgrowth, neuronal plasticity and learning and memory.

In consideration of the results obtained in the behavioral assessment, we also aim to perform an additional set of chronically stressed animals to validate our data and explore other behavioral dimensions, namely social behavior, in addition with the use of animal models of disease to further comprehend the association of SNXs with different neurological pathologies. Moreover, we would like to perform a more thorough characterization of the neuronal morphology of different brain regions giving particular interest to the hippocampus, prelimbic regions, amygdala and BNST, and to analyze cytokine production by immune cells population (as seen by our group, unpublished data). Electrophysiological studies would also be relevant to obtain a functional readout of the communication between distinct brain regions.

In addition, we would like to further extend the scope of our *in vitro* studies, namely by modulating the levels of different SNXs, either by down-regulation or up-regulation, in order to have a better understanding of SNXs function and how they are modulated by external factors. Membrane fractionation studies would also be relevant to determine SNXs subcellular localization biochemically.

FINAL REMARKS

Neurodegenerative and neuropsychiatric disorders have a crucial impact in individuals' well-being. Stress, a ubiquitous aspect of everyday life, is a major risk factor for the development of these brain disorders. In this thesis, we performed an extensive behavioral characterization of the SNX27$^{+/-}$ C57BL/6J mouse model and proved, for the first time, that reduction of SNX27 does not influence postnatal development and normal growth. Behavioral data indicated that upon stress-exposure, the emotional and cognitive behaviors are affected in animals with reduced levels of SNX27. Moreover, we demonstrated that increased glucocorticoids levels, a known risk factor for the development of neurodegenerative diseases, promote SNXs dysregulation. Nevertheless, the mechanisms behind these findings remain to be understood. The understanding of these mechanisms can bring us one step closer to the identification of potential novel pathways of intervention to improve the treatment of neurodegenerative diseases.

BIBLIOGRAPHY

Alves, N., Patrício, P., Correia, J., Mateus-Pinheiro, A., Machado-santos, A. R., Loureiro-campos, E., ... Pinto, L. (2017). Chronic stress targets adult neurogenesis preferentially in the suprapyramidal blade of the rat dorsal dentate gyrus. *Brain Structure and Function*, (223), 415–428. https://doi.org/10.1007/s00429-017-1490-3

Bacchelli, C., Jenkins, D., Thomas, A. C., Williams, H., Sullivan, M. O., Mengrelis, K., ... Stanier, P. (2014). Mutations in SNX14 Cause a Distinctive Autosomal-Recessive Cerebellar Ataxia and Intellectual Disability Syndrome. *The American Journal of Human Genetics*, *95*, 611–621. https://doi.org/10.1016/j.ajhg.2014.10.007

Bago, R., Malik, N., Munson, M. J., Prescott, A. R., Davies, P., Sommer, E., ... Alessi, D. R. (2014). Characterization of VPS34-IN1, a selective inhibitor of Vps34, reveals that the phosphatidylinositol 3-phosphate-binding SGK3 protein kinase is a downstream target of class III phosphoinositide 3-kinase. *Biochemical Journal*, *427*, 413–427. https://doi.org/10.1042/BJ20140889

Belzung, C., & Griebel, G. (2001). Measuring normal and pathological anxiety-like behaviour in mice : a review. *Behavioural Brain Research*, *125*, 141–149.

Berger-sweeney, J., Ricceri, L., & Branchi, I. (2003). Animal models of mental retardation : from gene to cognitive function. *Neuroscience and Biobehavioral Reviews*, *27*, 141–153. https://doi.org/10.1016/S0149-7634(03)00016-2

Bessa, J. M., Ferreira, D., Melo, I., Marques, F., Cerqueira, J. J., Palha, J. A., ... Sousa, N. (2009). The mood-improving actions of antidepressants do not depend on neurogenesis but are associated with neuronal remodeling. *Molecular Psychiatry*, *14*(8), 764–773. https://doi.org/10.1038/mp.2008.119

Binley, K. E., Ng, W. S., Tribble, J. R., Song, B., & Morgan, J. E. (2014). Sholl analysis: A quantitative comparison of semi-automated methods. *Journal of Neuroscience Methods*, *225*, 65–70. https://doi.org/10.1016/j.jneumeth.2014.01.017

Bourin, M., & Hascoe, M. (2003). The mouse light/dark box test. *European Journal of Pharmacology*, *463*, 55–65. https://doi.org/10.1016/S0014-2999(03)01274-3

Brown, E. S., Varghese, F. P., & Mcewen, B. S. (2004). Association of Depression with Medical Illness: Does Cortisol Play a Role? *Biological Psychiatry*, *55*, 1–9. https://doi.org/10.1016/S0006-3223(03)00473-6

Cai, L., Loo, L. S., Atlashkin, V., Hanson, B. J., & Hong, W. (2011). Deficiency of Sorting Nexin 27

(SNX27) Leads to Growth Retardation and Elevated Levels of N -Methyl-D-Aspartate Receptor 2C (NR2C). *Molecular and Cellular Biology*, *31*(8), 1734–1747. https://doi.org/10.1128/MCB.01044-10

Calabrese, F., Molteni, R., Racagni, G., & Riva, M. A. (2009). Neuronal plasticity : A link between stress and mood disorders. *Psychoendocrinology*, *34*, 208–216. https://doi.org/10.1016/j.psyneuen.2009.05.014

Cannon, W. B. (1929). Bodily Changes in Pain , Hunger , Fear and Rage: An Account of Recent Researches into the Function of Emotional Excitement . *The Psychological Clinic*, *19*(3), 100–101.

Castagn, V., Moser, P., Roux, S., & Porsolt, R. D. (2010). Rodent Models of Depression : Forced Swim and Tail Suspension Behavioral Despair Tests in Rats and Mice. *Current Protocols in Pharmacology*, *5.8*, 1–14. https://doi.org/10.1002/0471141755.ph0508s49

Castelhano-Carlos, M., Sousa, N., Ohl, F., & Baumans, V. (2010). Identification methods in newborn C57BL / 6 mice : a developmental and behavioural evaluation. *Laboratory Animals*, (44), 88–103. https://doi.org/10.1258/la.2009.009044

Cerqueira, J., Taipa, R., & Uylings, H. B. M. (2007). Specific Configuration of Dendritic Degeneration in Pyramidal Neurons of the Medial Prefrontal Cortex Induced by Differing Corticosteroid Regimens. *Cerebral Cortex*, *17*, 1998–2006. https://doi.org/10.1093/cercor/bhl108

Chan, A. S. M., Clairfeuille, T., Landao-Bassonga, E., Kinna, G., Ng, P. Y., Loo, L. S., … Pavlos, N. J. (2016). Sorting Nexin 27 couples PTHR trafficking to retromer for signal regulation in osteoblasts during bone growth. *Molecular Biol*, *27*(8), 1367–1382.

Chen, Y., Zhang, J., Tan, H., Li, J., & Yu, Y. (2020). Detrimental effects of hypercortisolism on brain structure and related risk factors. *Scientific Reports*, *10*, 1–12. https://doi.org/10.1038/s41598-020-68166-0

Conrad, C. D., Lupien, S. J., & Mcewen, B. S. (1999). Support for a Bimodal Role for Type II Adrenal Steroid Receptors in Spatial Memory. *Neurobiology of Learning and Memory*, *72*, 39–46.

Cullen, P. J. (2008). Endosomal sorting and signalling : an emerging role for sorting nexins. *Molecular Cell Biochemistry*, *9*, 574–582.

Day, B. L., & Fitzpatrick, R. C. (2005). The vestibular system. *Current Biology*, *15*(15), 583–586.

Deacon, R M J. (2009). Burrowing : A sensitive behavioural assay , tested in five species of laboratory rodents. *Behavioural Brain Research*, *200*, 128–133. https://doi.org/10.1016/j.bbr.2009.01.007

Deacon, Robert M J. (2006). Burrowing in rodents : a sensitive method for detecting behavioral

dysfunction. *Nature Protocols*, *1*, 118–121.

Douglas, P. M., & Dillin, A. (2010). Protein homeostasis and aging in neurodegeneration. *The Journal of Cell Biology*, *190*(5), 719–729. https://doi.org/10.1083/jcb.201005144

Ebner, K., & Singewald, N. (2017). Individual differences in stress susceptibility and stress inhibitory mechanisms. *Current Opinion in Behavioral Sciences*, *14*, 54–64. https://doi.org/10.1016/j.cobeha.2016.11.016

Fanselow, M. S., & Dong, H. (2010). Are the Dorsal and Ventral Hippocampus Functionally Distinct Structures ? *Neuron*, *65*(1), 7–19. https://doi.org/10.1016/j.neuron.2009.11.031

Farley, S., Dumas, S., Mestikawy, S., & Giros, B. (2012). Increased expression of the Vesicular Glutamate Transporter-1 (VGLUT1) in the prefrontal cortex correlates with differential vulnerability to chronic stress in various mouse strains: Effects of fluoxetine and MK-801. *Neuropharmacology*, *62*(1), 503–517.

Feng, T., Niu, M., Ji, C., Gao, Y., & Wen, J. (2015). SNX15 Regulates Cell Surface Recycling of APP and Aβ Generation. *Molecular Neurobiology*. https://doi.org/10.1007/s12035-015-9306-z

Gallon, M., & Cullen, P. J. (2015). Retromer and sorting nexins in endosomal sorting. *Biochemical Society Transactions*, *43*, 33–47. https://doi.org/10.1042/BST20140290

Gao, J.-Y., Chen, Y., Su, D.-Y., Marshall, C., & Xiao, M. (2017). Anxiety-like but not despair-like behaviors are further aggravated by chronic mild stress in the early stages of APPswe/PS1dE9. *BioRxiv*, (101), 1–57.

Godoy, L. D., Rossignoli, M. T., Delfino-pereira, P., Garcia-Cairasco, N., & Umeoka, E. H. de L. (2018). A Comprehensive Overview on Stress Neurobiology: Basic Concepts and Clinical Implications. *Frontiers in Behavioral Neuroscience*, *12*, 1–23. https://doi.org/10.3389/fnbeh.2018.00127

Gu, Y., Arruda-carvalho, M., Wang, J., Janoschka, S., Frankland, P., Ge, S., … Health, M. (2012). Optical controlling reveals time-dependent roles for adult-born dentate granule cells. *Nature Neuroscience*, *15*(12), 1700–1706. https://doi.org/10.1038/nn.3260.Optical

Guerra-Gomes, S., Cunha-Garcia, D., Marques-Nascimento, D., Duarte-Silva, S., Loureiro-Campos, E., Sardinha, V., … Oliveira, J. (2020). IP3R2 null mice display a normal acquisition of somatic and neurological development milestones. *European Journal of Neuroscience*. https://doi.org/10.1111/ejn.14724

Han, Big, Wang, J.-H., Geng, Y., Shen, L., Wang, H.-L., Wang, Y.-Y., & Wang, M.-W. (2017). Chronic Stress Contributes to Cognitive Dysfunction and Hippocampal Metabolic Abnormalities in APP/PS1 Mice. *Celluar Physiologu and Biochemistry*, *050031*, 1766–1776.

https://doi.org/10.1159/000471869

Han, Bing, Yu, L., Geng, Y., Shen, L., Wang, H., Wang, Y., & Wang, J. (2016). Chronic Stress Aggravates Cognitive Impairment and Suppresses Insulin Associated Signaling Pathway in APP/PS1 Mice. *Journal of Alzheimer's Disease*, *53*, 1539–1552. https://doi.org/10.3233/JAD-160189

Herman, J. P., Mcklveen, J. M., Ghosal, S., Kopp, B., & Wulsin, A. (2016). Regulation of the Hypothalamic-Pituitary- Adrenocortical Stress Response. *Comprehensive Physiology*, *6*, 603–621. https://doi.org/10.1002/cphy.c150015

Heyser, C. J. (2003). Assessment of Developmental Milestones in Rodents. *Behavioral Neuroscience*, 1–15.

Hill, J. M., Lim, M. A., & Stone, M. M. (2008). Developmental Milestones in the Newborn Mouse. *Neuromethods*, *39*, 131–149.

Hu, C., Luo, Y., Wang, H., Kuang, S., Liang, G., Yang, Y., … Yang, J. (2017). Re-evaluation of the interrelationships among the behavioral tests in rats exposed to chronic unpredictable mild stress. *PlosOne*, *12*(9), 1–15.

Hu, Y., Dammer, E. B., Ren, R., & Wang, G. (2015). The endosomal-lysosomal system : from acidification and cargo sorting to neurodegeneration. *Translational Neurodegeneration*, 1–10. https://doi.org/10.1186/s40035-015-0041-1

Huang, T. Y., Zhao, Y., Li, X., Wang, X., Tseng, I., Thompson, R., … Xu, H. (2016). SNX27 and SORLA Interact to Reduce Amyloidogenic Subcellular Distribution and Processing of Amyloid Precursor Protein. *The Journal of Neuroscience*, *36*(30), 7996–8011. https://doi.org/10.1523/JNEUROSCI.0206-16.2016

Jang, C. (2017). Correlation between retromer and neurological diseases including Alzheimer. *Biodesing*, *5*(3), 89–95.

Justice, N. J. (2018). The relationship between stress and Alzheimer's disease. *Neurobiology of Stress*, *8*, 127–133. https://doi.org/10.1016/j.ynstr.2018.04.002

Katz, R., & Hersh, S. (1981). Amitriptyline and Scopolamine in an Animal Model of Depression. *Neuroscience and Biobehavioral Reviews*, *5*, 265–271.

Katz, R., Roth, K., & Carrol, B. (1981). Acute and Chronic Stress Effects on Open Field Activity in the Rat : Implications for a Model of Depression. *Neuroscience and Biobehavioral Reviews*, *5*, 247–251.

Kaushik, S., & Cuervo, A. M. (2015). Proteostasis and aging. *Nature Medicine*, *21*(12), 1406–1415.

https://doi.org/10.1038/nm.4001

Kemeny, M. E. (2003). The Psychobiology of Stress. *Current Directions in Psychological Science*, *12*(4), 124–129.

Kheirbek, M. A., Drew, L. J., Burghardt, N. S., Costantini, D. O., Tannenholz, L., Fenton, A., … Zeng, H. (2013). Differential Control of Learning and Anxiety along the Dorsoventral Axis of the Dentate Gyrus. *Neuron*, *77*, 955–968. https://doi.org/10.1016/j.neuron.2012.12.038

Kiecolt-Glaser, J. K., Derry, H. M., & Fagundes, C. P. (2015). Inflammation : Depression Fans the Flames and Feasts on the Heat. *Mechanisms of Psychiatric Illness*, 1–17. https://doi.org/10.1176/appi.ajp.2015.15020152

Kirby, E. D., & Kaufer, D. (2010). Stress and Adult Neurogenesis in the Mammalian Central Nervous System. In *Stress - From Molecules to Behavior* (pp. 71–91).

Kirby, E. D., Muroy, S. E., Sun, W. G., Covarrubias, D., Leong, M. J., Barchas, L. A., … States, U. (2013). Acute stress enhances adult rat hippocampal neurogenesis and activation of newborn neurons via secreted astrocytic FGF2. *Neuroscience*, 1–23. https://doi.org/10.7554/eLife.00362

Kloet, E. R. De, Joëls, M., & Holsboer, F. (2005). STRESS AND THE BRAIN : FROM ADAPTATION TO DISEASE. *Nature Neuroscience*, *6*, 463–475. https://doi.org/10.1038/nrn1683

Kraeuter, A., Guest, P. C., & Sarnyai, Z. (2019). The Y-Maze for Assessment of Spatial Working and Reference Memory in Mice. *Pre-Clinical Models; Techniques and Protocols, Methods in Molecular Biology*, *1916*, 105–111.

Kurten, R. C., Cadena, D. L., & Gill, G. N. (1996). Enhanced Degradation of EGF Receptors by a Sorting Nexin , SNX1. *Science*, *272*, 1008–1010.

Kvainickas, A., Orgaz, A. J., Nägele, H., Diedrich, B., Kate, J., Dengjel, J., … Steinberg, F. (2016). Retromer/WASH dependent sorting of nutrient transporters requires a multivalent interaction network with ANKRD50. *Journal of Cell Science*, 1–35.

Lane, R. F., George-hyslop, P. S., Hempstead, B. L., Small, S. A., & Strittmatter, S. M. (2012). Vps10 Family Proteins and the Retromer Complex in Aging-Related Neurodegeneration and Diabetes. *The Journal of Neuroscience*, *32*(41), 14080–14086. https://doi.org/10.1523/JNEUROSCI.3359-12.2012

Lee, D. Y., Kim, E., & Choi, M. H. (2015). Technical and clinical aspects of cortisol as a biochemical marker of chronic stress. *Biochemistry and Molecular Biology*, *48*(4), 209–216.

Lee, H., Takamiya, K., Han, J., Man, H., Kim, C., Rumbaugh, G., … Huganir, R. L. (2003).

Phosphorylation of the AMPA Receptor GluR1 Subunit Is Required for Synaptic Plasticity and Retention of Spatial Memory. *Cell*, *112*, 631–643.

Leonard, B., & Maes, M. (2012). Mechanistic explanations how cell-mediated immune activation, inflammation and oxidative and nitrosative stress pathways and their sequels and concomitants play a role in the pathophysiology of unipolar depression. *Neuroscience and Biobehavioral Reviews*, *36*(2), 764–785. https://doi.org/10.1016/j.neubiorev.2011.12.005

Li, C., Zahid, S., Shah, A., Zhao, D., & Yang, L. (2016). Role of the Retromer Complex in Neurodegenerative Diseases. *Frontiers in Aging Neuroscience*, *8*, 1–12. https://doi.org/10.3389/fnagi.2016.00042

Li, J., & Pfeffer, S. R. (2016). Lysosomal membrane glycoproteins bind cholesterol and contribute to lysosomal cholesterol export. *ELife*, *5*, 1–16. https://doi.org/10.7554/eLife.21635

Lopes, S., Vaz-silva, J., Pinto, V., Dalla, C., Kokras, N., Bedenk, B., & Mack, N. (2016). Tau protein is essential for stress-induced brain pathology. *Proceedings of the National Academy of Sciences of the United States of America*, *113*(26), 1–9. https://doi.org/10.1073/pnas.1600953113

Lucassen, P. J., Pruessner, J., Sousa, N., Almeida, O. F. X., Marie, A., Rajkowska, G., … Czéh, B. (2014). Neuropathology of stress. *Acta Neuropathology*, *127*, 109–135. https://doi.org/10.1007/s00401-013-1223-5

Lupien, S. J., & McEwen, B. S. (1997). The acute effects of corticosteroids on cognition : integration of animal and human model studies. *Brain Research Reviews*, *24*, 1–27.

Mateus-Pinheiro, A., Pinto, L., Bessa, J. M., Morais, M., Alves, N. D., Monteiro, S., … Sousa, N. (2013). Sustained remission from depressive-like behavior depends on hippocampal neurogenesis. *Translational Psychiatry*, *3*. https://doi.org/10.1038/tp.2012.141

Mcallister, A. K. (2007). Dynamic Aspects of CNS Synapse Formation. *Annual Review of Neuroscience*, *30*, 425–450. https://doi.org/10.1146/annurev.neuro.29.051605.112830

Mccorry, L. K. (2007). Physiology of the Autonomic Nervous System. *American Journal of Pharmaceutical Education*, *71*(4), 1–11.

Mcewen, B. S. (2004). Protection and Damage from Acute and Chronic Stress Allostasis and Allostatic Overload and Relevance to the Pathophysiology of Psychiatric Disorders. *Annals New York Academy of Sciences*, 1–7. https://doi.org/10.1196/annals.1314.001

Mcewen, B. S., Nasca, C., & Gray, J. D. (2015). Stress Effects on Neuronal Structure: Hippocampus , Amygdala , and Prefrontal Cortex. *Neuropsychopharmacology*, *41*(1), 3–23. https://doi.org/10.1038/npp.2015.171

Miller, D. B., & Callaghan, J. P. O. (2005). Aging , stress and the hippocampus. *Ageing Research Reviews*, *4*, 123–140. https://doi.org/10.1016/j.arr.2005.03.002

Mineur, Y. S., Belzung, C., & Crusio, W. E. (2006). Effects of unpredictable chronic mild stress on anxiety and depression-like behavior in mice. *Behavioural Brain Research*, *175*, 43–50. https://doi.org/10.1016/j.bbr.2006.07.029

Miranda, A. M., Lasiecka, M., Xu, Y., Neufeld, J., Shahriar, S., Simoes, S., ... Paolo, G. Di. (2018). Neuronal lysosomal dysfunction releases harboring APP C-terminal fragments and unique lipid signatures. *Nature Communications*, *9*(291), 1–16. https://doi.org/10.1038/s41467-017-02533-w

Mirescu, C., & Gould, E. (2006). Stress and Adult Neurogenesis. *Hippocampus*, *16*(3), 233–238. https://doi.org/10.1002/hipo.20155

Monteiro, S., Roque, S., Sá-calçada, D. De, Sousa, N., Correia-neves, M., & Cerqueira, J. J. (2015). An efficient chronic unpredictable stress protocol to induce stress-related responses in C57BL / 6 mice. *Frontiers in Psychiatry*, *6*, 1–11. https://doi.org/10.3389/fpsyt.2015.00006

Moreira, P. S., Almeida, P. R., Leite-almeida, H., & Sousa, N. (2016). Impact of Chronic Stress Protocols in Learning and Memory in Rodents : Systematic Review and Meta-Analysis. *PlosOne*, 1–24. https://doi.org/10.1371/journal.pone.0163245

Morimoto, R. I., Driessen, A. J. M., Hegde, R. S., & Langer, T. (2011). The life of proteins: the good , the mostly good and the ugly. *Nature Publishing Group*, *18*(1), 1–4. https://doi.org/10.1038/nsmb0111-1

Mota, C., Taipa, R., Pereira, S., Monteiro-martins, S., Monteiro, S., Palha, J. A., ... Sousa, J. C. (2019). Structural and molecular correlates of cognitive aging in the rat. *Scientific Reports*, *9*, 1–14. https://doi.org/10.1038/s41598-019-39645-w

Nathanielsz, P., & Diehl-Rabadán, C. (2013). From Mice to Men: research models of developmental programming. *Journal of Developmental Origins of Health and Disease*, *4*, 3–9. https://doi.org/10.1017/S2040174412000487

Ness, S., Rafii, M., Aisen, P., Krams, M., Silverman, W., & Manji, H. (2012). Down's syndrome and Alzheimer's disease: towards secondary prevention. *Nature Reviews*, *11*, 655–656. https://doi.org/10.1038/nrd3822

Niu, Y., Dai, Z., Liu, W., Zhang, C., Yang, Y., Guo, Z., ... Liu, J. (2017). Ablation of SNX6 leads to defects in synaptic function of CA1 pyramidal neurons and spatial memory. *ELife*, (4), 1–41. https://doi.org/10.7554/eLife.20991

Nollet, M., Guisquet, A. Le, & Belzung, C. (2013). Models of Depression : Unpredictable Chronic Mild Stress in Mice. *Current Protocols in Pharmacology*, 1–17. https://doi.org/10.1002/0471141755.ph0565s61

Palumbo, A. L., Zubilete, A. A. Z., Cremaschi, G. A., & Mari, A. N. A. (2009). Different effect of chronic stress on learning and memory in BALB / c and C57BL / 6 inbred mice: Involvement of hippocampal NO production and PKC activity. *Stress*, *12*(4), 350–361. https://doi.org/10.1080/10253890802506383

Parente, D. J., Morris, S. M., Mckinstry, R. C., Brandt, T., Shinawi, M., Gabau, E., & Ruiz, A. (2020). Sorting nexin 27 (SNX27) variants associated with seizures, developmental delay, behavioral disturbance, and subcortical brain abnormalities. *Clinical Genetics*, *97*, 437–446. https://doi.org/10.1111/cge.13675

Paxinos, G., & Franklin, K. B. J. (2004). *The Mouse Brain in Stereotaxic Coordinates*. USA: Elsevier Science.

Pellow, S., Chopin, P., File, S. E., & Briley, M. (1985). Validation of open : closed arm entries in an elevated plus-maze as a measure of anxiety in the rat. *Journal of Neuroscience Methods*, *14*, 149–167.

Peña-bautista, C., Casas-fernández, E., Vento, M., Baquero, M., & Cháfer-pericás, C. (2020). Stress and neurodegeneration. *Clinica Chimica Acta*, *503*, 163–168. https://doi.org/10.1016/j.cca.2020.01.019

Petit-Demouliere, B., Chenu, F., & Bourin, M. (2005). Forced swimming test in mice : a review of antidepressant activity. *Psychopharmacology*, *177*, 245–255. https://doi.org/10.1007/s00213-004-2048-7

Pruett, S. B. (2003). Stress and the immune system. *Pathophysiology*, *9*, 133–153. https://doi.org/10.1016/S0928-4680(03)00003-8

Prut, L., Belzung, C., Rabelias, U. F., & Psychobiologie, E. (2003). The open field as a paradigm to measure the effects of drugs on anxiety-like behaviors : a review. *European Journal of Pharmacology*, *463*, 3–33. https://doi.org/10.1016/S0014-2999(03)01272-X

Raiborg, C., Schink, K. O., & Stenmark, H. (2013). Class III phosphatidylinositol 3 – kinase and its catalytic product PtdIns3P in regulation of endocytic membrane traffic. *FEBS Journal*, *280*, 2730–2742. https://doi.org/10.1111/febs.12116

Razzoli, M., Carboni, L., Andreoli, M., Ballottari, A., & Arban, R. (2011). Different susceptibility to social defeat stress of BalbC and C57BL6/J mice. *Behavioural Brain Research*, *216*, 100–108.

https://doi.org/10.1016/j.bbr.2010.07.014

Samuels, B. A., & Hen, R. (2011). Novelty-Suppressed Feeding in the Mouse. *Neuromethods*, *63*, 107–121. https://doi.org/10.1007/978-1-61779-313-4

Savignac, H. M., Finger, B. C., & Pizzo, R. C. (2011). Increased sensitivity to the effects of Chronic Social Defeat Stress in an innately anxious mouse strain. *Neurosci*, *192*, 524–536. https://doi.org/10.1016/j.neuroscience.2011.04.054

Schneiderman, N., Ironson, G., & Siegel, S. D. (2005). STRESS AND HEALTH : Psychological, Behavioral, and Biological Determinants. *Annual Review of Clinical Psychology*, 607–628. https://doi.org/10.1146/annurev.clinpsy.1.102803.144141

Schwarz, D. G., Griffin, C. T., Schneider, E. A., Yee, D., & Magnuson, T. (2002). Genetic Analysis of Sorting Nexins 1 and 2 Reveals a Redundant and Essential Function in Mice. *Molecular Biology of the Cell*, *13*, 3588–3600. https://doi.org/10.1091/mbc.E02

Schweizer, M. C., Henniger, M. S. H., & Sillaber, I. (2009). Chronic Mild Stress (CMS) in Mice : Of Anhedonia , "Anomalous Anxiolysis" and Activity. *PlosOne*, *4*(1), 1–11. https://doi.org/10.1371/journal.pone.0004326

Seiler, A., Fagundes, C. P., & Christian, L. M. (2019). The Impact of Everyday Stressors on the Immune System and Health. In *Stress Challenges and Immunity in Space* (pp. 71–92).

Serchov, T., Calker, D. Van, & Biber, K. (2016). Light / Dark Transition Test to Asses Anxiety-like Behavior in Mice. *Bio-Protocol*, *6*(19). https://doi.org/10.21769/BioProtoc.1957

Silva, J. M., Rodrigues, S., Sampaio-marques, B., Gomes, P., Neves-carvalho, A., Dioli, C., … Sotiropoulos, I. (2018). Dysregulation of autophagy and stress granule-related proteins in stress-driven Tau pathology. *Cell Death & Differentiation*, 1–17. https://doi.org/10.1038/s41418-018-0217-1

Sin, O., & Nollen, E. A. A. (2015). Regulation of protein homeostasis in neurodegenerative diseases : the role of coding and non-coding genes. *Cellular and Molecular Life Sciences*. https://doi.org/10.1007/s00018-015-1985-0

Slavich, G. M., & Irwin, M. R. (2014). From Stress to Inflammation and Major Depressive Disorder: A Social Signal Transduction Theory of Depression. *Psychological Bulletin*, *140*(3), 774–815. https://doi.org/10.1037/a0035302

Sotiropoulos, I., Catania, C., Pinto, L. G., Silva, R., Pollerberg, G. E., Takashima, A., … Almeida, O. F. X. (2011). Stress Acts Cumulatively To Precipitate Alzheimer's Disease-Like Tau Pathology and Cognitive Deficits. *The Journal of Neuroscience*, *31*(21), 7840–7847.

https://doi.org/10.1523/JNEUROSCI.0730-11.2011

Sotiropoulos, I., Catania, C., Riedemann, T., Fry, J. P., Breen, K. C., Michaelidis, T. M., & Almeida, O. F. X. (2008). Glucocorticoids trigger Alzheimer disease-like pathobiochemistry in rat neuronal cells expressing human tau. *Journal of Neurochemistry*, *107*, 385–397. https://doi.org/10.1111/j.1471-4159.2008.05613.x

Strange, B. A., Witter, M. P., Lein, E. S., & Moser, E. I. (2014). Functional organization of the hippocampal longitudinal axis. *Nature Publishing Group*, *15*(10), 655–669. https://doi.org/10.1038/nrn3785

Strekalova, T., Couch, Y., Kholod, N., Boyks, M., Malin, D., Leprince, P., & Steinbusch, H. M. W. (2011). Update in the methodology of the chronic stress paradigm: internal control matters. *Behavioral and Brain Functions*, *7*(9), 1–18. https://doi.org/10.1186/1744-9081-7-9

Strekalova, T., & Steinbusch, H. W. M. (2010). Measuring behavior in mice with chronic stress depression paradigm. *Progress in Neuropsychopharmacology & Biological Psychiatry*, *34*(2), 348–361. https://doi.org/10.1016/j.pnpbp.2009.12.014

Takashima, A., Wolozin, B., & Buee, L. (2019). *Tau Biology*.

Tang, N., Al-haddawi, M., Dawe, G. S., Hong, W., & Loo, L. S. (2014). A role for sorting nexin 27 in AMPA receptor trafficking. *Nature Communications*, *5*, 1–12. https://doi.org/10.1038/ncomms4176

Tatar, M., Tatar, M., Bartke, A., & Antebi, A. (2003). The Endocrine Regulation of Aging by Insulin-like Signals. *Science*, *299*, 1346–1351. https://doi.org/10.1126/science.1081447

Teasdale, R. D., & Collins, B. M. (2012). Insights into the PX (phox-homology) domain and SNX (sorting nexin) protein families : structures , functions and roles in disease. *Biochemical Journal*, *441*, 39–59. https://doi.org/10.1042/BJ20111226

Temkin, P., Lauffer, B., Jäger, S., Cimermancic, P., Krogan, N. J., & Zastrow, M. Von. (2011). SNX27 mediates retromer tubule entry and endosome-to-plasma membrane trafficking of signalling receptors. *Nature Cell Biology*, *13*(6), 1–9. https://doi.org/10.1038/ncb2252

Teplytska, L., Vaz-silva, J., Dioli, C., Trindade, R., Morais, M., Webhofer, C., … Filiou, M. D. (2016). Tau Deletion Prevents Stress-Induced Dendritic Atrophy in Prefrontal Cortex : Role of Synaptic Mitochondria. *Cerebral Cortex*, *27*(4), 1–12. https://doi.org/10.1093/cercor/bhw057

Vervoort, V. S., D Viljoen, R. S., Suthers, G., DuPont, B. R., Abbott, A., & Schwartz, C. E. (2002). Sorting nexin 3 (SNX3) is disrupted in a patient with a translocation t(6;13)(q21;q12) and microcephaly, microphthalmia, ectrodactyly, prognathism (MMEP) phenotype V. *Journal of Medical Genetics*, *3*,

893–899.

Vieira, N., Bessa, C., Rodrigues, A. J., Marques, P., Chan, F. Y., Carvalho, A. X. De, … Sousa, N. (2017). Sorting nexin 3 mutation impairs development and neuronal function in Caenorhabditis elegans. *Cellular and Molecular Life Sciences*. https://doi.org/10.1007/s00018-017-2719-2

Walf, A. A., & Frye, C. A. (2007). The use of the elevated plus maze as an assay of anxiety-related behavior in rodents. *Nature Protocols*, *2*, 322–328. https://doi.org/10.1038/nprot.2007.44

Walter, P., & Ron, D. (2011). The Unfolded Protein Response: From Stress Pathway to Homeostatic Regulation. *Science*, *334*, 1081–1086. https://doi.org/10.1126/science.1209038

Wang, X., Huang, T., Wang, X., Huang, T., Zhao, Y., Zheng, Q., … Zhang, Y. (2014). Sorting Nexin 27 Regulates Aβ Production through Modulating g-Secretase Activity. *Cell Reports*, *9*, 1023–1033. https://doi.org/10.1016/j.celrep.2014.09.037

Wang, X., Zhao, Y., Zhang, X., Badie, H., Zhou, Y., Mu, Y., … Xu, H. (2013a). Loss of sorting nexin 27 contributes to excitatory synaptic dysfunction by modulating glutamate receptor recycling in Down ' s syndrome. *Nature Medicine*. https://doi.org/10.1038/nm.3117

Wang, X., Zhao, Y., Zhang, X., Badie, H., Zhou, Y., Mu, Y., … Xu, H. (2013b). Loss of sorting nexin 27 contributes to excitatory synaptic dysfunction by modulating glutamate receptor recycling in Down ' s syndrome. *Nature Medicine*, (March), 1–10. https://doi.org/10.1038/nm.3117

Wang, Y., Lauwers, E., & Verstreken, P. (2017). Presynaptic protein homeostasis and neuronal function. *Current Opinion in Genetics & Development*, *44*, 38–46. https://doi.org/10.1016/j.gde.2017.01.015

Willner, P. (2017a). Reliability of the chronic mild stress model of depression : A user survey. *Neurobiology of Stress*, *6*, 68–77. https://doi.org/10.1016/j.ynstr.2016.08.001

Willner, P. (2017b). The chronic mild stress (CMS) model of depression : History , evaluation and usage. *Neurobiology of Stress*, *6*, 78–93. https://doi.org/10.1016/j.ynstr.2016.08.002

Winckler, X. B., Faundez, X. V., Maday, X. S., Cai, X. Q., Cla, X., & Almeida, G. (2018). The Endolysosomal System and Proteostasis : From Development to Degeneration. *The Journal of Neuroscience*, *38*(44), 9364–9374. https://doi.org/10.1523/JNEUROSCI.1665-18.2018

Wullschleger, S., Loewith, R., & Hall, M. N. (2006). TOR Signaling in Growth and Metabolism. *Cell*, *124*, 471–484. https://doi.org/10.1016/j.cell.2006.01.016

Xu, S., Zhang, L., & Brodin, L. (2017). Overexpression of SNX7 reduces Aβ production by enhancing lysosomal degradation of APP. *Biochemical and Biophysical Research Communications*, 1–8. https://doi.org/10.1016/j.bbrc.2017.10.127

Yaribeygi, H., Panahi, Y., Sahraei, H., & Johnston, T. P. (2017). The impact of stress on body function: A review. *EXCLI Journal*, *16*, 1057–1072.

Zaqout, S., & Kaindl, A. M. (2016). Golgi-Cox Staining Step by Step. *Frontiers in Neuroanatomy*, 1–7. https://doi.org/10.3389/fnana.2016.00038

Zhang, H., Huang, T., Hong, Y., Yang, W., & Zhang, X. (2018). The Retromer Complex and Sorting Nexins in Neurodegenerative Diseases. *Frontiers in Aging Neuroscience*, *10*, 1–11. https://doi.org/10.3389/fnagi.2018.00079

Zhang, P., Wu, Y., Belenkaya, T. Y., & Lin, X. (2011). SNX3 controls Wingless/Wnt secretion through regulating retromer-dependent recycling of Wntless. *Cell Research*, *21*(12), 1677–1690. https://doi.org/10.1038/cr.2011.167

Zhao, Y., Wang, Y., Yang, J., Wang, X., Zhao, Y., Zhang, X., & Zhang, Y. (2012). Sorting nexin 12 interacts with BACE1 and regulates BACE1-mediated APP processing. *Molecular Neurodegeneration*, *7*(30), 9–12.

Zheng, B., Tang, T., Tang, N., Kudlicka, K., Ohtsubo, K., Ma, P., … Lehtonen, E. (2006). Essential role of RGS-PX1 ¯sorting nexin 13 in mouse development and regulation of endocytosis dynamics. *Proceedings of the National Academy of Sciences*, *103*(45), 16776–16781.

Zhu, H., Tao, Y., Wang, T., Zhou, J., Yang, Y., Cheng, L., … Wu, X. (2019). Long-term stability and characteristics of behavioral , biochemical , and molecular markers of three different rodent models for depression. *Brain and Behavior*, 1–12. https://doi.org/10.1002/brb3.1508

Ziegler, M. G. (2012). Psychological Stress and the Autonomic Nervous System. In *Primer on the Autonomic Nervous System* (Third Edit, pp. 291–294). Elsevier Inc. https://doi.org/10.1016/B978-0-12-386525-0.00061-5

OTHER DOCUMENTS

(Grant proposal submitted to the Innovate Competition I iMed, Lisbon, 2020)

REGULATION OF SNX27 BY PHOSPHOTIDYLINOSITOL-3-PHOSPHATE AND GLUCOCORTICOIDS: IMPLICATIONS FOR ALZHEIMER'S DISEASE

Armada, G; Miranda, A and Vieira, N

Keywords: sorting nexins, PI3P, endolysosomes, neurodegeneration, stress

The endolysosomal pathway is fundamental for neuronal homeostasis and is increasingly linked to the pathogenesis of several neurodegenerative disorders such as Alzheimer's disease (AD) and stress-associated cognitive decline, among others (Y. Hu, Dammer, Ren, & Wang, 2015). The interpretation of these conditions as slowly progressing lysosomal storage disorders as prompted great interest in identifying novel molecular players implicated in pathogenesis and therapy. Sorting Nexins (SNXs) are a family of highly conserved proteins involved in protein trafficking and cell signaling underlying synaptic plasticity and cognition (Cullen, 2008). SNXs are characterized by the presence of a phosphoinositide binding PX-domain with increased affinity to phosphatidylinositol-3-monophosphate (PI3P) (Cullen, 2008; Teasdale & Collins, 2012), a master regulator of endolysosomal and autophagy pathways (Raiborg, Schink, & Stenmark, 2013). SNX27 is a brain-enriched SNX localized in early endosomes that promotes cargo retrieval from the endolysosomal pathway through the retromer complex (Temkin et al., 2011). Distinct studies highlight that retromer cargo sorting disruption due to SNX27 reduced expression/mutation occurs in AD and Down's syndrome (X. Wang et al., 2014, 2013b). Particularly, reduced SNX27 levels contribute to impaired glutamate receptor trafficking, increased amyloid-beta (Aβ) pathology and neuronal loss, whereas SNX27 overexpression limits Aβ production (Huang et al., 2016). Interestingly, our previous work (Miranda et al., 2018) has shown that reduced PI3P levels recapitulate endolysosomal defects reported in AD early stages, namely enlarged endolysosomes, aberrant autophagosomes and increased amyloidogenic processing of amyloid precursor protein (APP). Also, preliminary results indicate that chronic stress and elevated glucocorticoids (GC), known risk factors for AD, reduce SNX27 levels in rodents, whereas ageing promotes its increase. Moreover, *snx-27* KO worms display increased stress-susceptibility and memory impairments, similar to AD worm models. Herein, we aim to unravel SNX27 role in PI3P- and stress-induced endolysosomal dysfunction. Using pharmacological modulation of PI3P and GC levels in neuronal cultures, we will determine

SNX27 levels and subcellular localization using co-localization studies with endocytic markers (early endosomes e.g. EEA1; late endosomes e.g. Rab7; multivesicular bodies e.g. Hrs; lysosomes e.g. LAMP-1/2; autophagosomes e.g. LC3-II). We will test the effects of SNX27 modulation, via siRNA-mediated downregulation or plasmid overexpression, in lysosomal degradation and autophagy, using ligand-induced receptor degradation (e.g. EGFR) and autophagy flux assays. Levels of total APP/APP C-terminal fragments, APP subcellular distribution and Aβ production, as well as glutamate and GC receptors and other stress-associated disease markers, will be assessed under conditions of reduced PI3P or elevated GCs levels. Importantly, SNX27 findings will be compared to truncated SNX27ΔPX and SNX3, a functionally distinct and mutually exclusive PI3P-binding and retromer-associated SNX. Our preliminary results show that SNX27 expression levels in neuronal cells are markedly increased upon acute PI3P depletion and subacute GC treatment, whereas SNX3 levels were decreased. Under both conditions, we found accumulation of the autophagy receptor p62, suggesting autophagic degradation impairments. Our results suggest that reduced PI3P levels and elevated GC share a similar impact in SNX dysregulation, although further work is required to highlight their functional implications. Normalization of SNX expression will determine the therapeutic potential of SNX modulation in AD and stress-associated pathologies. Overall, our work will open new insights on SNXs role in neuronal physiology and neurodegeneration associated with endolysosomal dysfunction.

References

1. Hu Y, Dammer EB, Ren R, Wang G. The endosomal-lysosomal system : from acidification and cargo sorting to neurodegeneration. Transl Neurodegener. Translational Neurodegeneration; 2015; 1–10. doi:10.1186/s40035-015-0041-1
2. Cullen PJ. Endosomal sorting and signalling : an emerging role for sorting nexins. Mol Cell Biochem. 2008;9: 574–582.
3. Teasdale RD, Collins BM. Insights into the PX (phox-homology) domain and SNX (sorting nexin) protein families : structures , functions and roles in disease. Biochem J. 2012;441: 39–59. doi:10.1042/BJ20111226
4. Raiborg C, Schink KO, Stenmark H. Class III phosphatidylinositol 3 – kinase and its catalytic product PtdIns3P in regulation of endocytic membrane traffic. FEBS J. 2013;280: 2730–2742. doi:10.1111/febs.12116
5. Temkin P, Lauffer B, Jäger S, Cimermancic P, Krogan NJ, Zastrow M Von. SNX27 mediates

retromer tubule entry and endosome-to-plasma membrane trafficking of signalling receptors. Nat Cell Biol. Nature Publishing Group; 2011;13: 1–9. doi:10.1038/ncb2252

6. Wang X, Zhao Y, Zhang X, Badie H, Zhou Y, Mu Y, et al. Loss of sorting nexin 27 contributes to excitatory synaptic dysfunction by modulating glutamate receptor recycling in Down ' s syndrome. Nat Med. 2013; 1–10. doi:10.1038/nm.3117
7. Wang X, Huang T, Wang X, Huang T, Zhao Y, Zheng Q, et al. Sorting Nexin 27 Regulates Aβ Production through Modulating g-Secretase Activity. Cell Rep. 2014;9: 1023–1033. doi:10.1016/j.celrep.2014.09.037
8. Huang TY, Zhao Y, Li X, Wang X, Tseng I, Thompson R, et al. SNX27 and SORLA Interact to Reduce Amyloidogenic Subcellular Distribution and Processing of Amyloid Precursor Protein. J Neurosci. 2016;36: 7996–8011. doi:10.1523/JNEUROSCI.0206-16.2016
9. Miranda AM, Lasiecka M, Xu Y, Neufeld J, Shahriar S, Simoes S, et al. Neuronal lysosomal dysfunction releases harboring APP C-terminal fragments and unique lipid signatures. Nat Commun. 2018;9: 1–16. doi:10.1038/s41467-017-02533-w